The LINNEAN SOCIETY of London ZOOLOGICAL Journal of the Linnean Society

Zoological Journal of the Linnean Society, 2010, **160**, 139–194. With 13 figures

A revision of *Aceratherium blanfordi* Lydekker, 1884 (Mammalia: Rhinocerotidae) from the Early Miocene of Pakistan: postcranials as a key

PIERRE-OLIVIER ANTOINE[1,2,3]*, KEVIN F. DOWNING[4], JEAN-YVES CROCHET[5], FRANCIS DURANTHON[6], LAWRENCE J. FLYNN[7], LAURENT MARIVAUX[5], GRÉGOIRE MÉTAIS[8], ABDUL RAHIM RAJPAR[9] and GHAZALA ROOHI[9]

[1]*Université de Toulouse, UPS (SVT-OMP), LMTG, 14 Avenue Édouard Belin, F-31400 Toulouse, France*
[2]*CNRS, LMTG, 14 Avenue Édouard Belin, F-31400 Toulouse, France*
[3]*IRD, LMTG, 14 Avenue Édouard Belin, F-31400 Toulouse, France*
[4]*DePaul University, Chicago, IL 60604, USA*
[5]*Département de Paléontologie, Institut des Sciences de l'Évolution (CNRS-UMR 5554) Université Montpellier 2, c.c. 064, Place Eugène Bataillon, F-34095 Montpellier Cedex 5, France*
[6]*Laboratoire d'Étude et de Conservation du Patrimoine, Muséum d'Histoire naturelle de Toulouse, 39 allées Jules Guesde, F-31000 Toulouse, France*
[7]*Department of Anthropology and Peabody Museum, Harvard University, Cambridge, MA 02138, USA*
[8]*Laboratoire de Paléontologie, UMR 5143 CNRS, Muséum National d'Histoire Naturelle, 8 rue Buffon, F-75005 Paris, France*
[9]*Earth Sciences Division, Pakistan Museum of Natural History, Garden Avenue, Shakarparian, 44000 Islamabad, Pakistan*

Received 22 January 2009; accepted for publication 28 April 2009

Rhinocerotids are particularly abundant and diversified in Neogene deposits of the Indian subcontinent, but their systematics is far from being well defined. Based on the revision of old collections and new findings from the Early Miocene of the Bugti Hills and Zinda Pir, Pakistan, '*Aceratherium blanfordi* Lydekker, 1884' is a chimera, consisting of two dentally convergent but postcranially distinct rhinocerotid taxa: *Pleuroceros blanfordi* and ***Mesaceratherium welcommi* sp. nov.** Postcranial features appear to be much more diagnostic than craniodental morphology in this case. A phylogenetic analysis based on 282 morphological characters scored for 28 taxa (four outgroups and ingroup including both taxa of interest and a 'branching group') strengthens this statement and supports *Pleuroceros* and *Mesaceratherium* as monophyletic genera within Rhinocerotinae. Both genera are recognized for the first time outside Europe. In the Bugti Hills, *P. blanfordi* and *M. welcommi* are part of an exceptionally diversified rhinocerotid fauna, with up to nine species associated in the same locality (Kumbi 4f). This rhinocerotid assemblage confirms the earliest Miocene age (Agenian/Aquitanian) of the upper member of the Chitarwata Formation as a whole. Coeval homotaxic rhinocerotid faunas from Europe (France, Czech Republic) and East Africa (Uganda, Kenya) support broad and sustainable rhinocerotid interchanges amongst South Asia, Europe, and Africa under compatible environmental conditions throughout earliest Miocene times.

doi: 10.1111/j.1096-3642.2009.00597.x

ADDITIONAL KEYWORDS: Bugti Hills – Chitarwata Formation – cladistics – Indian subcontinent – *Mesaceratherium* – palaeobiogeography – Perissodactyla – *Pleuroceros* – Zinda Pir.

*Corresponding author. E-mail: poa@lmtg.obs-mip.fr

INTRODUCTION

The Tertiary deposits of the Bugti Hills (Balochistan, Pakistan; Fig. 1) have yielded innumerable fossil vertebrates, amongst which rhinocerotoids are particularly abundant and diversified. Despite the high productivity of fossil vertebrates, most of the recorded fossils were studied around a century ago (Blanford, 1876, 1879; Lydekker, 1881, 1884, 1886; Pilgrim, 1910, 1912; Forster-Cooper, 1924, 1934). Amongst Bugti Hills Rhinocerotidae, '*Aceratherium*' *blanfordi* Lydekker, 1884 is widely represented in original, classic collections (Natural History Museum, London; Indian Museum, Calcutta). Lydekker (1884: 2) named '*Aceratherium blanfordi*, n. sp., *nobis*' (his nomenclature) on the basis of a P4–M2 series from the 'Siwaliks of Punjab', which was originally referred to *Rhinoceros palaeindicus* by Lydekker (1881), and a few dental remains originating from the Bugti Hills area (Dera Bugti and Gandoi localities). Lydekker (1884: 2–11) split its hypodigm into two classes, including a 'larger race' and a 'smaller race'. Later, Pilgrim (1910: 66) proposed restriction of the species *A. blanfordi* Lydekker, 1884 to the hypodigm of the

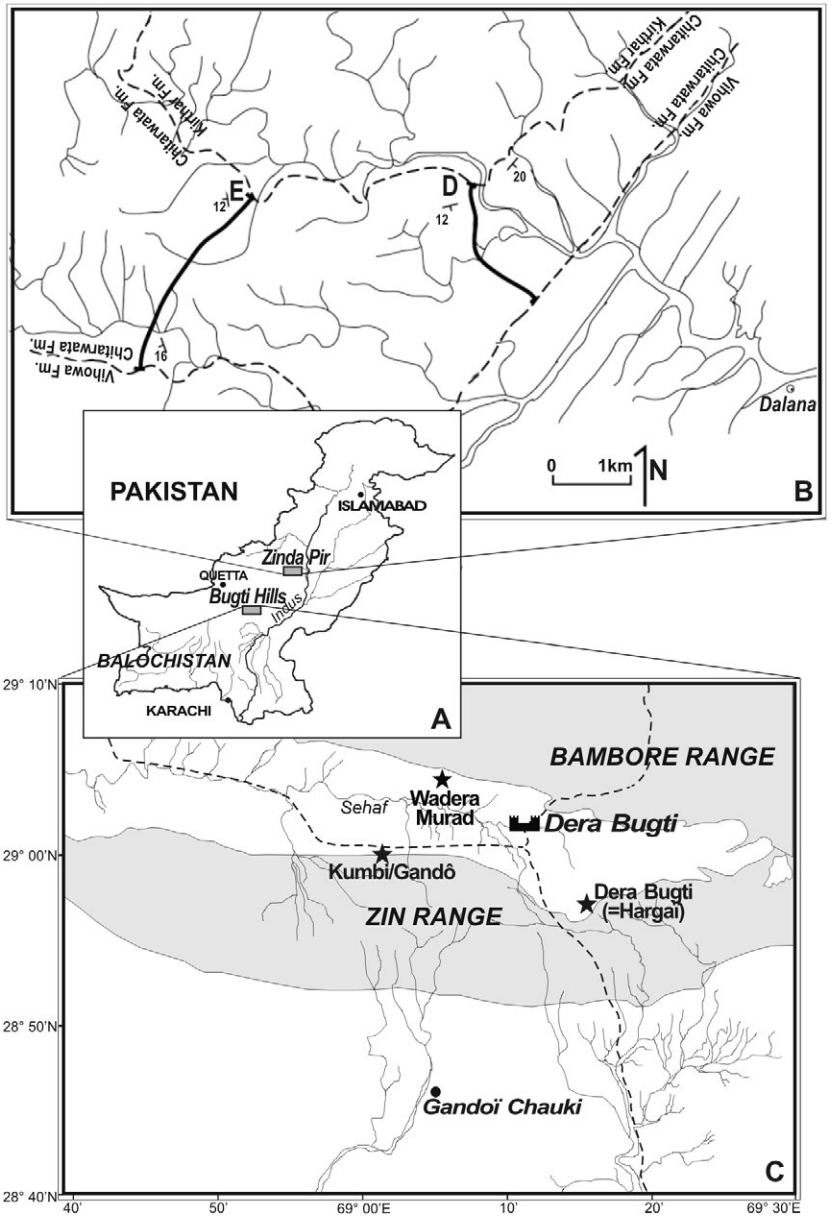

Figure 1. A, Index map of south-western Pakistan, showing the location of the main areas discussed in the text; B, enlargement of the Zinda Pir Dome area; C, enlargement of the Bugti area, with detailed location of mentioned localities.

larger series, via the awkward '*A. blanfordi* var. *majus* (probably a *Teleoceras*)'. This author then erected the new species '*Diceratherium naricum* Pilgrim, 1910' on the base of '*A. blanfordi* var. *minus* Lydekker (1884)'. In recent works (Antoine & Welcomme, 2000; Antoine *et al.*, 2003a; Antoine, Duranthon & Welcomme, 2003b; Métais *et al.*, 2009) the latter species was excluded from the waste-basket taxon *Diceratherium* Marsh, 1875 and referred to the genus *Plesiaceratherium* Young, 1937, owing to new interpretations of better fossil collections. However, the splitting proposed by Pilgrim (1910) did not clarify the affinities of the larger form, '*A. blanfordi*' *sensu stricto*, nor did it stabilize its generic assignment. In fact, this species was successively referred to *Teleoceras* Hatcher, 1894 by Pilgrim (1912), to *Chilotherium* Ringström, 1924 by Ringström (1924), Matthew (1929), and Forster-Cooper (1934), to *Aceratherium* Kaup, 1832 by Heissig (1972), to *Aprotodon* Forster-Cooper, 1915 by Welcomme *et al.* (1997), and to *Rhinoceros* von Linnaeus, 1758 by Downing (2005).

Recent fieldwork campaigns in the same area by a French–Balochi team (*Mission Paléontologique Franco-Balouche*, 1995–2004) led to the recovery of hundreds of new cranial, dental, and postcranial remains referred to hyracodontids, amynodontids, and rhinocerotids in a stratigraphically controlled context (Welcomme *et al.*, 1997, 1999, 2001; Antoine & Welcomme, 2000; Antoine *et al.*, 2003a, b, 2004; Métais *et al.*, 2009). As previously argued by Welcomme & Ginsburg (1997), the new stratigraphical framework in the field proved that the so-called 'Bugti fauna' was a set of distinct faunas from successive levels in this rock unit, ranging from the Early Oligocene up to the Late Miocene (Welcomme *et al.*, 1999, 2001; Antoine *et al.*, 2003b; Métais *et al.*, 2009). Thanks to these new findings, postcranials were for the first time attributed to '*A.*' *blanfordi* with confidence, some of them being recovered in association with both cranial and dental remains. Further comparison of these specimens has revealed wide morphological and metrical discrepancies, especially in the postcranial skeleton: the largest teeth (with thick enamel) are always associated with long and slender limb bones, whereas the smallest teeth (with thinner enamel) occur with somewhat shorter and more robust limbs. Comparison with the previously described specimens (including types), stored in the Natural History Museum, London, and with new material from the upper member of the Chitarwata Formation (Fm.) in the Zinda Pir (Downing, 2005; Lindsay *et al.*, 2005) confirms such a mismatch, and reveals that '*A.*' *blanfordi* is most probably a chimera, including two dentally convergent but postcranially distinct taxa that we describe and compare in this paper.

MATERIAL AND METHODS

Stratigraphical context

In the Bugti Hills, the outcrops usually extend over dozens of kilometres, so that several loci may document each fossiliferous level. For instance, different localities within Level 4 (earliest Miocene; Fig. 2) bear the name of the nearest spring or village (Dera Bugti, Kumbi, Gandô), associated with the number 4. As such, Dera Bugti 4, Kumbi 4a, Kumbi 4f, and Gandô 4 are laterally equivalent and considered as coeval. The same principle is applied for other levels or loci located in the Dera Bugti syncline (from 0 up to 7). Correlations get more complicated when considering coeval loci situated in the Gandoï Chauki syncline, i.e. south to the Zin Koh anticline (Fig. 1). In this area, the levels are also sorted chronostratigraphically, but they are labelled with letters rather than with numbers. Hypotheses of stratigraphical equivalences are summarized in Figure 2.

The fossiliferous levels document a long time range, spanning the Oligocene epoch and most of the Miocene times (Antoine *et al.*, 2003b). The lowest levels [Level 0 (= 0) to Level 3 (= J2)] correspond to Oligocene deltaic then fluvial deposits referred to the Bugti Member of the Chitarwata Fm. (Métais *et al.*, 2009); upper in the series, the levels 3bis (= M) and 4 (= Q) consist of river-lacustrine deposits attributed to the upper Member of the Chitarwata Fm., and referred to the earliest Miocene (Welcomme *et al.*, 2001; Antoine *et al.*, 2003a, b, 2004); overlying fossiliferous strata are Levels 5 (= T), 6, and 6sup (Welcomme *et al.*, 2001; Métais *et al.*, 2009) from the lowest deposits referred to the Vihowa Fm. (late Early Miocene), and considered as coeval to the Kamlial Fm. from the Potwar Plateau series (Welcomme *et al.*, 1997, 2001; Barry *et al.*, 2002; Lindsay *et al.*, 2005; Métais *et al.*, 2009). Much higher in the series another rhino-bearing locality is referred to as Sartaaf (= Djigani, Level 7), the mammal fauna of which indicates a Late Miocene age, equivalent to the Dhok Pathan Fm. of the Potwar Plateau (Antoine *et al.*, 2003b).

The new Bugti specimens mainly originate from localities referred to the upper member of the Chitarwata Fm. (level 4, earliest Miocene; Fig. 2); a few other were unearthed in the base of the overlying Vihowa Fm. (levels 5–6sup, Early Miocene; Fig. 2).

The specimens unearthed in the Zinda Pir area and described herein were recovered in distinct levels of sections D and E, in the Dalana area (Fig. 1; Lindsay *et al.*, 2005: fig. 3). They occur throughout the upper member of the Chitarwata Fm., which is tentatively parallelized with the Agenian European Land Mammal Age (Fig. 2; Downing, 2005; Lindsay *et al.*, 2005; Métais *et al.*, 2009). This period roughly

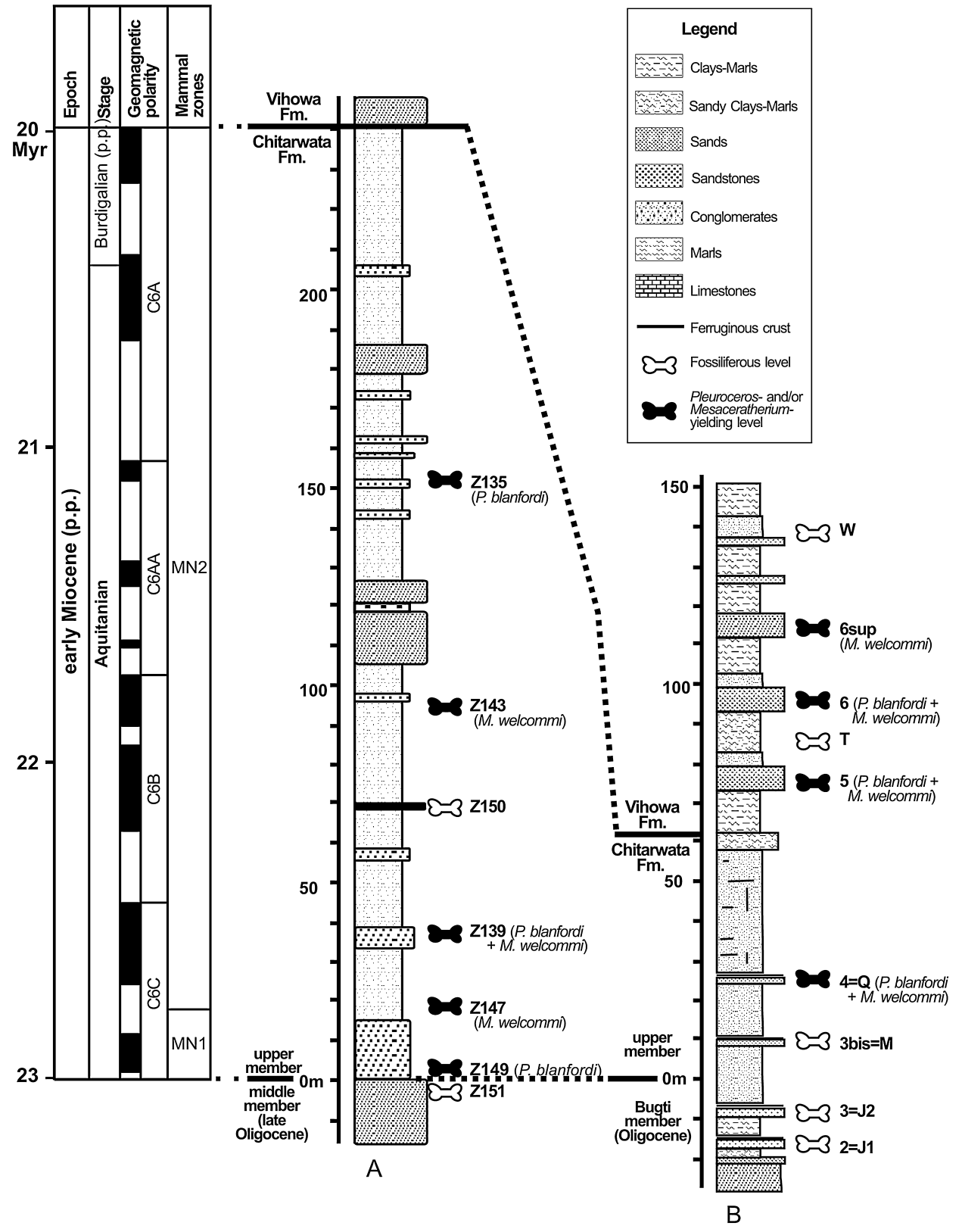
Epoch
Stage
Geomagnetic polarity
Mammal zones
20 Myr
21
22
23
early Miocene (p.p.)
Aquitanian
Burdigalian (p.p.)
C6A
C6AA
C6B
C6C
MN2
MN1
Legend
Clays-Marls
Sandy Clays-Marls
Sands
Sandstones
Conglomerates
Marls
Limestones
Ferruginous crust
Fossiliferous level
Pleuroceros- and/or Mesaceratherium-yielding level
Vihowa Fm.
Chitarwata Fm.
200
150
100
50
0m
Z135 (P. blanfordi)
Z143 (M. welcommi)
Z150
Z139 (P. blanfordi + M. welcommi)
Z147 (M. welcommi)
Z149 (P. blanfordi)
Z151
upper member
middle member (late Oligocene)
A
W
6sup (M. welcommi)
6 (P. blanfordi + M. welcommi)
T
5 (P. blanfordi + M. welcommi)
4=Q (P. blanfordi + M. welcommi)
3bis=M
3=J2
2=J1
upper member
Bugti member (Oligocene)
B

Figure 2. Synthetic stratigraphical sections and ranges of the rhinocerotids discussed in the text, in the Zinda Pir area (A) and the Bugti area (B). (A) is a composite section of the upper member of the Chitarwata Fm. based on sections D and E of Downing (2005: fig. 1) and Lindsay *et al.* (2005: fig. 3). (B) is modified from Welcomme *et al.* (2001), Antoine *et al.* (2003b, 2004) and Métais *et al.* (2009). Filled bone symbols indicate *Pleuroceros*- and/or *Mesaceratherium*-yielding levels whereas open bone symbols represent other fossiliferous levels. The upper member of the Chitarwata Formation corresponds to the classic 'Dera Bugti Fauna', which is correlated to the earliest Miocene (Aquitanian stage) based on fossil assemblages from levels 3bis-M and 4-Q. Comparisons between the Bugti faunas and biochronologic data from the Dalana area sections at Zinda Pir suggest that the best correlation is consistent with 'correlation B' of Lindsay *et al.* (2005: fig. 6B), which was also taken into account by Métais *et al.* (2009). Correlation of the Bugti and Zinda Pir faunas with standard European Neogene Mammal Zones (Steininger, 1999; Gradstein *et al.*, 2005) and with the Global Polarity Time Scale (Gradstein *et al.*, 2005; Lindsay *et al.*, 2005) is tentative and mostly based on rodent and perissodactyl assemblages.

corresponds to the Aquitanian stage (*c.* 23–20 Myr; Gradstein, Ogg & Smith, 2005). The available sample from the Zinda Pir (12 specimens) is much smaller than the one from the Bugtis, which may explain the shorter range observed in the former area.

The biochronological framework as it appears in Figure 2 is based on the geological time scale revised in 2004 (Gradstein *et al.*, 2005), whereas lithostratigraphical and magnetostratigraphical correlations between the Zinda Pir and Bugti areas follow 'interpretation B' of Lindsay *et al.* (2005: fig. 6) and the conclusions of Métais *et al.* (2009).

Field sampling: cranial/dental/postcranial associations

Most specimens were recovered isolated in the Dera Bugti and Zinda Pir areas. Thus postcranials had scarcely been identified in the past (Pilgrim, 1912; Forster-Cooper, 1934). Yet, recent collects in the Dera Bugti area have revealed several series associating cranial and dental and/or dental and postcranial remains: as an example, the association between the upper and lower dentitions has been established owing to the series Pak 1031, which includes both dentitions from the same individual. On account of the high specific diversity, we have classified the postcranial specimens after their dimensions, proportions, and morphology (structures, facets, and muscular insertions). A supplemental control was made owing to 'bone-to-bone' connections and associations.

Material for comparison

The fossils were further associated and determined by direct comparison with reference series: the 'historical' specimens from the Bugti Hills (Falconer & Cautley collection; Forster-Cooper collection; casts of the Pilgrim collection) stored in the Natural History Museum, London; the Early and Middle Miocene rhinocerotid faunas from the Aquitaine Basin, stored in the Muséum d'Histoire Naturelle, Toulouse (Antoine, Duranthon & Tassy, 1997) and in the Natural History Museum, London; the Oligocene and Early Miocene rhinocerotid faunas from western Europe stored in Lyon (Muséum d'Histoire naturelle; Laboratoire de Paléontologie, Claude-Bernard University) and Paris (Muséum National d'Histoire Naturelle); the Oligocene and Miocene rhinocerotids from Asia and North America stored in the American Museum of Natural History (New York); and the Late Oligocene and earliest Miocene rhinocerotids from Gannat, France (Rhinopolis).

Descriptions of rhinocerotids from the Miocene of Africa (Hooijer, 1966, 1971, 1973), Pakistan (Lydekker, 1881, 1884; Pilgrim, 1910, 1912; Heissig, 1972), Anatolia (Heissig, 1976), Arabia (Gentry, 1987), western Europe (Osborn, 1900; Guérin, 1980), and south-western France (de Bonis, 1973; Antoine *et al.*, 2006) provided further useful comparisons.

The specimens stored in the Natural History Museum (London) originate from the Cambridge-Sedgwick Museum Expeditions in the Bugti area, headed by Forster-Cooper in 1910–1911. Their labels generally mention only 'Near Dera Bugti', so it is impossible to determine the precise level(s) from which they were collected.

New specimens from the Dera Bugti area were collected by the French Paleontological Expeditions in Balochistan in 1995–1999. They are currently housed in the Muséum d'Histoire Naturelle in Toulouse, France.

Specimens originating from the Chitarwata Fm. in the vicinity of Dalana, in the Zinda Pir Dome, have their permanent repository in the Pakistan Museum of Natural History. Some of them are temporarily deposited in the Department of Anthropology and Peabody Museum (Harvard University, Cambridge, USA).

Anatomical terminology and phylogenetic characters

Capital letters are used for the upper teeth (I, incisor; C, canine; D, deciduous molar; P, premolar; M, molar), whereas lower case letters indicate lower teeth (i, c, d,

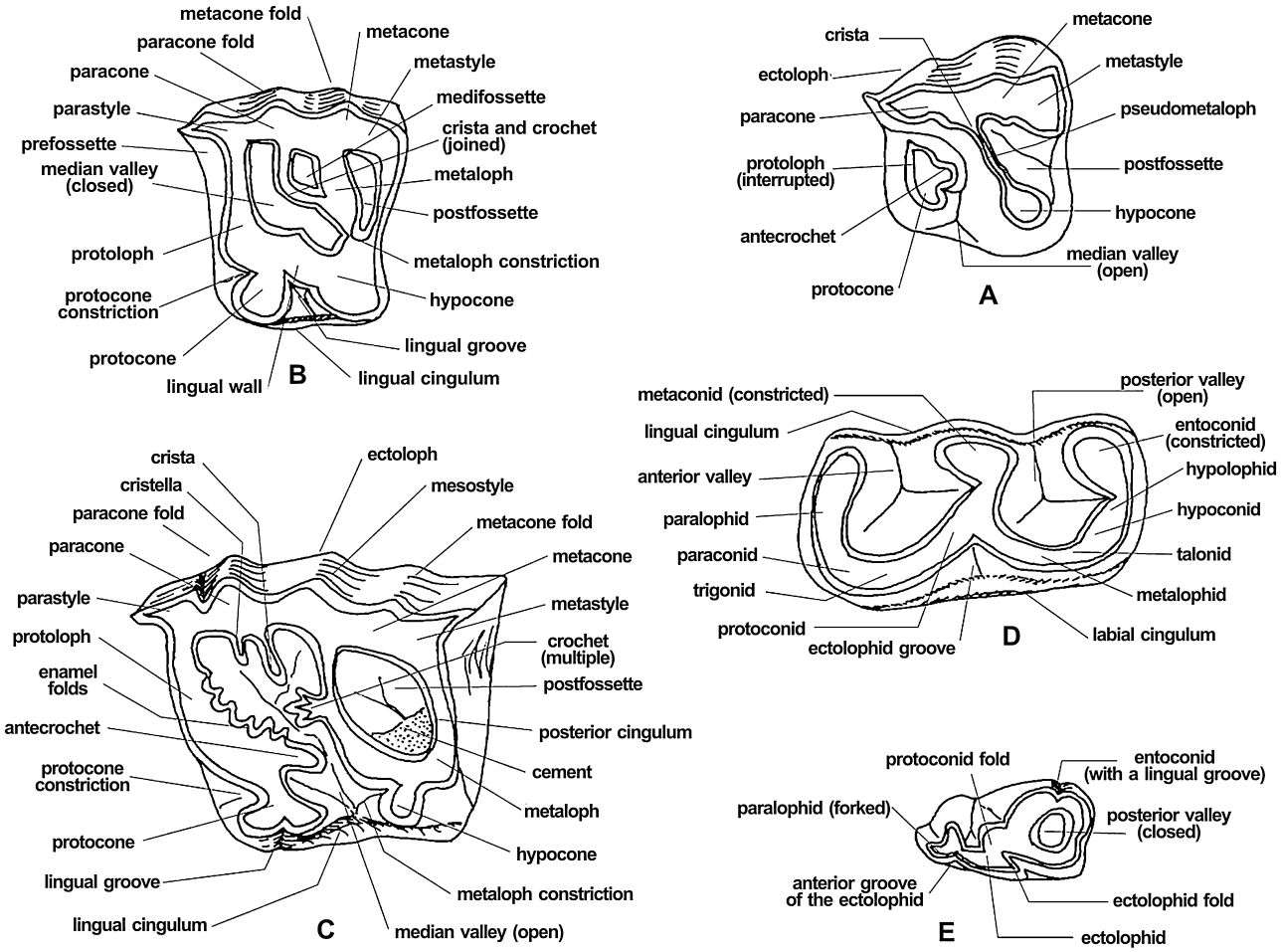

Figure 3. Dental terminology used for rhinocerotids. A, left P2 (hypothetical); B, left P3 or P4 (hypothetical); C, left upper molar (hypothetical); D, left lower molar (hypothetical); E, left d2. Modified from Antoine (2002, fig. 72).

p, m, respectively). Except when mentioned, the dimensions are given in mm.

Rhinocerotid dental terminology follows Heissig (1969: 11–12), Uhlig (1999: 15–16), and Antoine (2002: 122), as summarized in Figure 3; osteological and dental features described correspond basically to cladistic characters used and listed by Antoine (2002, 2003) and Antoine *et al.* (2003b). Postcranial dimensions follow the protocol defined by Guérin (1980).

Abbreviations

Anatomical orientation

ant, anterior; post, posterior; l, left; r, right; APD, anteroposterior diameter; H, height; L, length; TD, transversal diameter; W, width.

Institutions

BSP, Bayerische Staatssammlung für Paläontologie, Munich; IMC, Indian Museum, Calcutta; MHNT, Muséum d'Histoire naturelle, Toulouse; MNHN, Muséum National d'Histoire Naturelle, Paris; NHM, The Natural History Museum, London; PMNH, Pakistan Museum of Natural History, Islamabad.

Localities

DB, Dera Bugti; G, Gandô; K, Kumbi.

Taxa

P. b., *Pleuroceros blanfordi*; *M. w.*, *Mesaceratherium welcommi*.

SYSTEMATIC PALAEONTOLOGY

The suprageneric systematics within Rhinocerotidae follows the arrangement of the current phylogenetic analysis (see Phylogenetic relationships).

ORDER PERISSODACTYLA OWEN, 1848
SUPERFAMILY RHINOCEROTOIDEA GRAY, 1821
FAMILY RHINOCEROTIDAE GRAY, 1821
SUBFAMILY RHINOCEROTINAE GRAY, 1821
UNNAMED CLADE
PLEUROCEROS ROGER, 1898

Emended diagnosis: Short-limbed rhinocerotine with a concave occipital crest in dorsal view, a nearly horizontal mandibular symphysis, a reduced lingual cingulum on upper premolars, a strong antecrochet on P4, a protocone deeply constricted and a low and reduced posterior cingulum on M1–2, a smooth and U-shaped external groove on lower cheek teeth, a continuous lingual cingulum on lower premolars, a tridactyl manus (vestigial metacarpal V), a prominent insertion of the m. extensor carpalis on metacarpals, a slender tuber calcanei, and a short insertion of the m. interossei on lateral metapodials.

Type species: Pleuroceros pleuroceros (Duvernoy, 1853)

PLEUROCEROS BLANFORDI (LYDEKKER, 1884) **COMB. NOV.** (FIGS 4–7, 11A, 12A)

Rhinoceros palaeindicus Lydekker, 1881: 44–45; pl. 6, fig. 1
Aceratherium blanfordi sp. nov., *nobis* Lydekker, 1884: 2–11, text-fig. 2; pl. 2, figs 1–3
Aceratherium blanfordi var. *majus* Lydekker, 1884: 10; pl. 1, 1–2
Rhinoceros blanfordi var. *majus* Lydekker, 1886: 154
Aceratherium blanfordi Lyd. Pilgrim, 1908: 149
Aceratherium blanfordi var. *majus* Pilgrim, 1910: 66
Teleoceras blanfordi Lydekker Pilgrim, 1912: 3, 30–32, pl. 7, figs 4–7
Chilotherium blanfordi Ringström, 1924: 75
Chilotherium blanfordi Matthew, 1929: 508
Chilotherium blandfordi Forster-Cooper, 1934: 589–594; text-fig. 9, 12C; pl. 67, figs 34–38
« *Dicerorhinus* » cf. *abeli* (partim) Welcomme *et al.*, 1997: 532, 535
? « *Dicerorhinus* » cf. *abeli* (partim) Welcomme *et al.*, 1997: 534, 535, 536
Aprotodon blanfordi Welcomme & Ginsburg, 1997: 1001, table
Pleuroceros blanfordi Lindsay *et al.*, 2005: table 1
'*Aprotodon*' *blanfordi* Métais *et al.* 2009: 163, 164; table 2, fig. 5

Emended diagnosis: Differs from *P. pleuroceros* by its larger size (*c.* 15%), the presence of a posterior horizontal groove on the processus zygomaticus of the squamosal, the absence of a sagittal lingual groove on the corpus mandibulare, a shortened premolar series, higher tooth crowns, the abundance of coronary cement, a weaker labial cingulum, a multiple crochet always present, an unconstricted metaloph, a continuous lingual cingulum, and a thick lingual bridge on upper premolars, a transverse metaloph and a reduced protocone on P2, and the usually constricted protocone on P3–4, the absence of a crista on P3, the unconstricted metaloph on P4, the usual presence of a lingual cingulum (occasional in *P. pleuroceros*) on upper molars, a deep protocone constriction and the presence of a metacone fold on M1–2, a strong mesostyle on M2, a constricted metaconid on lower deciduous teeth, the absence of a posterior McIII-facet on McII, the absence of a fibula-facet on the calcaneus, and the concave proximal border of MtIII.

Lectotype: Right P4–M2 series unearthed in Gandoï, Bugti Hills (IMC C. 268) and figured by Lydekker (1884: pl. 1, fig. 1), proposed as a lectotype by Pilgrim (1912: 31).

Type locality: Gandoï, Bugti Hills, Pakistan (Early Miocene?).

Stratigraphical range: Chitarwata Fm. (Bugti and Zinda Pir areas) and base of the Vihowa Fm. (Bugti area). Early Miocene (*c.* 23–18.5 Myr; Lindsay *et al.*, 2005; Métais *et al.*, 2009).

Geographical range: Bugti and Zinda Pir area, Sulaiman Lobe, Balochistan, Pakistan.

Referred material
Old collections: 'Siwaliks of the Punjab' [?Early Miocene]. Left maxilla with P4–M2 IMC-without number; Gandoi [?Early Miocene, Bugti Hills]. Right mandible with p3–m1 and m2–3 salient (IMC C. 271); left M2 (IMC C. 259); right M1 or M2, worn (IMC C. 262); part of a right juvenile mandible, with d3 (IMC C. 267). Dera Bugti [?Early Miocene]. Part of left maxilla with M1–3 (IMC C. 268). 'Gaj of the Bugti Hills' [?Early Miocene]. M1–3 (IMC C. 266). 'Near Dera Bugti' [locality and age unknown]. Germ of a left P2 (NHM M 15335); left P2 and P3 from the same individual (NHM M without number [w.n.]); left P3 and P4 from the same individual (NHM M w.n.); fragment of a right maxilla with D2–4 and M1 (NHM M 15367) and germ of P3 extracted from the maxilla (NHM M 15368); right P2 (NHM M 15337); right P3 (NHM M 15338); left P3 and P4 from the same individual (NHM M 15333); right P3 and P4 from the

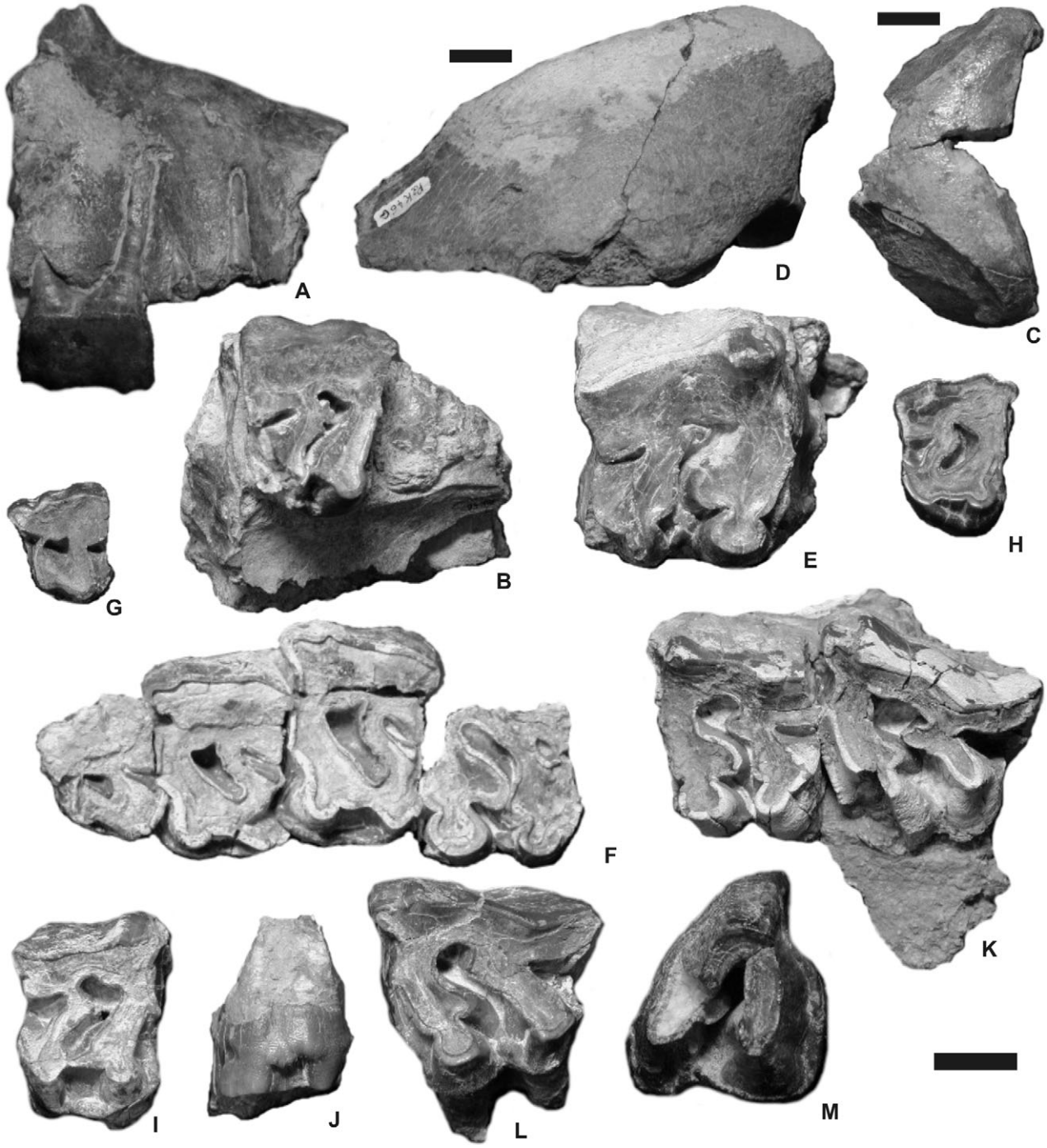

Figure 4. *Pleuroceros blanfordi* (Lydekker, 1884) from the Early Miocene of the Bugti Hills, Balochistan, Pakistan: cranial material and upper teeth. A, right fragmentary maxilla with P3 (MHNT Pak 46), lateral view. B, same, occlusal view; C, occipital crest (MHNT Pak 46A), dorsal view; D, left zygomatic arch and squamosal (MHNT Pak 46G), lateral view; E, right M1 (MHNT Pak 46D), occlusal view. The specimens illustrated in A–E belong to a single skull, from Kumbi 4a. F, left P2–M1 series (MHNT Pak 1031), occlusal view. Kumbi 4a; G, left P2 (MHNT Pak 751), occlusal view. Kumbi 4b; H, right P3 (MHNT Pak 1024), occlusal view. Kumbi 4a; I, right P4 (MHNT Pak 1046), occlusal view. Kumbi 4a; J, same, lingual view; K, left M1–M2 series (MHNT Pak 1022), occlusal view. Kumbi 4c; L, left M2 (MHNT Pak w/n), occlusal view; M, right M3 (MHNT Pak 918), occlusal view. Kumbi 4b. Scale bars = 2 cm.

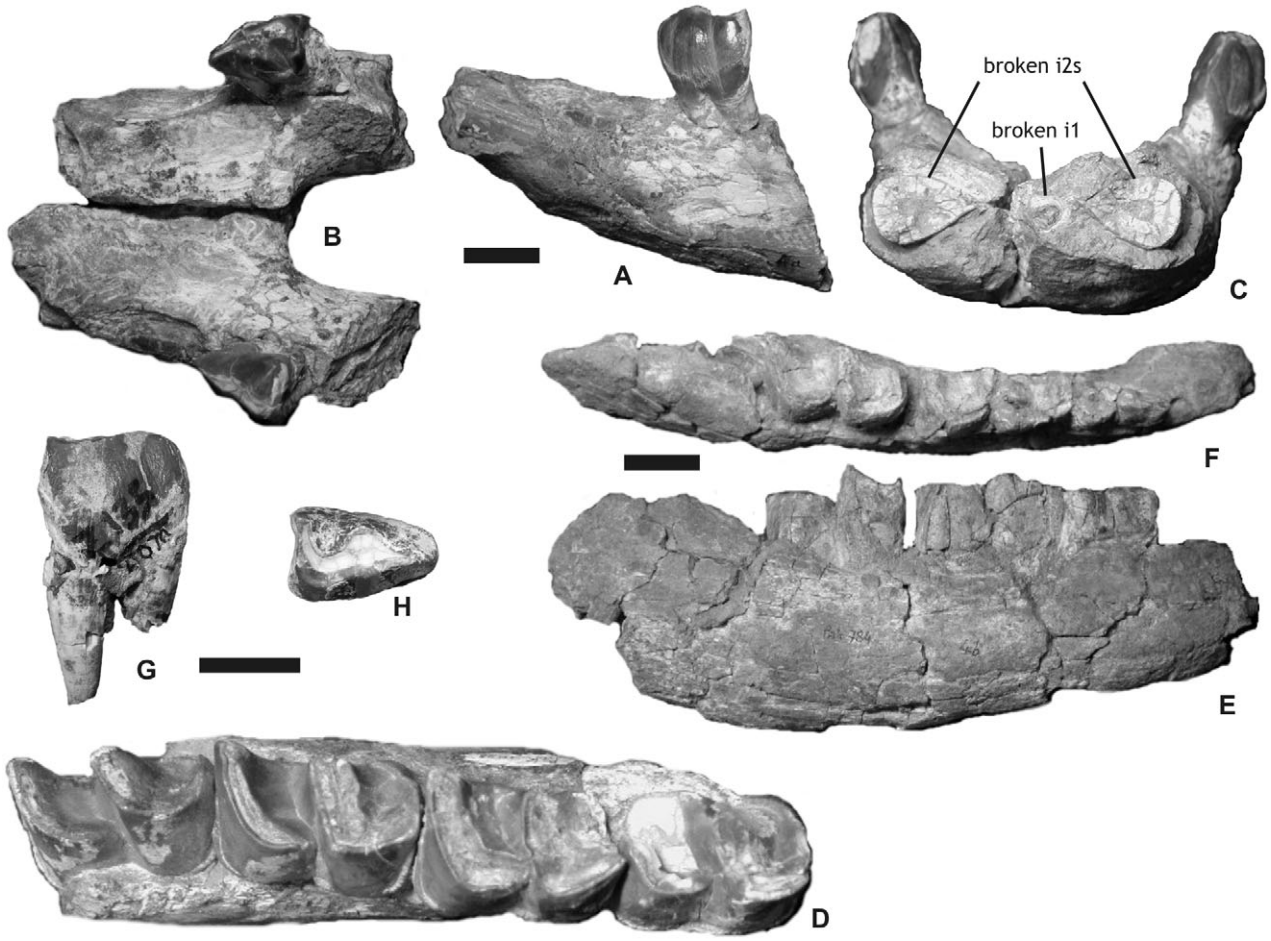

Figure 5. *Pleuroceros blanfordi* (Lydekker, 1884) from the Early Miocene of the Bugti Hills, Balochistan and of the Zinda Pir dome, Sind, Pakistan: mandibular material and lower teeth. A, mandibular symphysis with left and right p2 and alveoli of i2 (MHNT Pak 1038), lateral view; B, same, occlusal view. C, same, anterior view; D, right p4–m3 series from the same mandible, occlusal view. Kumbi 4a; E, right juvenile mandible with d2–d4 (MHNT Pak 784), lateral view. Kumbi 4b; F, same, occlusal view; G, right p2 (PMNH Z2070), lateral view. Z135 locus, Zinda Pir; H, same, occlusal view. Scale bars = 2 cm.

same individual (NHM M 15366); palate with left P2–M3 and right M1–2 (NHM M 15365).

New material

Bugti Hills (Figs 1, 2)

Kumbi 4a (Level 4, earliest Miocene). Mandible from a young adult, in three parts: left corpus with p4–m1, right corpus with p4–m3 and symphysis bearing left i1 and left and right i2, all of them broken (MHNT Pak 1038); fragment of a left mandible with p2 (broken) and p3 (MHNT Pak 1037); fragment of an toothless symphysis (MHNT Pak 1073); fragment of a right mandible with m3 (MHNT Pak 1068); fragment of a left maxilla with P2–P4, M1 without ectoloph and fragments of i2 and right p2 from the same individual (MHNT Pak 1031); right P3 (MHNT Pak 1024); right P3 (MHNT Pak 1059); left P4 (MHNT Pak 1058); right P4 d (MHNT Pak 1046); right P4 without ectoloph (MHNT Pak 1050); fragment of a left maxilla with M1–2 (MHNT Pak 1022), from the same individual as a right M2 (MHNT Pak 1019); right M1 (MHNT Pak 1061); fragment of a right M1 on a maxilla (MHNT Pak 1035); lingual fragment of a right M1 (MHNT Pak 1064); left crushed M2 (MHNT Pak 1045); lingual fragment of a right M2 (MHNT Pak 1027); left M3 (MHNT Pak 1013); right M3 (MHNT Pak 1014); rostral fragment of a left i2 (MHNT Pak 1021); lingual fragment of a right p3 (MHNT Pak w. n.); posterior fragment of a right m3 (MHNT Pak 1020); fragment of a humeral distal end (MHNT Pak 1085); fragment of a left humeral distal end (Pal 1198); proximal end of a left radius (MHNT Pak 1088); proximal end of a right radius (MHNT Pak 1087); proximal end of a right

Figure 6. *Pleuroceros blanfordi* (Lydekker, 1884) from the Early Miocene of the Bugti Hills, Balochistan, Pakistan: Forelimb remains. A, right radius, proximal end (MHNT Pak 1089), anterior view. Kumbi 4a; B, right radius, distal end (MHNT Pak 1090), anterior view. Kumbi 4a; C, right scaphoid (MHNT Pak 785), anteromedial view. Kumbi 4b; D, right scaphoid (MHNT Pak 1098), posterolateral view. Kumbi 4a; E, right semilunate (MHNT Pak 1101), anterior view. Kumbi 4a; F, same, lateral view; G, right trapezoid (MHNT Pak 787), dorsal view. Kumbi 4b; H, left magnum (MHNT Pak 1110), anterior view. Kumbi 4a; I, same, lateral view; J, right unciform (MHNT Pak 1114), anterior view. Kumbi 4a; K, left unciform (MHNT Pak 1112), dorsal view. Kumbi 4a; L, left McII (MHNT Pak 1733), anterior view. Kumbi 4f; M, same, lateral view; N, left McIII (MHNT Pak 1121), anterior view. Kumbi 4a; O, same, lateral view; P, same, dorsal view; Q, right McIII, distal end (MHNT Pak 1193), anterior view. Kumbi 4a. Scale bars = 2 cm.

radius (MHNT Pak 1089); distal end of a left radius (MHNT Pak 1091); distal end of a right radius (MHNT Pak 1090); distal end of a right radius (MHNT Pak 1206); right scaphoid (MHNT Pak 1098); right semilunate (MHNT Pak 1101); left magnum (MHNT Pak 1110); right magnum (MHNT Pak 1093); left unciform (MHNT Pak 1112); right unciform (MHNT Pak 1094); right unciform (MHNT Pak 1113); right unciform without posterior tuberosity (MHNT Pak 1114); proximal end of a left McIII (MHNT Pak

1118); proximal end of a left McIII (MHNT Pak 1119); proximal end of a left McIII (MHNT Pak 1120); left McIII (MHNT Pak 1121); right Mc III without distal end (MHNT Pak 1117); distal end of a right Mc III (MHNT Pak 1193); left patella (MHNT Pak 1131); left patella (MHNT Pak 1132); distal end of a left tibia (MHNT Pak 1124); distal end of a left tibia (MHNT Pak 1126); distal end of a right tibia (MHNT Pak 1127); distal end of a right tibia (MHNT Pak 1128); distal end of a right fibula (MHNT Pak 1129); left astragalus (MHNT Pak 1137); left astragalus (MHNT Pak 1138); left astragalus (MHNT Pak 1139); medial fragment of a left astragalus (MHNT Pak 1143); right astragalus (MHNT Pak 1140); right astragalus (MHNT Pak 1141); right tuber calcanei (MHNT Pak 1104); right calcaneus (MHNT Pak 1150; right calcaneus (MHNT Pak 1151); right calcaneus (MHNT Pak 1152); left navicular (MHNT Pak 1154); posterior fragment of a left navicular (MHNT Pak 1156); right cuboid (MHNT Pak 1158); right cuboid (MHNT Pak 1159); right ectocuneiform (MHNT Pak 1160); fragment of a left ectocuneiform (MHNT Pak 1161); right mesocuneiform (MHNT Pak 1590); proximal end of a left MtII (MHNT Pak 1163); distal end of a left MtII (MHNT Pak 1191); right MtII (MHNT Pak 1162); proximal end of a right MtIII (MHNT Pak 1096); distal end of a right MtIII (MHNT Pak 1192); distal end of a right MtIII (MHNT Pak 1194); right MtIII without proximal end (MHNT Pak 1195); distal end of a right MtIV (MHNT Pak 1097); right Mt IV (MHNT Pak 1165); proximal end of a right MtIV (MHNT Pak 1166); proximal end of a right MtIV (MHNT Pak 1167).

Kumbi 4b (Level 4, earliest Miocene). Fragment of an eroded right mandible with erupting m3 (MHNT Pak 772); right juvenile mandible with d2–4, m1 in the dentary and alveolus of d1 (MHNT Pak 784); left P2 (MHNT Pak 751); right P2 (MHNT Pak 844); left P3 without an ectoloph (MHNT Pak 842); right P3 without an ectoloph (MHNT Pak 758); fragment of a left M2 (MHNT Pak 760); fragment of a protoloph of left M3 (MHNT Pak 761); left M3 without a protoloph (MHNT Pak 763); right M3 (MHNT Pak 918); slightly worn left m3 (MHNT Pak 917); fragment of a left m3 (MHNT Pak 774); right scaphoid (MHNT Pak 785), fragment of a right semilunate (MHNT Pak 786) and right trapezoid (MHNT Pak 787) probably from the same individual; distal end of a left McII (MHNT Pak 789); distal end of a left MtII (MHNT Pak 790).

Kumbi 4c (Level 4, earliest Miocene). Right P2 (MHNT Pak 844); left P3 without an ectoloph (MHNT Pak 845); left M2 (MHNT Pak w. n.); left damaged patella (MHNT Pak 86); distal end of a right tibia (MHNT Pak 71).

Kumbi 4d (Level 4, earliest Miocene). Fragmentary skull with left and right squamosals (processus zygomaticus), left postglenoid apophysis, occipital, left and right maxilla bearing P3, right M1 and the alveoli of right P1–2, fragments of right M2–3 and undetermined fragments (MHNT Pak 46).

Kumbi 4f (Level 4, earliest Miocene). fragment of a right M3 (MHNT Pak 1676); proximal end of a left McII (MHNT Pak 1733); right patella (MHNT Pak 1687).

Gandô 4 (Level 4, earliest Miocene). Fragment of a right M3 (MHNT Pak 1864); left p3 (MHNT Pak 1862).

Dera Bugti 4 (Level 4, earliest Miocene). Fragment of a left P4 (MHNT Pak 1967); right P4 (MHNT Pak 1964).

Dera Bugti 5 (Level 5, Early Miocene). Posterolingual fragment of a left M2 (MHNT Pak 1258).

Dera Bugti 6 (Level 6, Early Miocene). left M2 g (MHNT Pak 1012a); lingual fragment of a right M3 (MHNT Pak 1444); lingual fragment of a left m1 (MHNT Pak 2215); damaged right astragalus (MHNT Pak 2235).

Wadera Murad (Early Miocene, northern side of the Dera Bugti syncline). Fragment of a left P4 (MHNT Pak 2458).

Zinda Pir Dome (Fig. 1)

Z149 (earliest Miocene). Left astragalus (PMNH Z2043); Z139 (earliest Miocene). Right fragmentary astragalus (PMNH Z2047). Z135 (earliest Miocene). Right p2 (PMNH Z2070).

Cranial material: The adult skull MHNT Pak 46 is fragmentary. The occipital, fragments of maxillae, squamosals (processus zygomaticus), and a postglenoid apophysis are preserved (Fig. 4A–D). The palate NHM M 15365 shows identical features. The foramen infraorbitalis was located above P4 and the nasal incisure above the middle of P3. The anterior border of the orbit is above M1. The zygomatic arch was high and thick (Fig. 4D). No processus postorbitalis is present on the dorsal border of the processus zygomaticus of the squamosal. The squamosal–jugal suture is smooth and regular. The caudal border of the processus zygomaticus is depressed by a transverse gutter-like groove (Fig. 4D). The articular tubercle is salient and regularly convex. The postglenoid apophysis, straight in anterior view, has a triangular cross-section, with a convex articular surface. The nuchal tubercle is prominent. The caudal border of the occipital crest is slightly concave. The frontoparietal crests converge rostrally, but their junction cannot be observed on this fragmentary specimen. The dorsal half of the occipital side is depressed. The dorsal side of the skull was narrow: the occipital crest is about 100 mm wide. The junction between the nuchal and temporal crests was very close to the auditory pseudomeatus. The foramen magnum is

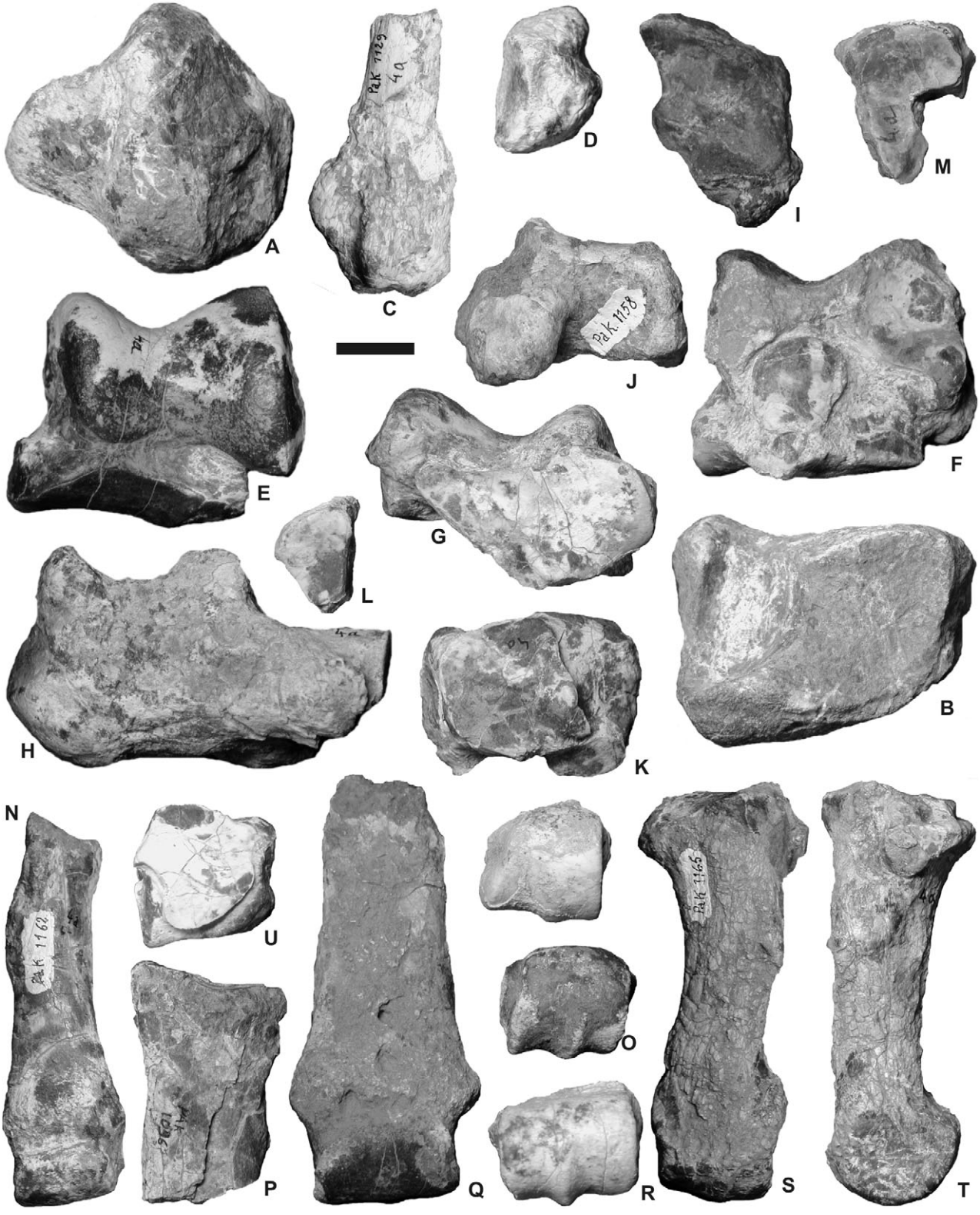
A
C
D
I
M
J
E
F
G
L
H
K
B
N
U
P
Q
O
R
S
T

Figure 7. *Pleuroceros blanfordi* (Lydekker, 1884) from the Early Miocene of the Bugti Hills, Balochistan, Pakistan: Hind limb remains. A, left patella (MHNT Pak 1132), anterior view; B, left tibia, distal end (MHNT Pak 1124), distal view; C, right fibula, distal end (MHNT Pak 1129), lateral view; D, same, distal view; E, left astragalus (MHNT Pak 1140), anterior view; F, right astragalus (MHNT Pak 1138), posterior view; G, same, distal view; H, right calcaneus (MHNT Pak 1150), lateral view; I, left navicular (MHNT Pak 1154), dorsal view; J, right cuboid (MHNT Pak 1158), lateral view; K, right cuboid (MHNT Pak 1159), dorsal view; L, right mesocuneiform (MHNT Pak 1590), dorsal view; M, right ectocuneiform (MHNT Pak 1160), dorsal view; N, right MtII (MHNT Pak 1162), anterior view; O, left MtII, distal end (MHNT Pak 1191), distal view; P, right MtIII, proximal end (MHNT Pak 1096), anterior view; Q, right MtIII without proximal end (MHNT Pak 1095), anterior view; R, right MtIII, distal end (MHNT Pak 1194), distal view; S, right MtIV (MHNT Pak 1165), anterior view; T, same, medial view; U, right MtIV (MHNT Pak 1167), proximal view; V, right MtIV, distal end (MHNT Pak 1097), distal view. A–V from Kumbi 4a. Scale bar = 2 cm.

Table 1. *Pleuroceros blanfordi* (Lydekker, 1884) and ***Mesaceratherium welcommi* sp. nov.** Compared dimensions of mandibular fragments (range, number of specimens in square brackets, and mean, in mm) from the Early Miocene of the Dera Bugti area (Balochistan, Pakistan)

	H corpus mandibulae						TD *corpus*			
Taxon	p2–3	p3–4	p4–m1	m1–2	m2–3	post m3	p4–m1	m2–3	L symphysis	H proc. coron.
M. w.	58–63	69–66	73–79	78–87	–	(81)	34.5–39	42	> 108	> 223
Mean	60.5 [2]	67.5 [2]	75.7 [3]	82.5 [2]	–	–	37.3 [3]	–	–	–
P. b.	50–53	(55)	70	75	71	–	37	(37)–41.5	(> 91)	–
Mean	51.5 [2]	–	–	–	–	–	–	–	–	–

H, height; L, length, *M. w.*; *M. welcommi*; *P. b.*, *P. blanfordi*; post, posterior; proc. coron., processus coronoideus; TD, transverse diameter. Approximate dimensions appear between brackets.

subcircular. A horizontal median ridge splits the occipital condyle into two parts. No medial truncation is visible on the latter.

Mandibular material: The most complete specimen is the mandible MHNT Pak 1038 (Fig. 5A–D). The symphysis, nearly horizontal, forms a plateau continuing the corpus mandibulae. It is thick and rather wide, lacking any lateral constriction at the diastema level. In anterior view, the lingual border of the symphysis is regularly concave and the ventral border is flattened, without a median depression. A sharp and winding ridge separates the lingual and labial borders of the symphysis, between the i2 and the lingual side of p1. The posterior border of the symphysis reaches the middle of p2, as does the wide foramen mentale. The latter is associated with accessory foramina, all along the ventral border of the symphysis. The spatium intermandibulare is very wide – from 32–40 mm between p2 and p3 according to the specimen. In frontal view the tooth rows are strongly divergent, the corpus mandibulae being very oblique (Fig. 5C). The corpus mandibulae gets regularly higher from the symphysis to m1, and notably lower backwards (MHNT Pak 1038, IMC C. 271; Table 1). There is no median sagittal groove (sulcus mylohyoideus) on the lingual side of the corpus mandibulae either in adults (MHNT Pak 1037, 1038, and 1068) or juveniles (MHNT Pak 784, IMC C. 267). The ramus is unknown, but Lydekker (1884: 6, fig. 2) figured a prominent angulus mandibulae (IMC C. 271). The mandible MHNT Pak 784 bears the alveolus of d1, the functional d2–4 series and the m1 included in the pars molaris (Fig. 5D–E). It belongs to a calf, referred to *P. blanfordi* owing to the shape of m1.

Dental material: The upper incisors are not known with certainty, but the flat wear surface on i2s is most probably because of large I1s. However, the mandibular symphysis MHNT Pak 1038, which is broken in its anterior part, bears cross-sections of the left i1 and both i2s (Fig. 5C). The former has an oval cross-section (5.5×7 mm) and it was located below the horizontal line defined by the i2s. The i2s, 22 mm away one from another, have a drop-shaped cross-section, as do the complete i2s MHNT Pak 1021 and 1031. A thin layer of enamel covers the crown. This enamel is fluted in the labial part of the crown. The i2s do not diverge.

The cheek teeth formula is 4P–3M, 4p–3m. No P1 or persistent D1 can be referred to this taxon. However, the maxilla MHNT Pak 46 bears the broken roots of a small triangular tooth in front of P2

Table 2. *Pleuroceros blanfordi* (Lydekker, 1884) (Early Miocene of the Bugti Hills, Balochistan, Pakistan) and *Pleuroceros pleuroceros* (Duvernoy, 1853) from Laugnac and Saint-Gérand-le-Puy (Early Miocene, France). Compared dimensions of the upper dentition (permanent and deciduous cheek teeth; range, mean, and number of specimens in square brackets, in mm)

	L		ant W		post W		H	
Tooth	*P. b.*	*P. p.*	*P. b.*	*P. p.*	*P. b.*	*P. p.*	*P. b.*	*P. p.*
P2	21–29.5	24–25	23–31	28–28	27–35	28–28	11–37	20–20
Mean	24.0 [6]	24.5 [2]	27.4 [7]	28.0 [2]	31.4 [5]	28.0 [2]	19.5 [4]	20.0 [2]
P3	25.5–35	29–29	38–47	36–36	37–48	33–33	14–27	23–23
Mean	31.3 [12]	29.0 [2]	43.0 [12]	36.0 [2]	42.4 [10]	33.0 [2]	20.4 [5]	23.0 [2]
P4	31.5–38.5	30–31	44.5–53	39	44.5–54	36	22–33	26–26
Mean	34.7 [6]	30.5 [2]	50.2 [6]	–	49.2 [5]	–	26.0 [3]	26.0 [2]
M1	42–56	36–36.5	53–57	41	50–56.5	36.5	34–60	20–21
Mean	49.0 [5]	36.2 [2]	55.4 [5]	–	53.2 [6]	–	45.1 [4]	20.5 [2]
M2	54–56	40–42	58–62	40–47	50–53	36–42.5	38–57	25–29
Mean	55.0 [4]	40.7 [3]	59.5 [4]	42.5 [4]	51.7 [5]	38.1 [4]	48.0 [3]	26.7 [4]
M3	44.5–48.5	33–36	53–57.5	32–41	L_{ect} = 57–60.5	40.5–45	21–55.5	23–30.5
Mean	47.2 [4]	34.7 [3]	54.8 [3]	37.7 [3]	58.2 [3]	41.8 [3]	36.1 [4]	26.8 [3]
D2	31.5	–	28	–	–	–	–	–
D3	35	–	38.5	–	37	–	–	–
D4	46	–	44	–	39	–	–	–

ant, anterior; H, height; L, length; L_{ect}, length of the ectometaloph; *P. b.*, *P. blanfordi*; *P. p.*, *P. pleuroceros*; post, posterior; W, width.

(Fig. 4B). The premolar row is short with respect to the molar one [$(L_{P3–4}/L_{M1–3}) \times 100 = 46$]. There is no enamel folding (Fig. 4F, K). The cement is abundant, covering the ectolophs and filling the valleys. The enamel is thinly wrinkled vertically and even squared because of horizontal striae (MHNT Pak 751, 1024, 1058; NHM M 15337). The crowns are high but still conical, with a strongly oblique ectoloph. The roots are thinly joined, long, and divergent (Fig. 4A).

P2 is trapezoid, wider in its posterior part (Fig. 4F–G; Table 2). The P3–4s are rectangular, wider than long. The labial cingulum is generally absent (ten P2–4 out of 11), but it forms a low ridge on the P3 MHNT Pak 1024 (Fig. 4H). The lingual cingulum is always strongly developed on P2–4 (Fig. 4F). Generally interrupted on the protocone and/or the hypocone (13/16 specimens), it can be continuous (three specimens out of 16). The crochet is lacking on every available P2 (Fig. 4G) and two worn P3s (MHNT Pak 758, 845). Yet, it is present and always multiple on the eight remaining P3s and the ten available P4s. The crochet is restricted to the top end of the crown, therefore vanishing with wear (Fig. 4B, F–H). The metaloph is complete, V-shaped in occlusal view, and without a constriction. The postfossette is narrow and deep. The median valley is still deeper. The antecrochet, lacking on P2–3, is always strongly developed on P4 (Fig. 4I). There is a lingual bridge joining the lingual cusps on P2–3 and joining the antecrochet with the hypocone on P4 (Fig. 4F). This bridge is thin in Early stages of wear, and it thickens in later stages. On P2, the metaloph is transverse and the protocone is less developed than the hypocone. The protoloph is narrow but continuous on every P2. There is no medifossette on the upper premolars (Fig. 4B, F–I), except for P4 MHNT Pak 1964. On P3–4, the anterior constriction of the protocone is generally present; the continuous metaloph forms a dihedron open backwards, in which the crochet is the anterior angle; the hypocone is posterior to the metacone. On P3, the protoloph is continuous and there is no crista. The parastyle is sagittal. The paracone and the metacone folds are always present on P2–4, the former being thicker.

The upper molars are generally lacking a labial cingulum: only two M2 have a cingular bulge very reduced, at the neck. The antecrochet and the crochet are always well developed, except on worn teeth, where the crochet may vanish (MHNT Pak 1031). The anterior constriction of the protocone is always deep, both in M1–2 and M3 (Fig. 4E–F, K–M). Therefore, the protoloph is 'trefoil-shaped' (*sensu* Antoine, 2003). The crochet is sagittally orientated and generally simple on the upper molars (11 specimens out of 15). Yet, the crochet is sometimes double in the top of the crown (MHNT Pak 760, 1012a, 1045, 1258). No crista

Table 3. *Pleuroceros blanfordi* (Lydekker, 1884) (Early Miocene of the Bugti Hills and of the Zinda Pir Dome, Pakistan) and *P. pleuroceros* (Duvernoy, 1853) from Laugnac and Saint-Gérand-le-Puy (Early Miocene, France). Compared dimensions of the lower dentition (permanent and deciduous cheek teeth; range, mean, and number of specimens in square brackets) in mm

	L		ant W		post W		H	
Tooth	*P. b.*	*P. p.*	*P. b.*	*P. p.*	*P. b.*	*P. p.*	*P. b.*	*P. p.*
p2	28–30	20–20.5	17–19	14–14	20–21	15–15	23–25	15–17
Mean	28.8 [3]	20.3 [3]	17.8 [3]	14.0 [3]	20.3 [3]	15.0 [3]	24 [3]	16.0 [2]
p3	(27)–32	26–28	17	16.5–18	19	18–19	19	12–18
Mean	–	26.8 [4]	–	17.4 [4]	–	18.3 [4]	–	16.5 [3]
p4	(35)–37	30–34	26–27	20–21	26–27.5	20.5–23	33–34	17–22
Mean	36.7 [3]	31.7 [3]	26.5 [2]	20.3 [3]	26.7 [2]	21.5 [3]	33.5 [2]	19.5 [2]
m1	(37)–38	31–34	25–26.5	20–23	27	20–24	24–28	12–23
Mean	–	32.7 [3]	25.7 [2]	21.0 [3]	–	21.7 [3]	26 [2]	17.5 [2]
m2	41.5	38–(40)	28	22–24.5	25–26	22–25	26–32	14–26
Mean	–	38.5 [2]	–	23.2 [2]	25.5 [2]	23.0 [3]	29 [2]	20.0 [2]
m3	45–46	38–40	26–27.5	22–24	25–29	20–22.5	19–45	16–28
Mean	45.5 [2]	39.0 [3]	26.7 [2]	22.7 [3]	26.5 [3]	20.8 [3]	28.3 [3]	22.0 [3]
d2	26.5	–	9	–	12	–	13	–
d3	(39)	–	(15)	–	(19)	–	18	–
d4 r	38.5	–	18.5	–	22	–	29	–

ant, anterior; H, height; L, length; *P. b.*, *P. blanfordi*; *P. p.*, *P. pleuroceros*; post, posterior; W, width. Approximate dimensions appear between brackets.

is present on M1–3, except on M2 MHNT Pak 1027. There is neither medifossette nor cristella. The lingual cingulum is generally reduced, determining a tubercle more or less developed, located at the entrance of the median valley. It forms a thin ridge on the protocone of two M3 (MHNT Pak 761, 918), but is absent from other molars (MHNT Pak 1019, 1022). The ectoloph is nearly straight on M1–2, with a sagittal parastyle, a weakly developed paracone fold, a weak mesostyle but no metacone fold. The metaloph is long on M1–2. A deep constriction notches the anterior side of the hypocone. This constriction is restricted to the base of the crown, deeper on M1 than on M2 (Fig. 4K–L). It is absent on M3, except on MHNT Pak 918. There is a shallow groove on the posterior side of the hypocone, close to the lingual tip of the posterior cingulum on M1–2. There is no junction between the antecrochet and the hypocone, even on worn molars. The postfossette is always present, deep and narrow. No lingual groove notches the protocone of M2. On M3, the ectoloph and the metaloph are fused into an ectometaloph (Fig. 4M). The posterior cingulum forms a thick spur restricted to the lingual half of the latter. Yet, M3 has a trapezoid outline, with a wide posterior side – corresponding to the remnant metaloph – supported by two divergent roots. The protoloph of M3 is sagittal and transverse.

The morphology of p1 is unknown. However, the size comparison between the alveolus of d1 (juvenile mandible MHNT Pak 784) and the one present in the adult mandible MHNT Pak 1038 leads us to assume the occurrence of true p1s in adults (Table 3). This p1 was single-rooted, with a cylindrical root section. The ectolophid of p2 is covered by vertical rugosities continuing the labial cingulum (PMNH Z2070, Fig. 5A, G). On p3–4, such rugosities are replaced by a sinuous and continuous cingulum. The external groove is shallow, U-shaped on every lower cheek tooth, vanishing above the neck. The trigonid is angular and forms a right or obtuse dihedron (Fig. 5D). The metaconid is constricted, contrary to the entoconid. The posterior valley is wide and V-shaped. The lingual cingulum, always present, is restricted to the anterior part of the lower cheek teeth. Continuing the anterior cingulum, it forms a thick ridge interrupted at the metaconide level. The labial cingulum is high and continuous on lower premolars, and reduced on lower molars, forming a short ridge in the external groove. The p2 has an isolated spur-like paralophid (Fig. 5B). The paraconid is developed and globular. The posterior valley of p2 is open. The base of the metaconid – between the roots – is depressed on the available specimens. The hypolophid of the lower molars is oblique. There is no lingual groove on the entoconid of m2–3.

The juvenile mandible MHNT Pak 784 bears no alveolus for deciduous incisors. d1 is one-rooted. The deciduous teeth are damaged, but the metaconid and

the entoconid seem to be constricted (Fig. 5E–F). It is impossible to observe the protoconid fold. d2–4 lack both labial and lingual cingula and external roughness. There is no ectolophid fold, but an anterior groove is present on the ectolophid of d2–3. The paralophid of d2 is simple and spur-like. The posterior valley of d2 is lingually open, but a thick oblique ridge lays posteriorly to the metaconid. The paralophid of d3 is double. There is no lingual groove on the entoconid of d3–4.

Postcranial skeleton: The material is very abundant, particularly in the Kumbi 4a locality. Postcranials are small- to medium-sized, very homogeneous in size and proportions (Tables 5–7, 9–13, 15–21, 23–27).

From the humerus, only two distal fragments are referred to this taxon (MHNT Pak 1085, 1198). The fossa olecrani is high. The trochlea is very constricted in its median part. The lateral lip is narrow (TD). Available dimensions are (mm): APD distal extremity = 86; APD trochlea = 71 (medial) (42) (middle), and 49.5 (lateral). The epicondyle is weakly developed and lacking any distal gutter.

No complete radius is preserved, but proximal and distal fragments are available (Fig. 6A–B; Table 5). In anterior view, the proximal end is much wider than the shaft. The proximal border is sigmoid, with a low medial border and high median part and lateral border. The weak insertion for the m. biceps brachii is slightly depressed medially. In proximal view, the anterior border of the proximal end is straight and the lateral lip of the cochlea forms a deep basin. The proximomedial ulna-facet is low and halfmoon-shaped. The proximolateral ulna-facet is high and concave. It is impossible to state whether they are fused or separate. Ulna and radius are independent all along the diaphysis. The distal end of the radius MHNT Pak 1090 (Fig. 6B) bears a huge lateral expansion, which supports the ulnar articular surface and takes the diaphyses away one from another. The diaphysis is slender and dorsoventrally flattened. The gutter for the m. extensor carpi is wide and deepened by a strong anterolateral tuberosity, above the semilunate-facet. The distal end is wide (TD) and flattened dorsoventrally. In anterior view, the distal border is oblique, much lower medially than laterally; the limit between the scaphoid- and the semilunate-facet is marked by a salient ridge. The scaphoid-facet, deep and sagittally shortened, is posteriorly extended by a medial high and triangular expansion. On the lateral side of the distal end, only one ulna-facet is present. Based on the available specimens, it is impossible to state the presence/absence of a pyramidal-facet.

The ulna is unknown.

The carpus is massive, with thick tuberosities and muscular insertions, especially on the scaphoid, the magnum and the unciform (Fig. 6C–K). The scaphoid is low and robust, with a large transverse diameter (Fig. 6C–D; Table 6). Its posterior height widely exceeds the anterior height. The medial side, short of articular facets, bears a very salient tuberosity in its posterior half. Such a tuberosity extends beyond the trapezium-facet. The latter is small and vertically developed. The scaphoid lacks a posteroproximal semilunate-facet, which is replaced by a thick tubercle. The trapezoid-facet is very wide (TD > APD). The magnum-facet, triangular, is sagittally concave and convex transversally. Its anterior end is located very rostrally with respect to the proximal articulation.

The semilunate MHNT Pak 1101 has no ulna-facet, which indicates the presence of a pyramidal-radius articulation (Fig. 6E–F). The proximal facet is convex and short sagittally. The posterior border of the distal pyramidal-facet is twisted posteriorly. The anterior side is smooth, with a rounded distal border. The magnum-facet does not reach the anterior side.

No pyramidal is preserved, neither the pisiform nor the trapezium.

The trapezoid is small and robust (Table 9). Its anterior side is as wide as high, with a proximal edge regularly convex (Fig. 6G).

The available magnums are broken: no posterior tuberosity is preserved (Fig. 6H–I). The anterior side is as wide as high (Table 10). Its proximal border is straight in anterior view. The articular process for the semilunate is semicircular in lateral view (diameter = 20 mm). On the medial side, the articular facets are not well separated, the anterior incisure being very shallow. Both facets form subvertical strips elongated sagittally. On the lateral side, the unciform-facet is rectangular and narrow sagittally. The distal McIII-facet is trapezoid.

The unciform is represented by four specimens, of which three are complete (Fig. 6J–K). This bone is low and wide in anterior view (Table 11). A strong tuberosity lies along the distal border of the anterior side; this tuberosity is more developed medially. The pyramidal- and McV-facets are always independent but close, especially on MHNT Pak 1113. The posterolateral expansion of the pyramidal-facet is present in this only specimen. In anterior view, the semilunate-facet is concave (MHNT Pak 1113, 1114) or flat (MHNT Pak 1094, 1112). In proximal view, the posterior tuberosity is slightly longer than the articular part. The former is wide and low. The distal facet has a wide articular surface for the magnum, McIII, McIV, and McV. The latter is regularly concave sagittally and forms an angle about 60° from the horizontal line, indicating a tridactyl manus (i.e. with a vestigial McV).

The metacarpals are small and robust, sagittally flattened, with wide diaphyses and salient insertions for the m. extensor carpalis (Tables 12–13).

McII is only represented by an eroded proximal end (MHNT Pak 1733; Fig. 6L–M) and a distal half (MHNT Pak 789). The proximal articulation has a quarter-circle outline in proximal view. The magnum-facet is curved in proximal and lateral views. It is impossible to state the presence/absence of a trapezium-facet. The distal end is wide, with a strong lateral tubercle close to the anteroproximal border of the distal articulation. According to the preserved region of the bone, the diaphysis was curved. The distal articulation is very wide, almost symmetrical, and slightly twisted posteromedially. The keel (or intermediate relief) is high and sharp.

Six McIII are preserved (Fig. 6N–Q). One is complete (Table 13). The proximal end is not widened with respect to the diaphysis. The wide McII-facet is comma-like, elongated sagittally. The magnum-facet is narrow and triangular in proximal view. It is visible in anterior view. The unciform-facet forms a narrow and elongated rectangle triangle. The insertion for the m. extensor carpalis is strikingly salient, with two huge tuberosities (medial and lateral). Thus, the lateral border of the diaphysis is laterally displaced in its proximal quarter (30–40 mm long). In anterior view, the diaphysis is slightly curved inwards, without distal widening. The intermediate relief, high and acute, is visible in anterior view. It is particularly salient in its posterior half. The anteroproximal border of the distal articulation is hardly separate from the diaphysis. No posterodistal tubercle is present on the diaphysis.

McIV and McV are not preserved. However, the tridactyly of the manus can be assumed owing to the shape of the unciform (Fig. 6J), especially from the orientation of the McV-facet, as argued by Antoine & Welcomme (2000) and Antoine (2002).

The coxal and the femur are unknown.

The patella is wide, i.e. as wide as high (Fig. 7A; Table 15). The muscular insertions are smooth on the anterior side. The most prominent one corresponds to the m. fascia lata. That for the m. rectus femoris is flat. On the articular side, the medial lip is wide, low, and shallow (MHNT Pak 1131). The proximal border of the articular surface is straight. The distal tip is smooth. The lateral lip is weakly notched transversally.

The tibia is represented by five distal ends (Table 16). There is no anterior groove on the anterior side (Fig. 7B). An oblique gutter notches the median part of the posterior side. The gutter corresponding to the m. tibialis posterior is always present and is deep and narrow. It is located on the posterior third of the medial side. The tibia and the fibula are independent, as the absence of any synostosis on the lateral border of the diaphysis indicates. The diaphysis has a drop-shaped cross-section (MHNT Pak 1126, 1128). The posterodistal apophysis is high and rounded. In distal view, the distal end has a trapezoid outline. The medial border of the cochlea is narrow and very deep. The lateral lip, much wider than the medial one, is almost flat transversally. The distal fibula-facet is semicircular. The contact area does not exceed 40 mm high.

Only one distal half of a fibula can be referred to this taxon (MHNT Pak 1129). The diaphysis is slender, short of any contact with the tibia. The distal end is robust, with a deep lateral gutter for the m. fibularis (Fig. 7C–D; Table 17). This vertical gutter is located in the posterior third of the head. The astragalus-facet is flat dorsoventrally, subvertical, and slightly concave sagittally.

Eight astragali are preserved (Fig. 7E–G; Table 18). They are morphologically and metrically homogeneous, wider than high (TD/H = 1.16) and deep (APD/H = 0.76). The fibula-facet is subvertical and flat transversally. It is very developed anteroposteriorly. The collum tali is high. The posteroproximal border of the trochlea is nearly straight. The trochlea is very oblique with respect to the distal articulation. The lateral lip is very prominent. The laterodistal expansion of calcaneus-facet 1 (*sensu* Heissig, 1972) is always present and is high and narrow. This facet is very deep sagittally. Calcaneus-facet 2 is flat and oval, higher than wide. Calcaneus-facet 3 is small (MHNT Pak 1140). Calcaneus-facets 2 and 3 are not connected and are separated by a deep notch. On the distal side, the posterior border of the cuboid-facet bears a strong and abrupt inflection. This facet is wide and short. The medial tubercle is salient, overhanging the medial border of the trochlea by about 15 mm.

The four available calcanei are robust, wide, and low (Table 19). They lack both fibular and tibial facets. The insertion for the m. fibularis longus is marked, forming a deep notch trimmed by a circular ridge (Fig. 7H). The tuber calcanei is high, slender, and oblique with respect to the processus calcanei. The latter is short and very thick (TD). The beak (rostrum calcanei) is low. The sustentaculum tali is wide. The cuboid-facet is sagittally flat and very deep transversally.

From the second tarsal row, two naviculars, two cuboids, a mesocuneiform, and two ectocuneiforms are preserved. The navicular is low (Table 20), with a lozengic outline in vertical view (Fig. 7I). The insertions for muscles and tendons are developed, especially towards the posteromedial tip, which bears a thick tubercle. The proximal articular surface for the astragalus is laterally displaced and splits into two parts because of a sharp transverse ridge (MHNT Pak 1154).

The cuboid is robust, wide (TD), and short (APD; Table 21). The anterior side, square in anterior view, is oblique with respect to a vertical transverse plane. The proximal facet, oval to lozengic, is split into two equal parts by a sagittal groove: the astragalus-facet is more posterior than the calcaneus-facet (Fig. 7K). The posterior tuberosity is well developed, with an oblique posterior border (Fig. 7J). The distal tip of this tuberosity overhangs the distal articulation by a few millimetres. The distal MtIV-facet is triangular (MHNT Pak 1158) or trapezoid (MHNT Pak 1159). In both cases, it is deeper than wide (APD > TD).

The mesocuneiform is wide, forming an isosceles triangle in proximal view (Fig. 7L; Table 23).

The ectocuneiform is high and narrow and is L-shaped in proximal view (Table 24). It lacks any posterolateral expansion (Fig. 7M). The distal border is regularly convex in anterior view.

The metatarsus is more slender than the metacarpus (Fig. 7N–V). The lateral metatarsals are almost as developed as MtIII. The insertions for the m. interossei are short and restricted to the proximal half of the shaft (Fig. 7N, S–T). Mt II bears a narrow proximal end, sagittally elongated (Fig. 7N; Table 25). Its outline forms a quarter oval. The mesocuneiform-facet is triangular (isosceles triangle). An oval posteromedial entocuneiform-facet nearly joins the proximal facet. On the lateral side, the anterior MtIII-facet is well developed, flat, and vertical. The diaphysis has a circular cross-section. The distal end is the most robust part of the bone. The distal articulation is roughly square in distal view (Fig. 7O). It is wide, nearly flat transversally, with a posteromedial expansion. The intermediate relief is salient, especially with respect to the medial lip of the pulley.

No complete MtIII has been recovered, but this bone was rather slender, according to the available fragmentary specimens (Fig. 7P–Q; Table 26). In proximal view, the anterior border of the articular facet is regularly convex. This facet is only for the ectocuneiform: there is no cuboid-facet. The proximal border of the anterior side is concave in anterior view. There are two flat and well-developed MtII-facets on the medial side of MtIII MHNT Pak 196. On the lateral side, the MtIV-facets are independent. The posterior facet is distally displaced with respect to the anterior one. The diaphysis widens distally (MHNT Pak 1194, 1195), reaching its maximal width (TD) immediately above the distal articulation: two symmetrical tuberosities considerably widen the diaphysis. The intermediate relief is displaced laterally. The medial lip of the trochlea is thus wider than the lateral one (Fig. 7R). No posterodistal tubercle is present on the diaphysis.

MtIV is robust, with thick ends and a cylindrical diaphysis (Fig. 7S–V; Table 27). In proximal view, the proximal end is trapezoid, with a right angle defined by its anterior and medial sides (Fig. 7U). The angle between the other sides exceeds 90°. The articular side is roughly triangular, even if the posterolateral border is strongly convex. The medial border is notched in its median part. The posterolateral tuberosity forms a strip and is split into two equal parts by a tendinous gutter (MHNT Pak 1166). On the medial side, the articular facets are flat and widely separate. They form an angle of about 150°. The posterior facet is oval and sagittally elongated. Its posterior end reaches the posterior tip of the bone. The diaphysis is curved outwards. The brutal curvature occurs at the distal end of the insertion for the m. interossei, in the proximal half of the shaft (Fig. 7S). The diaphysis is widened by a medial tubercle (muscular insertion), just above the distal articulation. The latter is wide and deeper (APD) than those of the other metatarsals. It is flat transversally in its medial part and concave in its lateral part. The intermediate relief is low and smooth (Fig. 7V).

Discussion

In the field, the fossil specimens here referred to *P. blanfordi* represent thus far the most abundant small to medium-sized rhinocerotid specimens, especially in Level 4 (earliest Miocene, *c*. 22.5 Myr; Fig. 2). The dimensions of the fragmentary skull MHNT Pak 46 fit with those of the palate NHM M 15365 figured by Forster-Cooper (1934: pl. 67, fig. 34).

Since its initial discovery through dental and fragmentary craniomandibular remains, this species has been referred to half a dozen distinct genera, which range from Recent times (*Rhinoceros* and *Dicerorhinus*) back to the Late Miocene (*Aceratherium*, *Chilotherium*, and *Teleoceras*), and even to the Late Oligocene (*Aprotodon*). However, to our knowledge, no comparison has been made with coeval rhinocerotid genera, such as the teleoceratine *Diaceratherium*, the aceratheres (*sensu lato*) *Mesaceratherium* and *Protaceratherium*, and the puzzling pair-horned *Pleuroceros*, which were abundant around the Oligocene–Miocene transition in Europe (Antoine *et al.*, 2003a). At first glance, the morphological similarity is striking with the type and only species of *Pleuroceros*, *P. pleuroceros*, as illustrated and described by Duvernoy (1854–1855) and de Bonis (1973), especially for the postcranials – which are referred to this taxon for the very first time in the present work.

Compared with the cranial features observable in both *P. blanfordi* and *P. pleuroceros* from France (Gannat, Laugnac, and Paulhiac localities; Duvernoy, 1854–1855; de Bonis, 1973), the Pakistani material is *c*. 15% larger. Both taxa share a concave occipital crest in dorsal view and they only differ by the horizontal posterior groove on the processus zygomaticus

of the squamosal, which is present in *P. blanfordi* and absent in *P. pleuroceros*, and by the nasal incision longer in *P. blanfordi*. The zygomatic arch is high, the processus postglenoidalis is thin and narrow, the frontoparietal crests converge similarly, and the distal border of the nuchal crest is irregular in both species. The occipital side (shape, orientation) and condyle (sigmoid medial border in occipital view) are identical.

The mandible of *P. blanfordi* is strongly reminiscent of that of *P. pleuroceros*: all observable mandibular characters are shared by *P. blanfordi* and *P. pleuroceros* (e.g. a nearly horizontal symphysis, with sharp sagittal edges running dorsally along the diastema, and a posterior border at the level of p2), with the exception of the lingual mandibular groove.

It is still more striking on the postcranial skeleton, with highly similar carpus, tarsus, and metapodials in terms of proportions, articular facets, tuberosities, and trochleae (Figs 11A–B, 12A–B). It may be noticed that *P. blanfordi* was most probably tridactyl, as is *P. pleuroceros* (de Bonis, 1973: 153, text-fig. 44.7). In both species, the metacarpals have a prominent insertion for the m. extensor carpalis, the tuber calcanei is elevated and slender, and the insertion of the m. interossei on the lateral metapodials is short. The astragali are identical (Fig. 12A–B). The only postcranial differences between both species are the stronger mediodistal tuberosity on the scaphoid in *P. blanfordi* (Fig. 11A–B) and on McII, the posterior McIII-facet on McII and the fibula-facet on the calcaneus (absent in *P. blanfordi*), and the proximal border of MtIII, which is concave in *P. blanfordi* and straight in *P. pleuroceros*.

Pleuroceros blanfordi and *P. pleuroceros* primarily differ in their dental characters, mainly the upper cheek teeth: in *P. blanfordi* larger dimensions (up to 30% larger; Table 2), a shortened premolar series, higher tooth crowns, abundant coronary cement, a weaker labial cingulum, a multiple crochet (only occasionally observed in *P. pleuroceros*), an unconstricted metaloph, a continuous lingual cingulum, the presence of a thick lingual bridge on the upper premolars, a transverse metaloph and a reduced protocone on P2, and the usually constricted protocone on P3–4, the absence of a crista on P3, the unconstricted metaloph on P4, the usual presence of a lingual cingulum (occasional in *P. pleuroceros*) on upper molars, a weak paracone fold, and the presence of a metacone fold on M1–2, a strong mesostyle on M2, and a constricted metaconid on the lower deciduous teeth.

Nevertheless, both species share several characters considered as synapomorphies in the phylogenetic analysis performed here (see Phylogenetic relationships): a reduced lingual cingulum on upper premolars, a strong antecrochet on P4, an occasional crista on upper molars, a strongly constricted protocone and a low reduced posterior cingulum on M1–2, a constricted hypocone on M1, a smooth and U-shaped external groove on lower cheek teeth, and a continuous lingual cingulum on lower premolars.

The mandibular symphysis figured by Forster-Cooper (1934: text-fig. 10A) is strongly similar to MHNT Pak 1038, especially for the wide spatium intermandibulare. None of these symphyses is very massive, neither enlarged rostrally nor displaying highly diverging incisors (i2). First lower incisors are retained. The foramen mentale is located under p2 in *P. blanfordi*, whereas it is situated in front of it in *Aprotodon*. An occasional postfossette occurs on the upper cheek teeth. The protoloph joins the ectoloph on P2. The protocone is deeply constricted on the upper molars. The posterior part of the ectoloph is concave on M1–2. A deep anterolingual groove marks the hypocone on M2. The external groove is smooth and U-shaped, and the trigonid is angular and sharp on the lower cheek teeth. The lingual opening of the posterior valley is deep, narrow, and V-shaped on the lower premolars, in lingual view. All of these mandibular and dental features make *P. blanfordi* differ from the species referred to *Aprotodon* Forster-Cooper, 1915. To our knowledge, no postcranial remain is referred to the latter genus (Forster-Cooper, 1915, 1934; Borissiak, 1944; Beliajeva, 1954; Qiu & Xie, 1997).

More features will be discussed in the phylogenetic analysis section, including differences with type species of some genera that *P. blanfordi* had been referred to, such as *Aceratherium* and *Chilotherium*.

MESACERATHERIUM HEISSIG, 1969: 90

Emended diagnosis: Medium-sized hornless rhinocerotine with a strong paracone fold on M1–2, a posterior McIII-facet on McII, no posterior MtII-facet on MtIII, and slender limbs.

Type species: Mesaceratherium gaimersheimense Heissig, 1969.

Included species: M. paulhiacense (Richard, 1937)

MESACERATHERIUM WELCOMMI ANTOINE & DOWNING **SP. NOV.** (FIGS 8–10, 11C, 12C)

Rhinoceros Falconer & Cautley, 1846: pl. 76, figs 12, 12a, 12b

Teleoceras blanfordi (partim) Pilgrim, 1912: 3, 30–32; pl. 7, figs 4, 7

Rhinoceros blandfordi (partim) Forster-Cooper, 1934: 589–594, text-figs 9A, 9C, 9E.

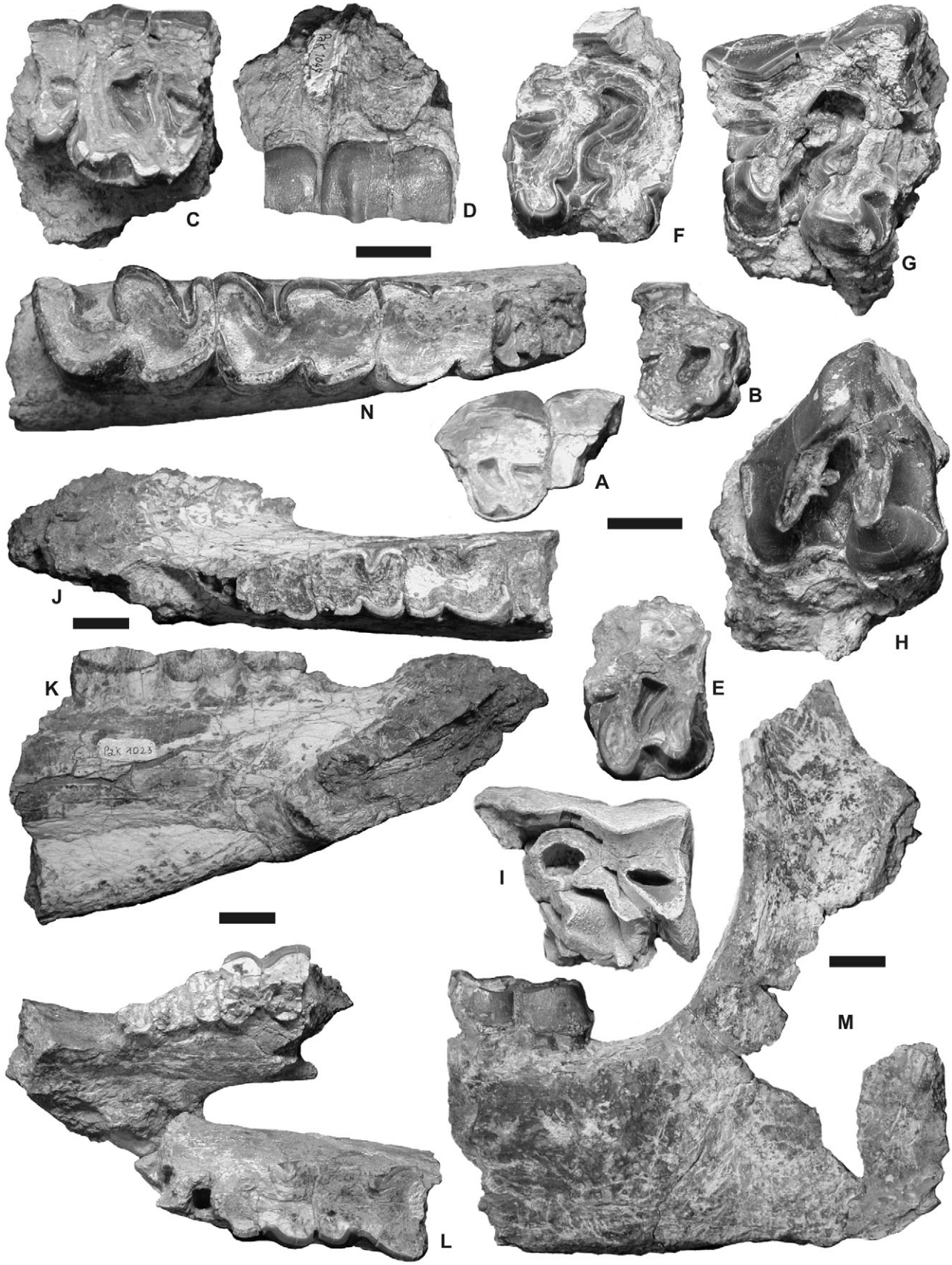
C
D
F
G
N
B
A
J
H
K
E
I
M
L

Figure 8. ***Mesaceratherium welcommi*** **sp. nov.** from the Early Miocene of the Bugti Hills, Balochistan, Pakistan: Cranial, mandibular, and dental remains. A, left P2 and fragmentary P3 (MHNT Pak 1044), occlusal view. Kumbi 4a; B, right P2 (MHNT Pak 1038bis), occlusal view. Kumbi 4a; C, left maxilla fragment, with posterior part of P2, and P3 (MHNT Pak 1047), occlusal view. Kumbi 4a; D, same, labial view; E, right P4 without ectoloph (MHNT Pak 1025), occlusal view. Kumbi 4a; F, broken right M1 (MHNT Pak 1060), occlusal view. Kumbi 4a; G, right M2 (MHNT Pak 1032A), occlusal view (holotype). Kumbi 4a; H, right M3 from the same individual as MHNT Pak 1032A (MHNT Pak 1032B), occlusal view (holotype); I, broken left M2 (MHNT Pak 2203), occlusal view (DB6); J, anterior part of a left hemimandible with p3–m1 and alveoli of i2, p1, and p2 (MHNT Pak 1023), occlusal view. Kumbi 4a; K, same, lingual view; L, fragment of a mandible with symphysis, left p4–m2, fragment of right p4, m1, m3, and alveoli of left and right p2–p3 (MHNT Pak 1054), occlusal view (paratype). Kumbi 4a; M, fragment of a left hemimandible with m3 and vertical ramus (MHNT Pak 1196), labial view. Kumbi 4a; N, fragment of a right hemimandible with m1–m3 (MHNT Pak 1648), occlusal view. Gandô 4. Scale bars = 2 cm.

« *Dicerorhinus* » cf. *abeli* (partim) Welcomme *et al.*, 1997: 532, 535

? '*Dicerorhinus*' cf. *abeli* (partim) Welcomme *et al.*, 1997: 534, 535, 536

Rhinocerotini, indeterminate genus and species Downing, 2005: 1–8, figs 2–3

Mesaceratherium sp. Métais *et al.*, 2009: 163, 164; table 2, fig. 5

Diagnosis: Differs from other species of *Mesaceratherium* by a shorter premolar series, a hypocone posterior to the metacone, and stronger than the protocone on P2, a protocone slightly constricted on P3–4 and deeply constricted on M1–2, lower cheek teeth with a constricted entoconid, and lower premolars without labial cingulum. Further differs from *Mesaceratherium gaimersheimense* by an upraised mandibular symphysis, a foramen mentale below the middle of p3, a thick and continuous protoloph on P2, the constant presence of a crochet on upper molars, a constricted entoconid but no lingual cingulid on lower premolars, and the occasional absence of d1/p1. Differs from *Mesaceratherium paulhiacense* by the presence of a lingual bridge on upper premolars (molariform in *M. paulhiacense*), by a labial cingulum on upper molars, and the absence of a mesostyle on M2, in the curved magnum-facet and fused McIII-facets on McII, fused calcaneus-facets 2 and 3 on the astragalus, the presence of a fibula-facet on the calcaneus, the proximal border of MtIII concave in anterior view, and in the presence of a distal widening of the diaphysis on MtIII.

Nomenclatural remark: This new species must be referred to as *Mesaceratherium welcommi* Antoine and Downing, 2010, following article 50.1 and the 'recommendation 50A concerning multiple authors' of the International Code of Zoological Nomenclature (ICZN, 1999: 52, 182).

Holotype: Right M2 (MHNT Pak 1032a), right M3 (MHNT Pak 1032b), and ectometaloph of a left M3 (MHNT Pak 1051) from the same individual, unearthed in the locality of Kumbi 4a (earliest Miocene; Bugti Hills, Balochistan, Pakistan).

Paratype: Fragment of mandible with symphysis, left p4–m2, fragments of right p4, m1, m3, and alveoli of left and right p2–3 (MHNT Pak 1054) from the locality of Kumbi 4a (earliest Miocene; Bugti Hills, Balochistan, Pakistan).

Etymology: In honour of Jean-Loup Welcomme, French palaeontologist, pioneer, and leader of the French Palaeontological Expeditions in the Bugti Hills (Balochistan, Pakistan), for his prominent role in the better understanding of mid-Cenozoic vertebrate assemblages from Pakistan.

Stratum typicum: Level 4 (earliest Miocene), parallelized with the Aquitanian, or Agenian European Land Mammal Age (MN2; Lindsay *et al.*, 2005; Métais *et al.*, 2009).

Type locality: Kumbi 4a, 30 km west of Dera Bugti (Balochistan, Pakistan).

Stratigraphical range: Chitarwata Fm. (Bugti and Zinda Pir areas) and base of the Vihowa Fm. (Bugti area). Early Miocene (*c.* 23–18.5 Myr; Lindsay *et al.*, 2005; Métais *et al.*, 2009).

Geographical range: Bugti and Zinda Pir area, Sulaiman Lobe, Balochistan, Pakistan.

Referred material

Old collections

'Near Dera Bugti' (? Early Miocene). Left maxilla with P2–4 (NHM M 15332) and right P2–3 (NHM M without number) from the same individual; right P3 (NHM M 15334); left P2 (NHM M 15336); right P2 (NHM M w.n.). Beloochistan Hills (? Early Miocene).

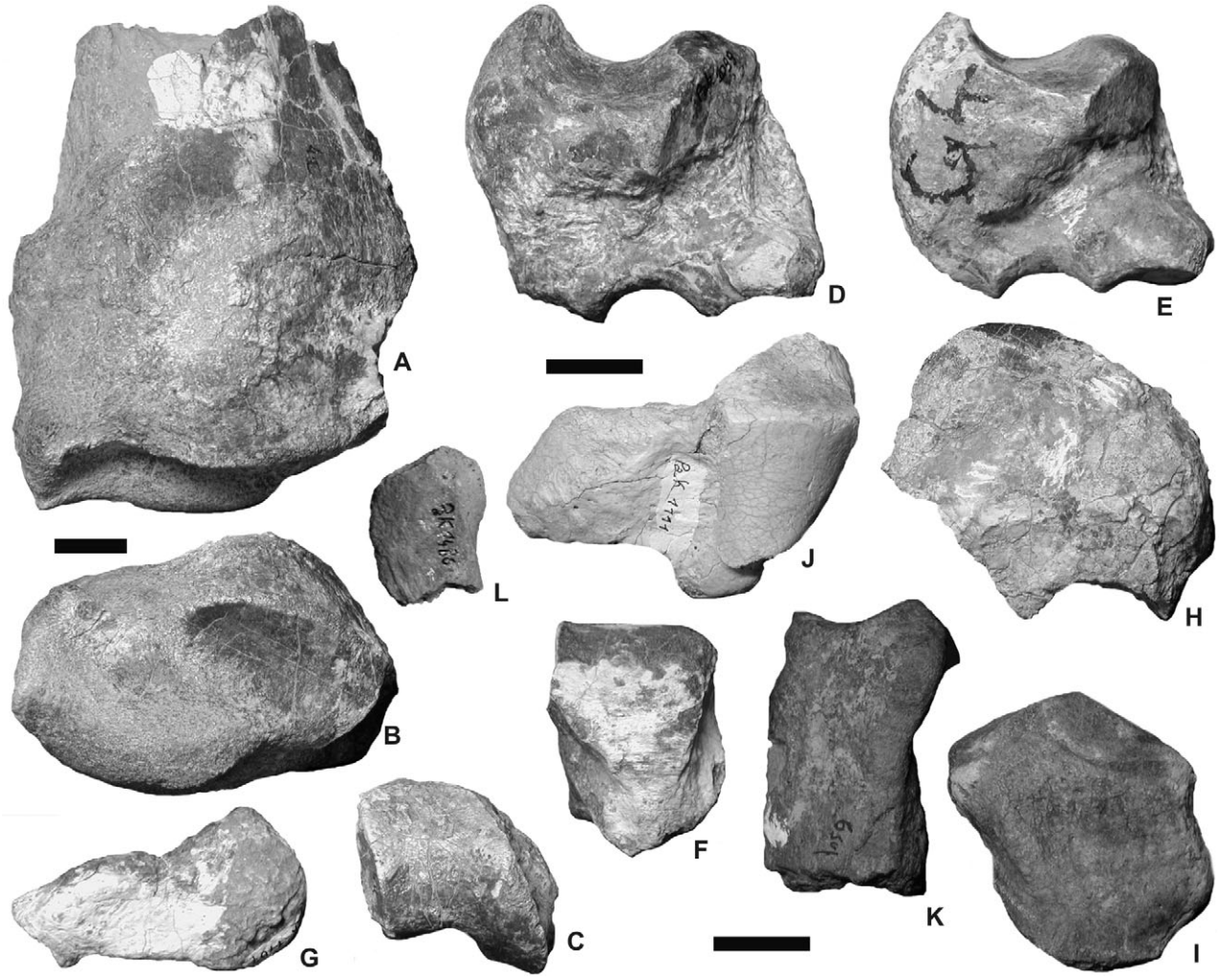

Figure 9. ***Mesaceratherium welcommi*** **sp. nov.** from the Early Miocene of the Bugti Hills, Balochistan, Pakistan: Fore limb remains. A, left radius, distal end (MHNT Pak 1092), anterior view. Kumbi 4a; B, same, distal view; C, left ulna, distal end (MHNT Pak 1184), distal view. Kumbi 4a; D, right scaphoid (MHNT Pak 1099), posteroproximal view. Kumbi 4a; E, right scaphoid (MHNT Pak 1868), posterolateral view. Gandô 4; F, left semilunate (MHNT Pak 1100), anterior view. Kumbi 4a; G, left pisiform (MHNT Pak 1107), medial view. Kumbi 4a; H, left magnum without posterior tuberosity (MHNT Pak 1109), medial view. Kumbi 4a; I, left unciform without posterior tuberosity (MHNT Pak 1709), anterior view. Kumbi 4f; J, right unciform (MHNT Pak 1111), dorsal view. Kumbi 4a; K, left McII, proximal end (MHNT Pak 1552), anterior view. Dera Bugti 6 sup; L, left McV, proximal end (MHNT Pak 1480), anterior view. Dera Bugti 6. Scale bar = 2 cm.

Distal end of a right radius (NHM M 10871). 'Gaj of the Bugti Hills' (? Early Miocene). P3 (IMC C. 295); P4 (IMC C. 311).

New material

Bugti Hills (Fig. 1).

Kumbi 4a (Level 4, earliest Miocene). Fragment of left mandible with p3–m1 and alveoli of i2, p1, and p2 (MHNT Pak 1023); fragment of left mandible with m1 (MHNT Pak 1040); fragment of left mandible with m3 and vertical branch (MHNT Pak 1196), maybe from the same individual as MHNT Pak 1023; left P2 and fragment of P3 (MHNT Pak 1044); right P2 (MHNT Pak 1038bis); fragment of left maxilla with P3 and posterior part of P2 (MHNT Pak 1047); right P3 without ectoloph (MHNT Pak 1025); left P4 without ectoloph (MHNT Pak 1026); fragment of a left P4 (MHNT Pak 1062); fragment of a right M1 (MHNT Pak 1060); right M2 (MHNT Pak 1032a), right M3 (MHNT Pak 1032b) and ectometaloph of left M3 (MHNT Pak 1051) from the same individual; left M2 without ectoloph (MHNT Pak 1049); lingual fragment

Figure 10. ***Mesaceratherium welcommi*** **sp. nov.** from the Early Miocene of the Bugti Hills, Balochistan, Pakistan: Hind limb remains. A, left astragalus (MHNT Pak 1135), anterior view. Kumbi 4a; B, same, distal view; C, right astragalus (MHNT Pak 1136), posterior view. Kumbi 4a; D, right astragalus (MHNT Pak 1144), medial view. Kumbi 4a; E, left calcaneus (MHNT Pak 1147), lateral view. Kumbi 4a; F, right calcaneus (MHNT Pak 1149), proximal view. Kumbi 4a; G, right navicular (MHNT Pak 1153), proximal view. Kumbi 4a; H, same, distal view; I, right cuboid (MHNT Pak 1990), lateral view. Dera Bugti 4; J, same, distal view; K, left entocuneiform (MHNT Pak 1095), anterior view. Kumbi 4a; L, left MtII, proximal end (MHNT Pak 1164), dorsal view. Kumbi 4a; M, left fragmentary MtIII (MHNT Pak 2126), anterior view. Kumbi 5; N, left MtIV, distal end (MHNT Pak 1190), anterior view. Kumbi 4a. Scale bar = 2 cm.

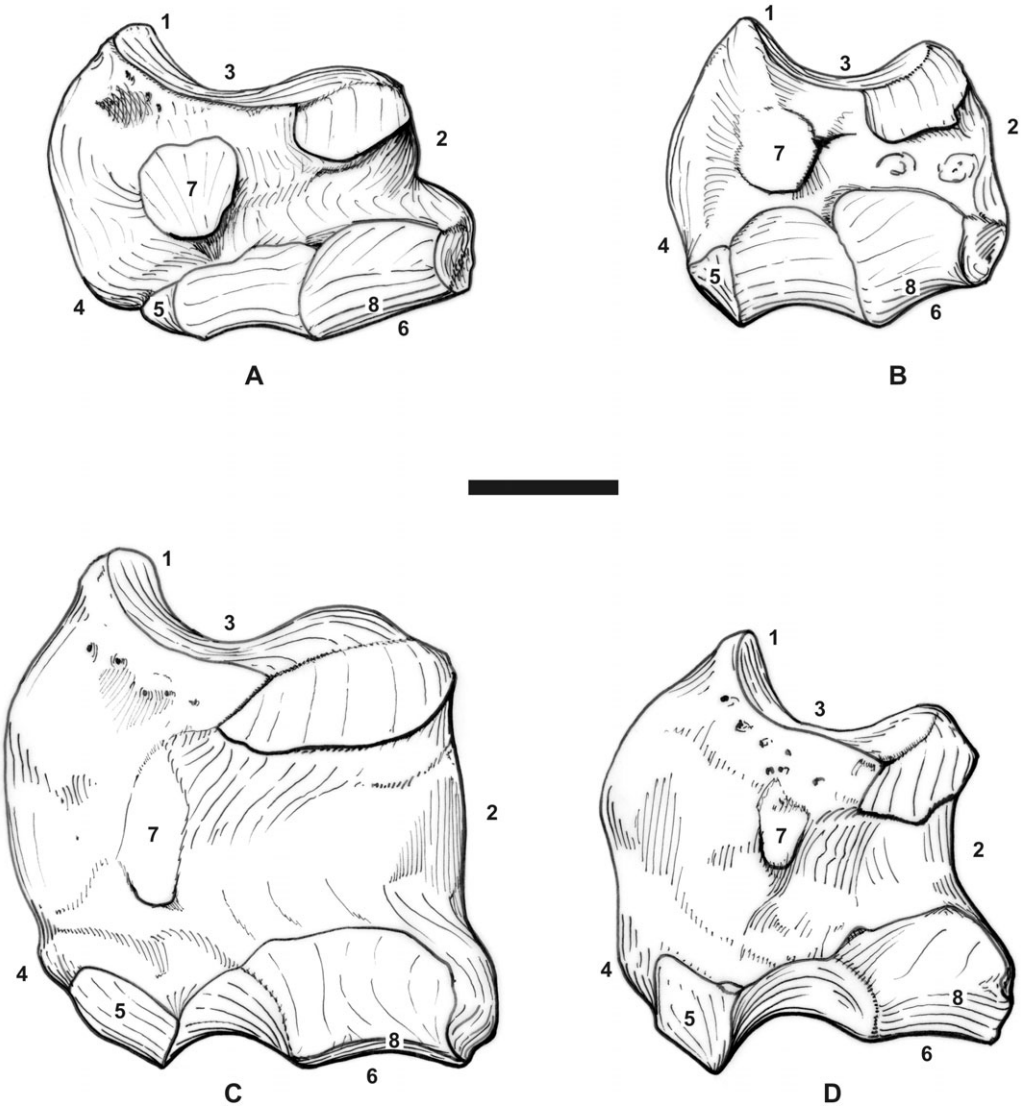

Figure 11. Morphological comparison amongst right scaphoids of four coeval fossil rhinocerotids (Early Miocene) referred to the genera *Pleuroceros* Roger, 1898 and *Mesaceratherium* Heissig, 1969, in lateral view. A, *Pleuroceros blanfordi* (Lydekker, 1884), Zinda Pir Dome, Pakistan; B, *Pleuroceros pleuroceros* (Duvernoy, 1853), Aquitaine Basin, France. 1. posterior height nearly equals anterior height; 2. robust and low bone; 3. shallow radial notch; 4. mediodistal tuberosity (thick in *P. blanfordi* but absent in *P. pleuroceros*); 5. small trapezium-facet; 6. flat magnum-facet; 7. prominent postero-proximal semilunate-facet; 8. no edge between anterodistal semilunate- and magnum-facets; C, ***Mesaceratherium welcommi* sp. nov.**, Zinda Pir Dome, Pakistan; D, *Mesaceratherium paulhiacense* (Richard, 1937), Aquitaine Basin, France. 1. posterior height much exceeding anterior height; 2. slender and elevate bone; 3. deep radial notch; 4. small mediodistal tuberosity; 5. large trapezium-facet; 6. concave magnum-facet; 7. no posteroproximal semilunate-facet (smooth pad); 8. sharp edge between anterodistal semilunate- and magnum-facets. (B) and (D) modified after de Bonis (1973). Scale bar = 2 cm.

of right M2 (MHNT Pak 1033); fragment of a worn right M1–2 (MHNT Pak 1063); fragment of a worn left M3 (MHNT Pak 1065); protoloph of a left M3 (MHNT Pak 1066); distal end of a left radius (MHNT Pak 1092); distal end of a left ulna (MHNT Pak 1184); right scaphoid (MHNT Pak 1099); left semilunate (MHNT Pak 1100); fragment of a left semilunate (MHNT Pak 1103); left pisiform (MHNT Pak 1107); broken left magnum (MHNT Pak 1109); right unciform (MHNT Pak 1111); distal end of a right tibia (MHNT Pak 1125); left astragalus (MHNT Pak 1134); left astragalus (MHNT Pak 1135); right astragalus (MHNT Pak 1136); medial part of a right astragalus (MHNT Pak 1144); fragment of an eroded right

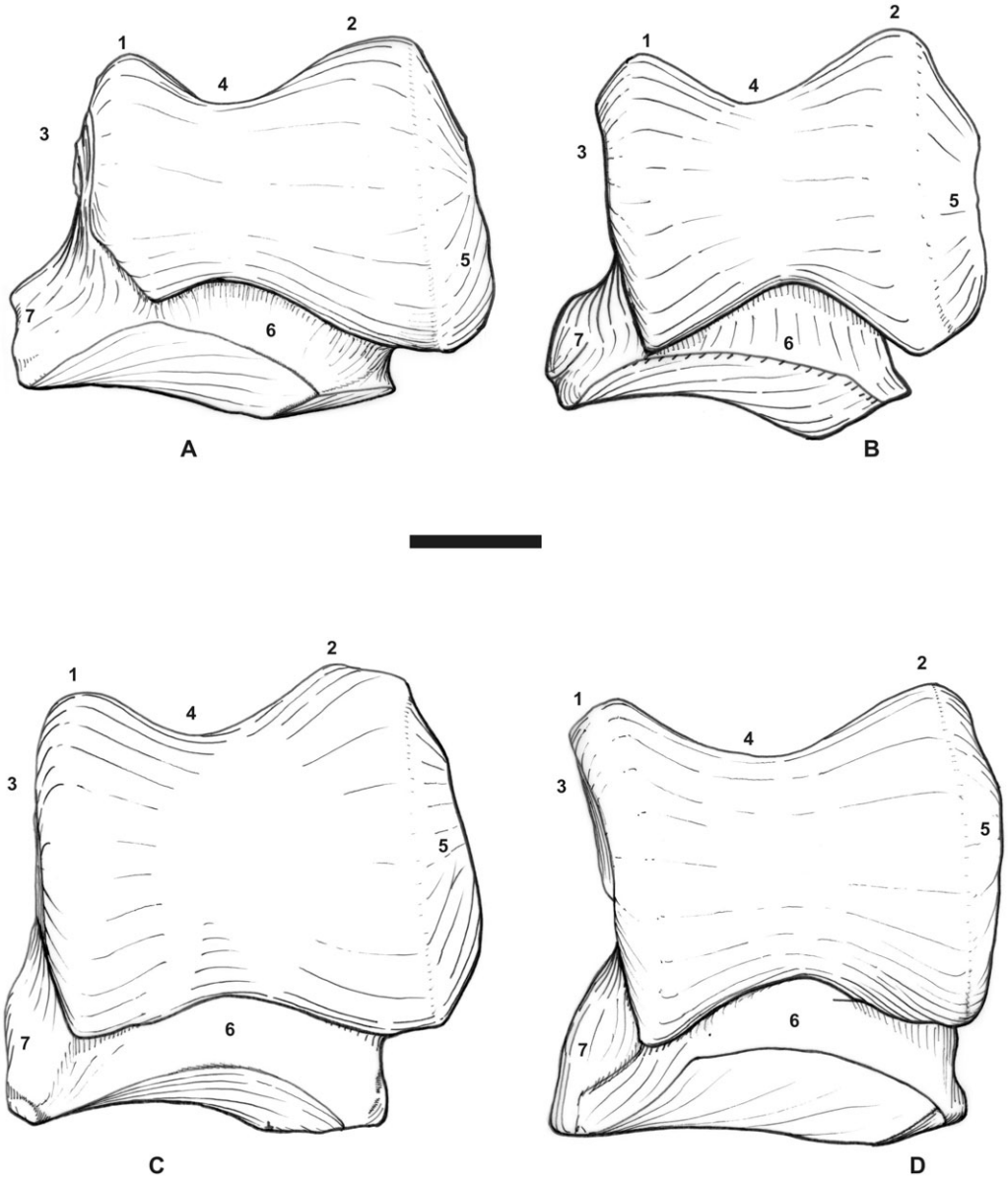

Figure 12. Morphological comparison amongst left astragali of four coeval fossil rhinocerotids (Early Miocene) referred to the genera *Pleuroceros* Roger, 1898 and *Mesaceratherium* Heissig, 1969, in lateral view. A, *Pleuroceros blanfordi* (Lydekker, 1884), Zinda Pir Dome, Pakistan; B, *Pleuroceros pleuroceros* (Duvernoy, 1853), Aquitaine Basin, France (reversed). 1. medial lip smaller than the lateral one; 2. lateral height much exceeding medial height; 3. robust, broad, and low bone; 4. deep trochlear notch; 5. broad and oblique fibula-facet; 6.high collum tali (with respect to total height); 7. medial tubercle low, salient, and laterally displaced.; C, ***Mesaceratherium welcommi* sp. nov.**, Bugti Hills, Pakistan; D, *Mesaceratherium paulhiacense* (Richard, 1937), Aquitaine Basin, France. 1. medial lip nearly equals the lateral one in size; 2. lateral height nearly equals medial height; 3. slender, narrow, and elevated bone; 4. narrow trochlear notch; 5. narrower and less oblique fibula-facet; 6.high collum tali (but lower with respect to total height); 7. medial tubercle high, smooth, and not-laterally displaced. (B) and (D) modified after de Bonis (1973). Scale bar = 2 cm.

astragalus (MHNT Pak 1145); left calcaneus (MHNT Pak 1147); right calcaneus (MHNT Pak 1149); right navicular (MHNT Pak 1153); left entocuneiform (MHNT Pak 1095); proximal end of a left Mt II (MHNT Pak 1164); distal end of a left Mt IV (MHNT Pak 1190). Kumbi 4c (Level 4, earliest Miocene). right P3 (MHNT Pak 77); distal end of a right tibia (MHNT Pak 70); right cuboid (MHNT Pak 851). Kumbi 4f (Level 4, earliest Miocene). Fragment of a right mandible with m1–3 (MHNT Pak 1648); broken left unci-

form (MHNT Pak 1709). Gandô 4 (Level 4, earliest Miocene). Right scaphoid (MHNT Pak 1868); medial fragment of a right astragalus (MHNT Pak 1873). Dera Bugti 4 (Level 4, earliest Miocene). Right cuboid (MHNT Pak 1990); posterior tuberosity of a right cuboid (MHNT Pak 1991). Kumbi 5 (Level 5, Early Miocene). Proximal end of a right Mt III (MHNT Pak 2126). Dera Bugti 5 (Level 5, Early Miocene). Left patella (MHNT Pak 1260). Dera Bugti 6 (Level 6, Early Miocene). Right M1 without ectoloph (MHNT Pak 165); left M2 without ectoloph (MHNT Pak 1435); left broken M2 (MHNT Pak 2203); fragment of a right M2 (MHNT Pak 1438); fragment of a right M3 (MHNT Pak 1437); proximal end of a left McV (MHNT Pak 1480). Dera Bugti 6sup (Level 6, Early Miocene). Proximal end of a left McII (MHNT Pak 1552); fragment of a right patella (MHNT Pak 2234). Zinda Pir Dome (Fig. 1).

Z147 (earliest Miocene). Right M1 (PMNH Z2268). Z139 (earliest Miocene). Right scaphoid (PMNH Z2046); left pyramidal (PMNH Z2048). Z143 (earliest Miocene). Left P2, right M2, left M3, and right M3 with 'fractured and dislocated partial maxilla' (PMNH Z2269; Downing, 2005: 3).

Description

Skull: The only available cranial element (PMNH Z2269C, from Zinda Pir) is fragmentary and dislocated (Downing, 2005: fig. 3). The anterior base of the zygomatic arch was high. The position of the anterior border of the orbit with respect to M3 is not observable.

Mandible: Three fragments are available (MHNT Pak 1023, 1054, 1196; Fig. 8J–M). The corpus mandibulae was about 440 mm long (from MHNT Pak 1023 + MHNT Pak 1196). The short symphysis is raised about 30° with respect to the corpus mandibulae, and a little more on MHNT Pak 1054 (Fig. 8K). It is thick, slightly constricted at the diastema level, and weakly widened in its anterior tip. The posterior border of the symphysis reaches the middle of p3, as does the foramen mentale (Fig. 8J–K). The latter is large, deep, and stretched sagittally. A sharp sagittal ridge runs on the dorsal border throughout the diastema, prior to joining the lingual side of the p1. The ventral side of the symphysis is convex in anterior view. There is a thick spina mentalis, forming a rounded axial tubercle at the caudal tip of the symphysis (MHNT Pak 1054). The spatium intermandibularis is very narrow near the symphysis: only 12–15 mm between the branches at the p4 level (Fig. 8L). No median sagittal groove (sulcus mylohyoideus) is present on the lingual side of the corpus mandibulae. The latter gets regularly higher backwards until m2, with a straight ventral border (Table 2). Behind, its height becomes constant. The horizontal branches deviate regularly. In cross-section, they are vertical. The angulus mandibulae, incompletely preserved (MHNT Pak 1196), is not very salient. The ramus mandibulae is vertical, with a processus coronoideus long and well developed sagittally, although broken (Fig. 8M). The foramen mandibulare is located below the neck line.

Dentition: The presence of upper incisors and i1 cannot be confirmed from the available material. Still, the alveoli of i2 are preserved on the mandible MHNT Pak 1023 (Fig. 8K). These incisors were subcircular in cross-section, parallel, and *c*. 25 mm away from one another. The cheek teeth formula is 4P–3M and 4p–3m. No P1 (or persistent D1) is known, but each P2 bears contact facets with the former. The upper premolar series is long with respect to the molar series: $L_{P3–4}/L_{M1–3} \times 100) \approx 52$. Some cement is visible on a few ectolophs, ectolophids, and in the bottom of some valleys (MHNT Pak 1648). There are no secondary enamel foldings (Fig. 8A–I). The enamel is thick and wrinkled throughout the crowns (lower and upper teeth). The crowns are low and conical; the roots are independent, long and divergent.

The labial cingulum is totally absent on the upper teeth except for an isolated spur at the posterior tip of the ectometaloph of M3. By contrast, the lingual cingulum is always present. It is high and thickly developed on the upper premolars, sometimes interrupted on the protocone (MHNT Pak 1038) and/or on the hypocone (MHNT Pak 1026, 1047). This cingulum is reduced to a tubercle at the entrance of the median valley on all the upper molars. On M2 MHNT Pak 1438 and 2203, it forms a transverse spur that splits the valley in two parts. The anterior and posterior cingula are thick and continuous. There is neither crista, nor cristella nor medifossette on the upper cheek teeth. The postfossette is narrow and as deep as the median valley (Fig. 8C, E–G, I).

The upper premolars are quadrangular, short, and wide (Fig. 8A–D; Table 4). The crochet is generally lacking at the observed stages of wear (12 specimens out of 16). When present, it is restricted to a short tubercle. The metaloph is continuous, lacking any constriction, but very thin until late stages of wear. However, a thin lingual bridge connects the protocone and hypocone much earlier on the upper premolars, but there is no antecrochet. The hypocone is posterior to the metacone on all premolars. On P2, the protocone is weaker than the hypocone. The protoloph is thin and usually complete, except on NHM M 15336. The anterior constriction of the protocone is weak but always present on P3–4. The protoloph is continuous

Table 4. ***Mesaceratherium welcommi*** **sp. nov.** Dental dimensions (range, number of specimens in square brackets, and mean, in mm) from the Early Miocene of the Bugti Hills (Balochistan, Pakistan)

Tooth	L	ant W	post W	H
P2	27–32.5	31–35	37–39.5	13–17
Mean	29.4 [5]	32.7 [4]	37.5 [6]	15.3 [3]
P3	32–38	47–50	46.5–51	17–20
Mean	34.9 [4]	48.5 [4]	48.1 [4]	18.5 [2]
P4	(> 35)–39	55	52	–
M1	(> 46)	(> 63)	(59)	22
M2	57–58	68	58	35
Mean	57.5 [2]	–	–	–
M3	54	61	L_{ect} = 63–64	43–43
Mean	–	–	63.5 [2]	43 [2]
p3	25	17	22.5	7
p4	32	22.5	30.5–32	10–13
Mean	–	–	31.2 [2]	11.3 [3]
m1	31–41	23–30	27.5–33	8–25
Mean	35.5 [5]	26.7 [4]	29.1 [4]	14.7 [4]
m2	39.5–49.5	26.5–29	29.5–32	10–14
Mean	44.5 [2]	27.7 [2]	30.7 [2]	12 [2]
m3	46.5–53.5	26.5–29	26–27.5	8–19
Mean	49.2 [3]	27.8 [3]	26.5 [3]	14.3 [3]

ant, anterior; H, height; L, length; L_{ect}, length of the ectometaloph; post, posterior; W, width. Approximate dimensions appear between brackets.

and thick on P3. The paracone fold is strong on the premolars, whereas the metacone fold is poorly developed or absent. The parastyle is sagittal.

The antecrochet, which is strongly detached on the upper molars, is oblique and very elongated, so that it joins the hypocone on worn molars (MHNT Pak 1049, 1063, 1065). The anterior constriction is very deep on the protocone, which gives a trefoil-shape to the protoloph (Fig. 8F–I). The crochet is always present, sagittal and generally simple (12 specimens out of 14). M3 MHNT Pak 1032b has a double crochet, whereas it is simple on the symmetric M3 of the same individual (MHNT Pak 1051) and on M3s PMNH Z2269. The ectoloph of M2 is straight, with a sagittal parastyle and a weak paracone fold. Only the most posterior part of the ectoloph is concave. The mesostyle is lacking, as is the metacone fold. The metastyle is long on M1–2. The M1 are rectangular and the M2 subrectangular, with a metaloph almost as long as the protoloph is (Table 4). The protocone is elongated sagittally, with a lingual side flattened on M2 and convex on M3, but without any lingual groove. The posterior cingulum is continuous but lowered next to the postfossette. On all the upper molars, especially on M2, the hypocone is strongly constricted by a deep anterior groove, still restricted to the base of the crown. On some M2 (MHNT Pak 1032a, 1435) there is also a shallow posterolingual constriction at the base of the hypocone. A few enamel tubercles can occur at the bottom of the median valley (MHNT Pak 1033, 1065, 2203; PMNH Z2269). On M3, the ectoloph and the metaloph are fused into an ectometaloph without any remaining groove. Yet, the M3 have a quadrangular outline, with a wide posterior part sustained by two diverging transverse roots (Fig. 8H).

All the available lower cheek teeth are worn (Fig. 8J–N). The presence of a one-rooted p1, or persistent d1, is revealed by a small alveolus located in front of the anterior alveolus of p2 (MHNT Pak 1023). Nevertheless, there is no trace of any tooth anterior to p2 on the symphysis MHNT Pak 1054, belonging to an old individual. There is no lingual cingulid on the lower cheek teeth, except on m3 MHNT Pak 1196 (small ridge at the entrance of the posterior valley). On most specimens, the labial cingulid is also absent. If not, it is reduced to a small ridge closing the ectolophid groove (MHNT Pak 1023). This sharp groove is interrupted above the neck. The trigonid is rounded, forming a right dihedron. The metaconid lacks any constriction at the available stages of wear. The lingual side of the metaconid is flat and very elongated sagittally (as is the protocone on the upper molars), thus forming a right dihedron with the posterior border of this cuspid. The entoconid is constricted on the lesser worn teeth (m1 MHNT Pak 1040, m2–3 MHNT Pak 1648). The posterior valley is narrow and V-shaped on both the premolars and m1–2, whereas it is wide and U-shaped on m3. The hypolophid of the molars is almost transverse. There is no lingual groove on the entoconid of m2–3. The posterior cingulid is weak, reduced to a smooth median tubercle on m3 (Fig. 8M).

No deciduous tooth has been unearthed.

Postcranial skeleton: The bones are large and slender (Figs 9–10; Tables 5–8, 10–12, 14–16, 18–22, 25–27). The rachis, the scapula, and the humerus are unknown.

The radius is represented by a distal end (MHNT Pak 1092; Fig. 9A–B). The diaphysis has a drop-like cross-section. The radius and the ulna were independent throughout their diaphysis: no trace of contact or synostosis is visible. The distal end is not much widened with respect to the diaphysis (Table 5). Only one distal ulna-facet is present, well developed and almond-shaped. The m. extensor carpi groove is wide and deepened by the strong tuberculum dorsale lying beside it. The distal articulation is wide. The scaphoid-facet is very short in its anterior part and very convex behind. This facet is deep (APD), with a wide and low triangular posterior expansion. The semilunate-facet is narrow whereas the pyramidal-

Table 5. *Pleuroceros blanfordi* (Lydekker, 1884) and ***Mesaceratherium welcommi* sp. nov.** Compared dimensions of the radii (range, number of specimens in square brackets, and mean, in mm) from the Early Miocene of the Bugti Hills (Balochistan, Pakistan)

	prox. ext.		proximal art.			Diaphysis		dist. ext.		dist. art.	
Taxon	TD	APD	TD	medAPD	latAPD	TD	APD	TD	APD	TD	APD
P. b.	77–78.5	48.5–51.5	77	40–44	24–26	39–46	26–28	80–82.5	56	(65)	(31)–32
Mean	77.7 [2]	50 [2]	–	42 [2]	25 [2]	42.5 [2]	27 [2]	81 [3]	–	–	–
M. w.	–	–	–	–	–	–	–	80	(53)	75	(40)

APD, anteroposterior diameter; art., articulation; dist., distal; ext., extremity; lat, lateral; med, medial; *M. w.*, *M. welcommi*; *P. b.*, *P. blanfordi*; prox., proximal; TD, transverse diameter. Approximate dimensions appear between brackets.

facet is very developed, transversally and sagittally. The latter forms a wide oblique band that extends onto the posterior side.

A distal end of an ulna is preserved (MHNT Pak 1184; Fig. 9C). There is no lateral tubercle. The cross-section of the diaphysis forms a flattened lozenge. On the medial side, the only radius-facet is spindle-shaped and oblique with respect to the vertical. The distal articulation corresponds only to the pyramidal and the pisiform. The pyramidal-facet is narrow (TD = 31; APD = 48), subrectangular and more rounded behind than anteriorly. The wide pisiform-facet forms a triangle restricted to the posterior side of the bone. This facet is very high.

The carpus is high and rather slender (Figs 9D–J, 11C; Tables 6–8, 10–11).

Three scaphoids have been collected. Even though their size range reaches *c*. 15% (Table 6), the morphology is identical. The APD and H are similar (Figs 9D–E, 11C). There is no tubercle on the medial side, but a shallow depression hollowing its antero-distal corner. The anterior border of this medial side is straight, inclined downwards, whereas the posterior border is vertical and regularly convex. The radius-facet is as wide (TD) as deep (APD). It is much upraised in its posterior part, so the bone is much less elevated anteriorly than posteriorly (Fig. 11C). On the lateral side, only two semilunate-facets are present. There is neither posteroproximal facet nor tubercle. The trapezium-facet is well developed, high, and narrow (APD). In distal view, the trapezoid-facet is rectangular, longer (APD) than wide (TD). The magnum-facet forms an equilateral triangle, transversally flat and sagittally concave.

The semilunate is high and narrow (Fig. 9F; Table 7). The anterior side bears a thick and angulous tubercle for the m. interossei dorsales. Its distal border is sharp. The magnum-facet reaches the anterior side of the bone. It is weakly hollow in its posterior part. The unciform-facet is oval and biconcave. The posterior tuberosity is narrow and higher than wide.

The pyramidal PMNH Z2048 is badly preserved and eroded. It is roughly cubic (TD ≈ 36; APD ≈ 45; anterior height ≈ 51). The proximal facet, for the ulna, is small. The pisiform-facet is eroded. Some parts of a strong tubercle remain on the lateral side. The medial facets for the semilunate are not preserved; yet the distal one probably had an asymmetric outline. On the distal side, the biconcave unciform-facet forms a quarter-circle in distal view.

Both trapezium and trapezoid are unknown.

The pisiform MHNT Pak 1107, doubtfully attributed to this taxon, is slender and elongated sagittally (Fig. 9G; Table 8). The pyramidal-facet is comma-like, whereas the ulna-facet is semicircular. The median part, between the articular area and the posterior tuberosity, is constricted.

A broken and large-sized magnum is available (MHNT Pak 1109; Table 10). The posterior tuberosity is not preserved (Fig. 9H). The anterior side, bearing a thick tubercle surrounded by sharp ridges, is higher than wide. The proximal border is straight. The semilunate-facet reaches the anterior side. It is long (APD) and slightly convex transversally, with a 'question-mark'-like lateral profile. In proximal view, the articular apophysis bears two dissymmetrical sides. The medial side is narrow and subvertical, restricted to the anterior side of the bone. The lateral one, for the semilunate, is much more developed laterally and sagittally. On the medial side, the articular facets are connected throughout their length (APD) and delimited by a sharp ridge. This ridge is anteriorly shortened by a shallow indentation. On the lateral side, the unciform-facet forms a narrow and elongated stripe. Distally, the McIII-facet has a sigmoid lateral border.

Two unciforms are attributed to this taxon (Fig. 9I–J). The anterior side is as high as wide (Table 11). The tubercles for the m. interossei dorsales are almost lacking, except for a small mediodistal pad. The posterior tuberosity is very long. Thus, the proximal articular area only reaches the anterior third of the bone. The proximal facets are triangular and sagit-

Table 6. *Pleuroceros blanfordi* (Lydekker, 1884) and ***Mesaceratherium welcommi* sp. nov.** Compared dimensions of the scaphoids (range, number of specimens in square brackets, and mean, in mm) from the Early Miocene of the Bugti Hills and of the Zinda Pir (Pakistan)

			Height			Rad.-fac.	Trapz.-fac.		Trapzd.-fac.		Mag.-fac.		
Taxon	TD	APD	ant	mid.	post	APD	H	APD	TD	APD	TD	APD	D SL- fac.
P. b.	39–43	58–60	40–40	30–33	44–44	37–39	12–16	6–7	28–28	20–22	22–24	22	9–9
Mean	41 [2]	60 [2]	40 [2]	31.5 [2]	44 [2]	38 [2]	14 [2]	6.5 [2]	28 [2]	21 [2]	23 [2]	22 [2]	9 [2]
M. w.	38.5–46.5	60–66.5	48–57	41.5–50	57–68	40–(46)	23–25	10–13	22–25	23–26	19–24	18–23	12–14
Mean	41.7 [3]	63 [3]	53.3 [3]	46.2 [3]	64 [3]	42.5 [2]	24 [2]	11.5 [2]	23.7 [3]	24.3 [3]	21.7 [3]	19.7 [3]	13 [2]

ant, anterior; APD, anteroposterior diameter; D, distance; fac., facets; H, height; Mag., magnum; mid., middle; *M. w.*, *M. welcommi*; *P. b.*, *P. blanfordi*; post, posterior; Rad., radius; TD, transverse diameter; Trapzd, trapezoid. Approximate dimensions appear between brackets.

tally convex. The semilunate-facet is flat transversally on MHNT Pak 1709 and slightly concave on MHNT Pak 1111. The pyramidal-facet, lacking any posterolateral expansion, is distant from the McV-facet. The latter is about 60° to the vertical line.

The metacarpus is only represented by two proximal ends (McII and McV; Fig. 9K–L).

McII MHNT Pak 1552 has a large proximal end, without any salient insertion for the m. extensor carpalis (Fig. 9K). In proximal view, the trapezoid-facet is pentagonal. The longest border is next to the lateral magnum-facet. This facet forms a curved stripe, vertical and elongated sagittally. The McIII-facets are distinct. The anterior facet is the most developed. It follows the magnum-facet, without marked edge between them. The posterior facet is reduced. A small trapezium-facet is present on the posteromedial side. It joins the proximal facet. The diaphysis has an oval cross-section, sagittally flattened (Table 12).

The McV was functional, with an elongated diaphysis (Fig. 9L; Table 14). The unciform-facet is convex and narrow sagittally. The adjoining McIV-facet is high (7 mm) and almond-shaped.

The femur and the fibula are unknown.

The patellae are damaged. The most complete (MHNT Pak 1260) is higher than wide (TD; Table 15). The muscular insertions are smooth on the anterior side. The most salient corresponds to the m. fascia lata. On the articular side, the medial lip is wide and triangular, not very hollow. The proximal border of the articular area is strongly delimited laterally. The distal tip is high and sharp, displaced outwards. The lateral lip is wide and very hollow.

Two distal ends of a tibia are preserved. They have different sizes (Table 16) but the same morphology. The anterior side is short of any anterodistal groove. At the contrary, the m. tibialis posterior groove is wide and deep on both specimens. The lateral border of the diaphysis shows high and wide (APD) rough scars corresponding to the contact with the fibula: this bone, although lacking, would have had a very developed sagittally distal end. The fibula-facet is small. The posteromedial apophysis is high and sharp. In distal view, the distal end forms a trapezium, with a straight anterior border and a high APD.

Six astragali are available, amongst which three are complete. The morphology is homogenous, but two series can be distinguished, with a size difference of *c*. 10–15% (Table 18). The astragalus is slightly wider than high (TD/H = 1.08; Figs 10A–C, 12C). It is robust in medial view (APD/H = 0.70; Fig. 10D). The fibula-facet is high, subvertical, and flat transversally. The collum tali, usually low, is high on one specimen (MHNT Pak 1135). The medial tubercle is not very

Table 7. *Pleuroceros blanfordi* (Lydekker, 1884) and ***Mesaceratherium welcommi* sp. nov**. Compared dimensions of the semilunates (mm) from the Early Miocene of the Bugti Hills (Balochistan, Pakistan)

					Magnum-fac.		Uncif.-fac.			
Taxon	TD	APD	H	post TD	TD	APD	TD	APD	D Scaph.- fac.	D Pyram.- fac.
P. b.	34	55	36	24	15	30	20	26	11	8
M. w.	(> 36)	61.5	50	27.5	16	41	25	31	–	–

ant, anterior; APD, anteroposterior diameter; D, distance; fac., facet(s); H, height; *M. w.*, *M. welcommi*; *P. b.*, *P. blanfordi*; post, posterior; Pyram., pyramidal; Scaph., scaphoid; TD, transverse diameter; Uncif., unciform. Approximate dimensions appear between brackets.

Table 8. ***Mesaceratherium welcommi* sp. nov.** Dimensions of the pisiform (mm) from the Early Miocene of the Bugti Hills (Balochistan, Pakistan)

		Tuberosity			
TD	APD	H	APD	Ulna-fac. TD	TD Pyram.-fac.
23.5	62.5	34	20	13	18

APD, anteroposterior diameter; fac., facet; H, height; Pyram., pyramidal; TD, transverse diameter.

Table 9. *Pleuroceros blanfordi* (Lydekker, 1884). Dimensions of the trapezoid (mm) from the Early Miocene of the Bugti Hills (Balochistan, Pakistan)

		Height			
TD	APD	ant	mid.	post	Trapz.-fac. min. APD
(21)	(30)	21	16.5	21	9

ant, anterior; APD, anteroposterior diameter; fac., facet(s); mid., middle; min, minimal; post, posterior; TD, transverse diameter; Trapz., trapezium. Approximate dimensions appear between brackets.

salient (Fig. 12C). In proximal view, the caudal border of the trochlea is nearly straight. On the posterior side, the calcaneus-facet 1 (see Heissig, 1972: pl. 13) is concave, with a long and narrow laterodistal expansion. The calcaneus-facets 2 and 3 are fused. In distal view, the axis of the trochlea is very oblique with respect to the distal articulation. The cuboid-facet forms an oblique stripe, posteriorly interrupted by a brutal inflexion. The navicular-facet is lozengic (Fig. 10B).

The calcaneus is robust (Table 19). The processus calcanei is short, with a wide and massive tuber calcanei (Fig. 10E–F). The latter is not very salient in lateral view, with a laterally displaced anterior tip. The beak is low, with a convex astragalus-facet, nearly angulous. There is a small fibula-facet (MHNT Pak 149), but no tibia-facet. The trochlea fibularis is marked by a sharp circular ridge. The sustentaculum tali is rather narrow. The astragalus-facets 2 and 3 are fused. On the distal side, the cuboid-facet is semicircular and biconcave.

The navicular MHNT Pak 1153 is low, with a lozengic outline (Fig. 10G–H; Table 20). The TD and APD are similar. In proximal view, the lateral border is concave. A small articular area is isolated on the astragalus-facet, in the posterolateral corner of the proximal side. This area touches the astragalus in the extreme flexion movements.

The cuboid is large and robust (Fig. 10I–J; Table 21). The anterior side is pentagonal. This side is inclined, with a set back proximomedial border. In proximal view, the articular region is subcircular, occupying half of the APD. It is split into two equal facets, weakly separated by a shallow sagittal groove. The medial facet is damaged on all the available specimens. The navicular-facet was high. The posterior tuberosity is wide and very high (Table 21). Its distal tip exceeds the distal articular faced by about 15 mm. In lateral view, the posterior border is vertical. The distal facet is triangular, long (APD), and narrow (TD).

The mesocuneiform and ectocuneiform are unknown.

A broken entocuneiform was attributed to this taxon owing to the shape of the navicular-facet, which fits with the available naviculars (Fig. 10K). In medial view, it forms a rectangle higher than wide (Table 22). The navicular-facet is subcircular and biconcave. Contiguous to it, the mesocuneiform-facet is comma-like. A tiny MtII-facet is present in the middle of the lateral side of the bone.

The metatarsus is documented by a fragment of MtII, a damaged MtIII, and a distal end of a MtIV. The preserved diaphyseal parts indicate that the metatarsals were long, slender, and not very curved (Tables 25–27).

Table 10. *Pleuroceros blanfordi* (Lydekker, 1884) and ***Mesaceratherium welcommi* sp. nov.** Compared dimensions of the magnums (range, number of specimens in square brackets, and mean, in mm) from the Early Miocene of the Bugti Hills (Balochistan, Pakistan)

					McIII-fac.	
Taxon	TD	ant H	H	SL-fac. APD	TD	APD
P. b.	(34)–34 [2]	(24.5)–27 [2]	45–(48) [2]	39–(43) [2]	(30)–31 [2]	–
M. w.	41.5	38	(63)	58	38	–

ant, anterior; APD, anteroposterior diameter; fac., facet; H, height; *M. w.*, *M. welcommi*; *P. b.*, *P. blanfordi*; SL, semilunate; TD, transverse diameter. Approximate dimensions appear between brackets.

Table 11. *Pleuroceros blanfordi* (Lydekker, 1884) and ***Mesaceratherium welcommi* sp. nov.** Compared dimensions of the unciforms (range, number of specimens in square brackets, and mean, in mm) from the Early Miocene of the Bugti Hills (Balochistan, Pakistan)

					post tuber.		SL-fac.		Pyram.-fac.		McV-fac.	
Taxon	TD	H	max APD	APD	TD	H	TD	APD	TD	APD	TD	APD
P. b.	48–51	44–46	61–67	54–58	29–30	19–22.5	23–(26)	23–28	24–26	28–29	(19)	(21)–(26)
Mean	49.2 [4]	44.5 [4]	63.7 [3]	56 [4]	29.7 [3]	20.8 [3]	23.3 [3]	25.7 [3]	24.7 [3]	28.5 [3]	–	22 [3]
M. w.	59–60	54–55	75	63	30	22	25–27	(26)–30	31–32.5	30	20	31
Mean	59.5 [2]	54.5 [2]	–	–	–	–	26.0 [2]	[2]	31.7 [2]	–	–	–

APD, anteroposterior diameter; fac., facet; H, height; max, maximal; McV, fifth metacarpal; *M. w.*, *M. welcommi*; *P. b.*, *P. blanfordi*; post, posterior; post tuber., posterior tuberosity; Pyram., pyramidal; SL, semilunate; TD, transverse diameter. Approximate dimensions appear between brackets.

Table 12. *Pleuroceros blanfordi* (Lydekker, 1884) and ***Mesaceratherium welcommi* sp. nov.** Compared dimensions of McII (range, number of specimens in square brackets, and mean, in mm) from the Early Miocene of the Bugti Hills (Balochistan, Pakistan)

	prox. art.		Trapzd.-fac.		lat. fac. H			diaphysis		dist. art.	
Taxon	TD	APD	TD	APD	ant	mil.	post	TD	APD	TD	APD
P. b.	(25)	(33)	(19)	(29)	12	8	14	24.5	15–15	33	31
Mean	–	–	–	–	–	–	–	–	15.0 [2]	–	–
M. w.	32.5	41	25	35	20	13	18	–	–	–	–

ant, anterior; APD, anteroposterior diameter; art., articulation; dist., distal; fac., facet; H, height; lat., lateral; *M. w.*, *M. welcommi*; *P. b.*, *P. blanfordi*; post, posterior; prox., proximal; TD, transverse diameter; Trapzd, trapezoid. Approximate dimensions appear between brackets.

The proximal end of Mt II has a semicircular outline in proximal view (Fig. 10L). The mesocuneiform-facet is triangular and biconcave, with smooth angles. On the lateral side, there are two distinct MtIII-facets. The anterior facet is large, circular and vertical, sagittally directed, and separated from the proximal facet. By contrast, the posterior facet joins the mesocuneiform-facet. The top of the entocuneiform-facet is preserved on the posteromedial side of the bone.

MtIII MHNT Pak 2126 bears a concave proximal border in anterior view (Fig. 10M). The proximal end is lacking any salient ligamentary insertion on its anterior side. In proximal view, the anterior border is regularly convex. The anterior MtIV-facet is vertical and triangular. The posterior one is not preserved. There is no cuboid-facet. The diaphysis widens distally. It is slender and flattened sagittally (Table 26). The insertion for the m. interossei is long, especially on the lateral side.

Table 13. *Pleuroceros blanfordi* (Lydekker, 1884). Dimensions of McIII (mean values appear in bottom line and number of specimens in square brackets) from the Early Miocene of the Bugti Hills (Balochistan, Pakistan)

	prox. art.		McIV-fac. D	Uncif.-fac.		Mag.-fac.		Diaphysis		dist. ext.	dist. art.	
L	TD	APD		TD	APD	TD	APD	TD	APD	TD	TD	APD
123	46–54	(>37)–40	7–11	30–35	37–38	14–19	18–25	37–42	14–17	47–(48)	39.5–42	33–34
–	50.2 [4]	39 [4]	11 [4]	33 [3]	37.5 [2]	16.7 [4]	21.6 [4]	39.8 [3]	15.3 [3]	–	40.7 [2]	33.5 [2]

APD, anteroposterior diameter; art., articulation; D, distance; dist., distal; ext., extremity; fac., facet; L, length; Mag., magnum; McIV, fourth metacarpal; prox., proximal; TD, transverse diameter; Uncif., unciform. Approximate dimensions appear between brackets.

Table 14. ***Mesaceratherium welcommi* sp. nov.** Dimensions of McV (mm) from the Early Miocene of the Bugti Hills (Balochistan, Pakistan)

TD	APD	McIV-fac.		Uncif.-fac. APD
		H	APD	
20.5	23	9	17	21

APD, anteroposterior diameter; fac., facet; H, height; McIV, fourth metacarpal; TD, transverse diameter; Uncif., unciform.

The diaphysis of MtIV MHNT Pak 1190 (Fig. 10N) has a triangular to oval cross-section, medially stretched. The distal trochlea is deeper (APD) than wide (TD), with a salient and sharp intermediate relief (Table 27). This relief is located on the lateral third of the trochlea. The latter is essentially concave transversally in its medial part.

Discussion

The hypodigm of '*Aceratherium blanfordi* Lydekker, 1884' as described successively by Lydekker (1884), Pilgrim (1912), and Forster-Cooper (1934) based on Bugti Hills specimens, included only a palate, a partial mandible, and three dozen upper and lower cheek teeth. With the exception of an unusual size range and a few morphological features on upper cheek teeth (coronary cement weak/abundant; low/high crown heights; lingual cingulum continuous/reduced on upper premolars; metaloph oblique/transverse on P2; antecrochet absent/present on P4; metacone fold absent/present and posterior cingulum reduced/continuous on M1–2; mesostyle absent/present on M2), it was virtually impossible to distinguish two taxa within the available sample.

Nevertheless, Lindsay *et al.* (2005: 6) described upper teeth and a portion of maxilla from the Early Miocene of the Zinda Pir, Pakistan, and referred them to an 'enigmatic large rhinocerotid', mentioning that 'of the fossils [Forster-Cooper (1934)] discussed, the specimens assigned to *Rhinoceros blandfordi* [· · ·] show the closest affinities' to it. Finally, this author concluded to their distinction, on the same grounds as discussed above, without assigning the Zinda Pir specimens to any known genus and species.

The new specimens from the Early Miocene of the Bugti Hills provide a new insight into this taxon. Associated cranials, mandibles, dentals, and postcranials found in the last decade by the MPFB allowed us (1) to split the sample of '*Aceratherium blanfordi* Lydekker, 1884' *sensu lato* into two consistent and homogeneous series ('*A. blanfordi*' *sensu stricto*, here referred to as *Pleuroceros blanfordi*, and a new taxon erected on the larger specimens); (2) to define further distinctive characters between them, especially on postcranials (Figs 11–12); and (3) to include the enigmatic large rhino from coeval deposits of the Zinda Pir (Lindsay *et al.*, 2005) within the latter sample, formerly referred to as '*Mesaceratherium* sp.' (Métais *et al.*, 2009). As a matter of fact, based on dimensions and morphology, the concerned remains cannot be assigned to other taxa described in the same deposits as listed by Métais *et al.* (2009), such as the hippo-like teleoceratines *Brachypotherium fatehjangense* (Pilgrim, 1910), *Brachypotherium gajense* (larger and much more robust), and *Prosantorhinus shahbazi* (small and brachypod), the tiny and minute *Protaceratherium* sp., *Plesiaceratherium naricum* (rhinocerotines), *Bugtirhinus praecursor* (elasmotheriine), and the modern-like rhinocerotines *Gaindatherium* cf. *browni* and 'Rhinocerotina indet., cf. *Rhinoceros*'.

Once its hypodigm is completed – with *c*. 80 available remains – this large and slender taxon differs significantly from *P. blanfordi* in a large amount of features, amongst which are (1) a mandibular character (symphysis upraised); (2) three general dental characters (cement less abundant; lower tooth crowns; distinct roots on cheek teeth); (3) 17 characters of the upper dentition (neither labial cingulum nor crochet, but continuous lingual cingulum on

Table 15. *Pleuroceros blanfordi* (Lydekker, 1884) and ***Mesaceratherium welcommi* sp. nov**. Compared dimensions of the patellae (range, number of specimens in square brackets, and mean, in mm) from the Early Miocene of the Bugti Hills (Balochistan, Pakistan)

		APD			Articulation			lat. trochl.	
Taxon	TD	max.	min.	H	TD	H	TD med. trochl.	TD	H
P. b.	(73)–73.5	(33)–44	27–35	(61)–82	61	56–64	35.5	25–25.5	42
Mean	–	42.0 [3]	33.0 [4]	76.3 [4]	61	60 [2]	35.5	25.3 [3]	42
M. w.	–	53–55	(36)–(39)	(> 97)	–	–	–	29	–
Mean	–	54.0 [2]	–	–	–	–	–	–	–

APD, anteroposterior diameter; H, height; lat., lateral; max, maximal; med., medial; min, minimal; *M. w.*, *M. welcommi*; *P. b.*, *P. blanfordi*; TD, transverse diameter; trochl., trochlea. Approximate dimensions appear between brackets.

Table 16. *Pleuroceros blanfordi* (Lydekker, 1884) and ***Mesaceratherium welcommi* sp. nov**. Compared dimensions of the tibiae (range, number of specimens in square brackets, and mean, in mm) from the Early Miocene of the Bugti Hills (Balochistan, Pakistan)

					Astragalus-cochlea			
	Diaphysis		dist. ext.			APD		
Taxon	TD	APD	TD	APD	TD	med.	mid.	lat.
P. b.	47–47	33.5–36	73–78.5	(50)–57.5	59–(67)	35–39	25–32	40–(43)
Mean	47 [2]	34.5 [3]	76.1 [4]	52.9 [4]	60.0 [4]	37.0 [3]	29.7 [4]	41.2 [4]
M. w.	74	43	93	66–75.5	71	(52)–55	41.5	47
Mean	–	–	–	70.7 [2]	–	–	–	–

APD, anteroposterior diameter; dist., distal; ext., extremity; med., medial; mid., middle; *M. w.*, *M. welcommi*; *P. b.*, *P. blanfordi*; TD, transverse diameter. Approximate dimensions appear between brackets.

Table 17. *Pleuroceros blanfordi* (Lydekker, 1884). Dimensions of the fibula (mm) from the Early Miocene of the Bugti Hills (Balochistan, Pakistan)

Diaphysis		dist. ext.		Tibia-fac.		Astrag.-fac.	
TD	APD	TD	APD	APD	H	APD	H
12	18.5	25	37.5	17	7	26	18

APD, anteroposterior diameter; Astrag., astragalus; dist., distal; ext. extremity; fac., facet; H, height; TD, transverse diameter.

upper premolars; hypocone posterior to metacone on P2; medifossette always absent and protocone constriction always present on P3–4; no antecrochet on P4; labial and lingual cingula always present but no crista on upper molars; continuous posterior cingulum and no metacone fold on M1–2; no mesostyle on M2); (4) 11 characters of the lower dentition (no lower canine; V-shaped ectolophid groove, rounded trigonid, entoconid constriction present but no metaconid constriction on lower cheek teeth; neither lingual nor labial cingulum on lower premolars; d1 usually retained in adults; lingual and labial cingula usually absent and transverse hypolophid on lower molars); and (5) 15 postcranial characters (posterior expansion of the scaphoid-facet low on the radius; large trapezium-facet on the scaphoid; distal border of the keeled anterior side acute on the lunate; no posterior expansion on the pyramidal-facet of the unciform posterior McIII-facet present on McII; functional McV; insertion of the M. extensor carpalis flat on metacarpals; tibia and fibula in contact; posterior apophysis acute on the tibia; calcaneus-facets 2 and 3 fused and fibula-facet always present on the astragalus; tuber calcanei massive; no posterior MtII-facet on MtIII; insertion of the M. interossei long on lateral metapodials). About a third of these features are morphoclines based on frequency (see the Phylogenetic relationships section below), i.e. their recognition as distinct character states necessitates a wide sample.

However, and thanks to the phylogenetic analysis detailed in the next section, this new species appears to be unambiguously referable to the hornless

Table 18. *Pleuroceros blanfordi* (Lydekker, 1884) and ***Mesaceratherium welcommi* sp. nov**. Compared dimensions of the astragali (range, number of specimens in square brackets, and mean, in mm) from the Early Miocene of the Bugti Hills (BH) and of the Zinda Pir Dome (ZP), Pakistan

				Height			Calc.-fac.1		Calc.-fac.2		distal art.		Cub.-art.	
Taxon	max TD	TD trochl.	max APD	med.	mid.	lat.	TD	H	TD	H	maxTD	APD	L	W
P. b. (BH)	71.5–75.5	59–62.5	47–49.5	54–62	48–51	(58)–64.5	26–30	43	22–25	25–33	56–62	29–35	38–43	13–17
Mean	73.6 [5]	61.0 [6]	48.1 [5]	58.1 [7]	49.5 [5]	62.5 [5]	28.5 [6]	37.0 [2]	23.7 [4]	29.0 [2]	59.4 [5]	32.2 [4]	40.5 [2]	15.4 [5]
P. b. (ZP)	(71)–73	59	44	52	48	58–(62)	(29)	42	27	–	–	–	–	18
Mean	–	–	–	–	–	–	–	–	–	–	–	–	–	–
M. w. (BH)	73–85	64–76	50.5–57	66–75	57–62	70–77	34–42	45–50	26–28	36–40	63–71	35–41	39–42	15–16
Mean	80.3 [3]	70.0 [3]	53.1 [4]	71.5 [4]	60.3 [3]	74.3 [3]	38.3 [3]	47.7 [3]	27.0 [3]	38 [3]	67.1 [4]	39.0 [3]	40.5 [2]	15.3 [3]

APD, anteroposterior diameter; art., articulation; Calc., calcaneus; Cub., cuboid, fac., facet; lat., lateral; H, height; L, length; max, maximal; med., medial; mid., middle; *M. w.*, *M. welcommi*; *P. b.*, *P. blanfordi*; TD, transverse diameter; W, width. Approximate dimensions appear between brackets.

Table 19. *Pleuroceros blanfordi* (Lydekker, 1884) and ***Mesaceratherium welcommi* sp. nov**. Compared dimensions of the calcanei (range, number of specimens in square brackets, and mean, in mm) from the Early Miocene of the Bugti Hills (Balochistan, Pakistan)

			Tuberosity						Astrag.-fac.3		Cub.-fac.	
Taxon	H	H art.	TD	APD	Beak APD	sust. TD	min. TD post.	min. APD post	TD	H	TD	H
P. b.	(97)–105	56–59	39–44	55–63	53–(54)	(67)	30–38	41–49	22–27	8–11	19	–
Mean	104.0 [2]	57.5 [2]	42.2 [3]	59.7 [3]	–	–	35.3 [3]	45.3 [2]	24.5 [2]	9.7 [3]	–	
M. w.	122–126	73–75	45–45	59–59.5	57–57	(> 69)–70	30.5–(< 35)	50–51.5	–	12	23.5–23.5	43–44
Mean	124.0 [2]	74.0 [2]	45.0 [2]	59.2 [2]	57.0 [2]	–	–	50.7 [2]	–	–	23.5 [2]	43.5 [2]

APD, anteroposterior diameter; art., articulation; Astrag., astragalus; Cub., cuboid; fac., facet; min, minimal; H, height; *M. w.*, *M. welcommi*; *P. b.*, *P. blanfordi*; sust., sustentaculum tali; TD, transverse diameter. Approximate dimensions appear between brackets.

Table 20. *Pleuroceros blanfordi* (Lydekker, 1884) and ***Mesaceratherium welcommi* sp. nov.** Compared dimensions of the naviculars (range, number of specimens in square brackets, and mean, in mm) from the Early Miocene of the Bugti Hills (Balochistan, Pakistan)

			Height			
Taxon	TD	APD	ant	mid.	post	prox. art. APD
P. b.	38–39	56	22	19	24–24	50.5
P. b.	38.5 [2]	–	–	–	24 [2]	–
M. w.	44	50	24	18	26	42

ant, anterior; APD, anteroposterior diameter; art., articulation; mid., middle; *M. w.*, *M. welcommi*; *P. b.*, *P. blanfordi*; post, posterior; prox., proximal; TD, transverse diameter.

Table 21. *Pleuroceros blanfordi* (Lydekker, 1884) and ***Mesaceratherium welcommi* sp. nov**. Compared dimensions of the cuboids (range, number of specimens in square brackets, and mean, in mm) from the Early Miocene of the Bugti Hills (Balochistan, Pakistan)

	TD			H		proximal art.		distal art.		Medial face	
Taxon	ant	post	APD max	ant	post	TD	APD	TD	APD	antD	postH
P. b.	34–38	39.5–39.5	53.5–61	30.5–32.5	42–42	32–32	37–37	28–30	33–36.5	12	18–20
Mean	36.0 [2]	39.5 [2]	57.2 [2]	31.5 [2]	42.0 [2]	32.0 [2]	37.0 [2]	29.0	34.7 [2]	–	19.0 [2]
M. w.	37–40	40–(41)	68	37.5–40	(53)–56	(39)–40	(39)–40	33–34	41–(43)	–	–
Mean	38.5 [2]	–	–	38.7 [2]	–	–	–	33.5 [2]	–	–	–

ant, anterior; APD, anteroposterior diameter; art., articulation; D, distance; H, height; max, maximal; *M. w.*, *M. welcommi*; *P. b.*, *P. blanfordi*; post, posterior; TD, transverse diameter. Approximate dimensions appear between brackets.

Table 22. ***Mesaceratherium welcommi* sp. nov**. Dimensions of the entocuneiform (mm) from the Early Miocene of the Bugti Hills (Balochistan, Pakistan)

			Navic.-fac.		Mesocf.-fac.		
TD	APD	H	TD	APD	TD	H	D ant. fac.
(31)	19	42	14	20	25	13	14

ant, anterior; APD, anteroposterior diameter; D, distance; fac., facets; H, height; Mesocf., mesocuneiform; Navic., navicular; TD, transverse diameter. Approximate dimensions appear between brackets.

rhinocerotine genus *Mesaceratherium* Heissig, 1969, so far restricted to the Late Oligocene and Early Miocene of western Europe, in sharing at least three synapomorphies: a strong paracone fold on M1–2, a posterior McIII-facet on McII, and no posterior MtII-facet on MtIII. Within this monophyletic genus, the Bugti species is more closely related to the Late Oligocene species *M. gaimersheimense* Heissig, 1969 in having a lingual bridge on P2–4, whereas the lingual cusps are separate in the Early Miocene species *M. paulhiacense* (Richard, 1937).

It appears as further distinct from *M. gaimersheimense* in possessing an upraised mandibular symphy-

Table 23. *Pleuroceros blanfordi* (Lydekker, 1884). Dimensions of the mesocuneiform (mm) from the Early Miocene of the Bugti Hills (Balochistan, Pakistan)

			Ectocun.-fac.		Entocun.-fac.	
TD	APD	H	APD	H	TD	H
20	29.5	14	12	8	12	3

APD, anteroposterior diameter; Ectocun., ectocuneiform; Entocun., entocuneiform; fac., facet; H, height; TD, transverse diameter.

sis, a foramen mentale below the middle of p3, a thick and continuous protoloph on P2, a crochet on all upper molars, a constricted entoconid but no lingual cingulum on lower premolars, and occasionally no d1/p1.

Mesaceratherium welcommi sp. nov. can be distinguished from *M. paulhiacense* (Richard, 1937) by the presence of a lingual bridge on upper premolars (molariform in *M. paulhiacense*), of a labial cingulum on upper molars, and the absence of a mesostyle on M2, in the curved magnum-facet and fused McIII-facets on McII, fused calacaneus-facets 2 and 3 on the astragalus, the presence of a fibula-facet on the calcaneus, the proximal border of MtIII concave in anterior view, and in showing a distal widening of the diaphysis of MtIII. Other postcranial features are shared by both species (Figs 11C–D, 12C–D), but were not controlled in *M. gaimersheimense*, the postcranial skeleton of which is virtually unknown (Heissig, 1969; Laudet & Antoine, 2004).

Finally, *M. welcommi* sp. nov. differs from all other species of *Mesaceratherium* in having a shorter premolar series, a hypocone posterior to the metacone and stronger than the protocone on P2, a protocone slightly constricted on P3–4 and deeply constricted on M1–2, lower cheek teeth with a constricted entoconid, and lower premolars without labial cingulum.

Based on current phylogenetic results and contrary to what was stated by Antoine *et al.* (2006), *M. gaimersheimense* Heissig, 1969 cannot be considered as a junior synonym of *M. paulhiacense* (Richard, 1937): the former can be distinguished from the latter in possessing a very upraised mandibular symphysis (upraised in *M. paulhiacense*), a lingual bridge on upper premolars (lingual cusps separate), an interrupted protoloph on P2 (continuous), a labial cingulum always present (always absent) and a crochet

Table 24. *Pleuroceros blanfordi* (Lydekker, 1884). Dimensions of the ectocuneiform (mm) from the Early Miocene of the Bugti Hills (Balochistan, Pakistan)

			Navic.-fac.	
TD	APD	H	TD	APD
35.5	42	20	28	36

APD, anteroposterior diameter; fac., facet; H, height; Navic., navicular; TD, transverse diameter.

Table 25. *Pleuroceros blanfordi* (Lydekker, 1884) and ***Mesaceratherium welcommi* sp. nov.** Compared dimensions of MtII (range, number of specimens in square brackets, and mean, in mm) from the Early Miocene of the Bugti Hills (Balochistan, Pakistan)

		prox.art.		Mesocun.-fac.		Diaphysis		dist. art.	
Taxon	L	TD	APD	TD	APD	TD	APD	TD	APD
P. b.	101.5	(21)–22.5	34.5	16–20	26	21	19	28–30	28.5–29
Mean	–	–	–	18 [2]	–	–	–	29 [2]	28.7 [2]
M. w.	–	(24)	(35)	17	28	–	–	–	–

APD, anteroposterior diameter; art., articulation; dist., distal; L, length; Mesocun., mesocuneiform; *M. w.*, *M. welcommi*; *P. b.*, *P. blanfordi*; prox., proximal; TD, transverse diameter. Approximate dimensions appear between brackets.

Table 26. *Pleuroceros blanfordi* (Lydekker, 1884) and ***Mesaceratherium welcommi* sp. nov**. Compared dimensions of MtIII (mm) from the Early Miocene of the Bugti Hills (Balochistan, Pakistan)

	prox. art.			Diaphysis			dist. art.	
Taxon	TD	APD	TD diag.	TD	APD	max TD dia.	TD	APD
P. b.	41	(34)	24.5	32	15.5	–	–	–
P. b.	–	–	–	–	–	44	36	31.5
P. b.	–	–	–	33	16	42.5	36	30
P. b.	–	–	–	31.5	(17)	47	35	32.5
M. w.	50	–	–	39.5	–	–	–	–

APD, anteroposterior diameter; art., articulation; dia., diaphysis; diag., diagonal; dist., distal; max., maximal; *M. w.*, *M. welcommi*; *P. b.*, *P. blanfordi*; prox., proximal; TD, transverse diameter. Approximate dimensions appear between brackets.

Table 27. *Pleuroceros blanfordi* (Lydekker, 1884) and ***Mesaceratherium welcommi* sp. nov**. Compared dimensions of MtIV (range, number of specimens in square brackets, and mean, in mm) from the Early Miocene of the Bugti Hills (Balochistan, Pakistan)

		prox. ext.		prox. art.		medial facets				Diaphysis			dist. art.	
Taxon	L	TD	APD	TD	APD	antAPD	antH	postAPD	postH	TD	APD	Max TD dia.	TD	APD
P. b.	107	31–36	35.5–37.5	25–26	30–32.5	14–15	12–15	16–(18)	12–14	22–23	16–20	34–34	32–32	31–33
P. b.	–	34.0 [3]	36.3 [3]	25.7 [3]	31.2 [3]	14.7 [3]	13.7 [3]	16 [2]	13 [3]	22.5 [2]	18.0 [2]	34.0 [2]	32.0 [2]	32.0 [2]
M. w.	–	–	–	–	–	–	–	–	–	29	20	32	32	36

ant, anterior; APD, anteroposterior diameter; art., articulation; dia., diaphysis; dist., distal; ext., extremity; H, height; L, length; max, maximal; *M. w.*, *M. welcommi*; *P. b.*, *P. blanfordi*; post, posterior; prox., proximal; TD, transverse diameter. Approximate dimensions appear between brackets.

usually absent (always present) on upper molars, and the mesostyle absent (present) on M2.

Mandibular dimensions fit the average dimensions of Recent *Dicerorhinus sumatrensis*, but postcranials are larger: their size corresponds to the mean values observed in Recent *Diceros bicornis* (Guérin, 1980). Moreover, most postcranial bones referred to *M. welcommi* sp. nov. can be split into two series, with a size difference reaching 10–15% on the scaphoids, tibias, and astragali (Tables 6, 16, 18). This might be interpreted as a sexual dimorphism based on size, as observed in other rhinocerotoids (Antoine *et al.*, 2004; Mihlbachler, 2005). Yet, no morphological evolution has been observed between the specimens originating from level 4 (earliest Miocene, ≈ Aquitanian, ≈ MN2) on the one hand, and levels 5, 6, and 6sup (Early Miocene, ≈ Early Burdigalian', ≈ MN3), on the other.

PHYLOGENETIC RELATIONSHIPS

METHODS

Basically, the data set (character list, character states) is that of Antoine (2002, 2003) and Antoine *et al.* (2003b), with 282 morphological characters (52 cranial, ten mandibular, 100 on permanent cheek teeth, 20 on deciduous teeth, and 100 postcranial), originally used for proposing a phylogeny of Elasmotheriina within Rhinocerotidae.

The inclusion of intraspecifically variable characters (caused either by sexual dimorphism, individual, and/or ontogenetic variations) in a cladistic analysis has been debated for decades. As they 'can contain useful phylogenetic information' (Wiens, 2001: 690), such characters have been included in the current analysis. All of them were treated the same way as character 264 (Appendix 1), which corresponds to the presence/absence of a fibula-facet on the calcaneus. This facet is always absent in several taxa (in 29 specimens of the recent rhinocerotine *Diceros bicornis*; Guérin, 1980: 131), always present in others [in 14 specimens of the elasmotheriine *Hispanotherium beonense* (Antoine, 1997)], and absent in 15 specimens out of 18 for *Plesiaceratherium mirallesi* (Crusafont, Villalta & Truyols, 1955). Therefore, the binary states ('0, absence; 1, presence') were replaced by multistate quantitative states based on frequency ['0, always absent (100%); 1, generally absent (50–99%); 2, generally present (50–99%); 3, always present (100%)'], as detailed by Antoine (2002, 2003). The corresponding characters are additive and considered as morphoclines.

All the characters have an equal weight. Characters 72, 94, 102, and 140 are unordered whereas all other characters are ordered (Wagner parsimony).

Table 28. Character coding sources (direct observation and/or literature) for each terminal taxon included within the present phylogenetic analysis

	Character coding (source)	
Terminal	Direct observation	Literature
Aceratherium incisivum Kaup, 1832	MHNT; MNHN	Kaup, 1832; Guérin, 1980; Hünermann, 1989
Alicornops simorrense (Lartet, 1851)	MHNT; MNHN; NHM	Guérin, 1980; Cerdeño & Sánchez, 2000
Brachypotherium brachypus (Lartet, 1837)	MHNT; MNHN; UCBL	Roman & Viret, 1930, 1934; Guérin, 1980; Ginsburg & Bulot, 1984; Cerdeño, 1993
Bugtirhinus praecursor Antoine & Welcomme, 2000	MHNT; pers. obs. (P.-O. A.)	Antoine & Welcomme, 2000
Diaceratherium aginense (Répelin, 1917)	MHNT; MHNH; UCBL; Rhinopolis	Répelin, 1917; de Bonis, 1973
Diceratherium armatum Marsh, 1875	AMNH	Prothero, 2005
Dicerorhinus sumatrensis (Fischer Von Waldheim, 1814)	MNHN	Cuvier, 1822; Guérin, 1980
Diceros bicornis (von Linnaeus, 1758)	MNHN	Guérin, 1980
Gaindatherium browni Colbert, 1934	AMNH; HUPM	Colbert, 1934; Heissig, 1972
Hispanotherium beonense (Antoine, 1997)	MHNT	Antoine, 2002, 2003; Antoine, Bulot & Ginsburg, 2000
Hyrachyus eximius Leidy, 1871	AMNH	Leidy, 1871
Lartetotherium sansaniense (Lartet, 1837)	MHNT; MNHN; NHM	Klaits, 1973; Guérin, 1980
Menoceras arikarense (Barbour, 1906)	AMNH	Tanner, 1969; Prothero, 2005
Mesaceratherium paulhiacense (Richard, 1937)	MHNT; Rhinopolis	Richard, 1937; de Bonis, 1973
Mesaceratherium gaimersheimense Heissig, 1969	MHNT	Heissig, 1969; Laudet & Antoine, 2004; Antoine *et al.*, 2006
***Mesaceratherium welcommi* sp. nov.**	MHNT; HUPM	Falconer & Cautley, 1846; Pilgrim, 1912; Forster-Cooper, 1934; Lindsay *et al.*, 2005
Plesiaceratherium mirallesi (Crusafont, Villalta & Truyols, 1955)	MHNT; MNHN; UCBL	Crusafont *et al.*, 1955; Yan & Heissig, 1986; Antoine *et al.*, 2000
Pleuroceros pleuroceros (Duvernoy, 1853)	MHNL; UCBL; Rhinopolis; MNHN	Duvernoy, 1853; de Bonis, 1973
Pleuroceros blanfordi (Lydekker, 1884) **comb. nov.**	MHNT; HUPM	Lydekker, 1884; Pilgrim, 1912; Forster-Cooper, 1934
Prosantorhinus douvillei (Osborn, 1900)	MHNT; MNHN; UCBL	Wermelinger, 1998; Antoine *et al.*, 2000
Protaceratherium albigense (Roman, 1912)	MHNT; FSL	Duvernoy, 1853; Roman, 1912; Antoine *et al.*, 2008; Lihoreau *et al.*, 2009
Protaceratherium minutum (Cuvier, 1822)	MHNT; MNHN; UCBL	Roman, 1924; de Bonis, 1973
Rhinoceros unicornis von Linnaeus, 1758	MNHN	Blainville, 1839; Guérin, 1980
Subhyracodon occidentalis (Leidy, 1851)	–	Scott, 1941; Prothero, 1998, 2005
Ronzotherium filholi (Osborn, 1900)	LGPH; MHNT	Osborn, 1900; Heissig, 1969; Brunet, 1979
Tapirus terrestris (von Linnaeus, 1758)	MHNT, MNHN AC	Blainville, 1839
Trigonias osborni Lucas, 1900	AMNH	Lucas, 1900; Wood, 1927; Scott, 1941; Prothero, 2005

Taxa are arranged in alphabetical order. The 'direct observation' column indicates the institution where the material is stored.

Gaps are treated as 'missing'. Using PAUP 4.0 v.10 (Swofford, 1998), starting trees were obtained via stepwise addition, and heuristic islands were avoided by multiple starts with random taxon additions (1000 replicates).

TAXONOMIC SAMPLING

Twenty-eight terminal taxa were included in the phylogenetic analysis (Table 28). Four terminals were selected as outgroups: the extant tapirid *Tapirus terrestris* von Linnaeus, 1758, the Eocene

hyrachyid rhinocerotoid *Hyrachyus eximius* Leidy, 1871, the Eocene rhinocerotid *Trigonias osborni* (Lucas, 1900) from North America, and the Oligocene rhinocerotid *Ronzotherium filholi* (Osborn, 1900) from Europe.

The ingroup *sensu lato* consists of both taxa of interest (in-group *sensu stricto*: exhaustive specific sampling for *Mesaceratherium* Heissig, 1969 and *Pleuroceros* Roger, 1898) and selected taxa forming a 'branching group', *sensu* Antoine (2002).

The ingroup *sensu stricto* includes *P. blanfordi* Lydekker (1884), *M. welcommi* sp. nov. (Early Miocene of Pakistan), and all other known species of *Mesaceratherium* Heissig, 1969 [*M. paulhiacense* (Richard, 1937) and *M. gaimersheimense* Heissig, 1969, from around the Oligocene–Miocene limit in Europe] and *Pleuroceros* Roger, 1898 [*P. pleuroceros* (Duvernoy, 1853), from the Early Miocene of Europe].

The branching group includes (1) type species or well-represented species of type genera of suprageneric groups recognized within Rhinocerotidae; and (2) early representatives of these suprageneric groups, in order to branch the taxa of interest within the Rhinocerotidae, to define their generic and suprageneric affinities, and to avoid long-branch attraction artefacts because of parallelism (e.g. late representatives of Elasmotheriinae vs. Rhinocerotinae; Antoine, 2002). The present branching group comprises well-known Elasmotheriinae (early Elasmotheriina: *Hispanotherium beonense* (Antoine, 1997) and *Bugtirhinus praecursor* Antoine & Welcomme, 2000 from the Early Miocene of Europe and Pakistan, respectively; Menoceratina: *Menoceras arikarense* (Barbour, 1906), from the Early Miocene of North America; 'diceratheres': *Diceratherium armatum* Marsh, 1875 and *Subhyracodon occidentalis* (Leidy, 1851), from the Oligocene of North America) and Rhinocerotinae (Rhinocerotina: *Rhinoceros unicornis* von Linnaeus, 1758, *Diceros bicornis* (von Linnaeus, 1758), and *Dicerorhinus sumatrensis* (Fischer Von Waldheim, 1814) (recent), *Lartetotherium sansaniense* (Lartet, 1837) and *Gaindatherium browni* Colbert, 1934, from the Miocene of Europe and South Asia, respectively (extinct); Teleoceratina: *Brachypotherium brachypus* (Lartet, 1837), *Prosantorhinus douvillei* (Osborn, 1900), and *Diaceratherium aginense* (Répelin, 1917), from the Early and/or Middle Miocene of Europe; Aceratheriini: *Aceratherium incisivum* Kaup, 1832, *Alicornops simorrense* (Lartet, 1851), and *Chilotherium anderssoni* Ringström, 1924, from the middle and/or Late Miocene of Eurasia; other selected hornless rhinos ('aceratheres *sensu lato*'): *Protaceratherium minutum* (Cuvier, 1822), *Protaceratherium albigense* (Roman, 1912), and *Plesiaceratherium mirallesi* (Crusafont *et al.*, 1955) from the Oligocene of Eurasia (*Protaceratherium albigense, Pr. a.*; Lihoreau *et al.*, 2009) and the Early Miocene of Europe (*Protaceratherium minutum, Pr. m.* and *Plesiaceratherium mirallesi, Pl. m.*).

The character coding was performed through direct observation and/or the literature (Table 28).

RESULTS

Two equally parsimonious trees (1237 steps; consistency index = 0.27; retention index = 0.42) were obtained by using the 'mh*bb*' command of Hennig86, 1.5 (Farris, 1988) and the heuristic search of PAUP 4.0 v.10 (Swofford, 1998). They only differ in the relationships between the Aceratheriina included in the analysis (*Aceratherium incisivum*, *Chilotherium anderssoni*, and *Alicornops simorrense*; Fig. 13).

The suprageneric and interspecific phylogenetic relationships within Rhinocerotidae are discussed below, as well as the distribution of unambiguous synapomorphies, detailed in Table 29, and based on the consensus tree (1244 steps; consistency index = 0.27; retention index = 0.41) as illustrated in Figure 13. Both indexes are low, which indicates a large amount of unstructured homoplasy. The ingroup is not monophyletic, with the extra-group *Ronzotherium filholi* as the first offshoot of Elasmotheriinae. Nevertheless, suprageneric taxa such as Rhinocerotidae, Elasmotheriinae, Elasmotheriini and Elasmotheriina, Rhinocerotinae, Aceratheriini, Rhinocerotina, and Teleoceratina are monophyletic in the consensus tree (Fig. 13). Moreover, suprageneric relationships are consistent with those resulting from recent analyses with better indexes (e.g. Antoine, 2002, 2003; Antoine *et al.*, 2003b), pointing to terminal taxa homoplasy. Twenty-three characters are uninformative in the current analysis (cranial: 5, 7, 32, 43; dental: 64, 69, 92, 93, 106, 117, 123, 126, 127, 131, 132, 137, 141, 153, 167, 171, 175; postcranial: 217, 273; Appendix 1).

Within the available taxonomic sample, Rhinocerotidae (Fig. 13, node 1) are characterized by 11 synapomorphies, of which two are nonhomoplastic (i2 tusk-like and i3 absent). The other ones are a brachycephalic skull, an upraised mandibular symphysis, the c1 absent, the antecrochet usually absent on upper molars, the alar notch present on the atlas, the long posterior tuberosity on the magnum, the transverse diameter/height ratio between 1.0 and 1.2 on the astragalus, the anteroposterior diameter/height ratio higher than 0.65 on the astragalus, and the proximal border of MtIII concave in anterior view.

Node 2 (Fig. 13) puts the clades Rhinocerotinae and Elasmotheriinae as sister groups. This node is defined by the absence of I3 (nonhomoplastic), a spur-like paralophid on p2 (unique reversion), a straight occipi-

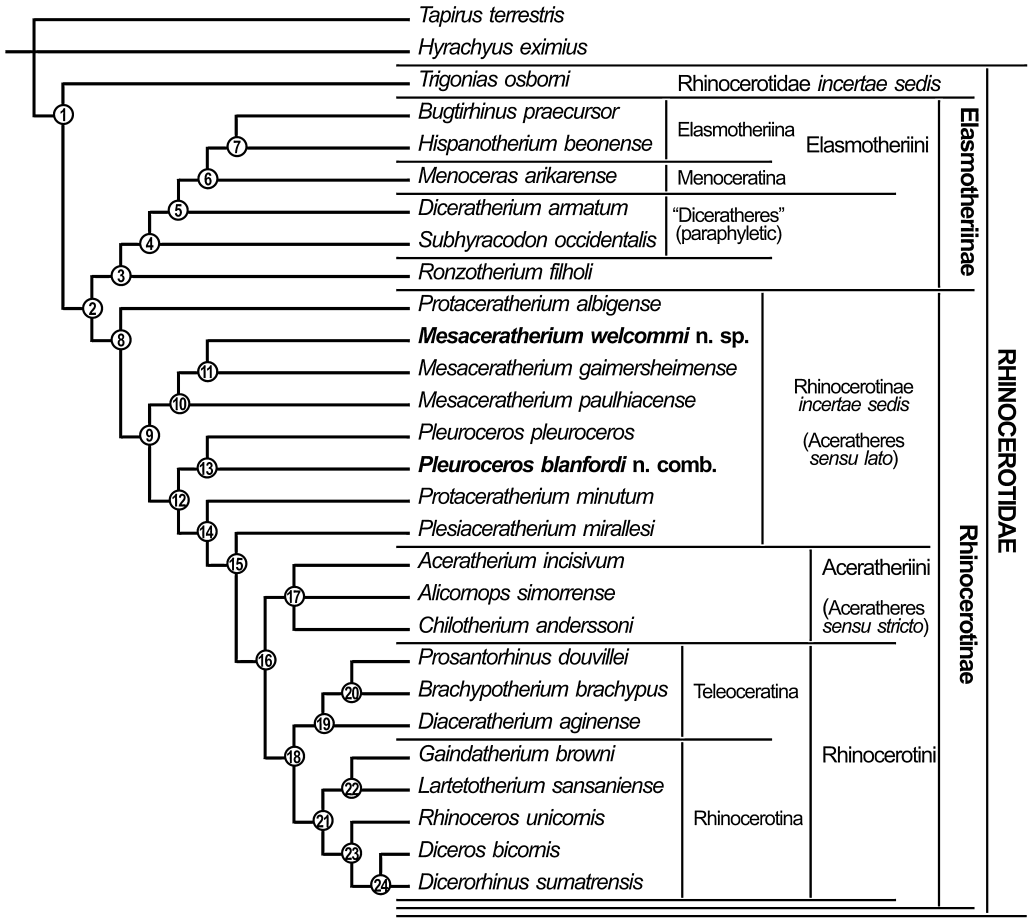

Figure 13. Strict consensus tree of two most parsimonious trees (1237 steps; consistency index = 0.27; retention index = 0.42) obtained using Hennig86 1.5 (Farris, 1988) and PAUP 4.0 v.10 (Swofford, 1998), based on 282 morphological characters, and performed on 28 rhinocerotid, rhinocerotoid, and tapirid taxa, with *Tapirus terrestris*, *Hyrachyus eximius*, *Trigonias osborni*, and *Ronzotherium filholi* as outgroups. Suprageneric group names are based on current phylogenetic relationships. Taxa of interest are in bold.

tal crest, a convex processus postglenoidalis, the absence of C1, and the antecrochet usually present on upper molars.

The controlled Elasmotheriinae (Fig. 13, node 3) have seven homoplastic synapomorphies, such as an open external auditory pseudomeatus (reversion), a rounded vomer, a lingual wall on P3–4, a forked paralophid on d2, no foramen transversarium on the atlas, fused proximal ulna-facets on the radius, and a McIV with a triangular outline in proximal view.

Node 4 (Fig. 13, unnamed clade) joins the diceratheres (*Subhyracodon occidentalis* + *Diceratherium armatum*; paraphyletic) and the Elasmotheriini (Elasmotheriina + Menoceratina), based on nine homoplastic features: a depressed area between temporal and nuchal crests on the temporal, a dolichocephalic skull (reversion), a trigonid forming an acute dihedron on lower cheek teeth, a continuous lingual cingulum on lower premolars, d1/p1 absent in adults, an oblique hypolophid on lower molars, radius and ulna in contact or fused, a proximal fibula-surface proximally displaced on the tibia, and a proximal border of MtIII sigmoid in anterior view.

Diceratherium armatum appears as the sister group of the Menoceratina + Elasmotheriina clade because of a low anterior base of the processus zygomaticus maxillari, a well-developed nuchal tubercle, a concave occipital crest (reversion), the presence of cement on cheek teeth, the hypocone posterior to the metacone on P3–4, the antecrochet always present on upper molars, the protocone usually constricted on M1–2, the absence of a posteroproximal lunate-facet on the scaphoid, calcaneus-facets 2 and 3 always fused on the astragalus (Antoine, 2002), and the tibia-facet always present on the calcaneus.

The Elasmotheriini (Fig. 13, node 6), i.e. Menoceratina (*Menoceras arikarense*) + Elasmotheriina, share 20 synapomorphies (Table 29), amongst which the

Table 29. Distribution of unambiguous synapomorphies in the strict consensus tree illustrated in Figure 13

Node 1 (Rhinocerotidae): 23^1, 53^1, **79^1**, **81^1**, 82^1, 110^1, 184^1, 220^1, 252^1, 253^1, 271^1
Node 2 (Rhinocerotinae + Elasmotheriinae): 36^1, 42^1, **74^1**, 75^1, 110^2, $\underline{-154^0}$
Node 3 (Elasmotheriinae): -18^0, 38^1, 102^3, 179^1, 188^1, 199^3, 230^2
Node 4: 17^1, $\underline{-23^0}$, 143^1, 148^1, 151^3, 161^1, 201^1, 248^1, 271^2
Node 5: 10^1, 20^2, -36^0, 65^1, 103^1, 110^3, 115^2, 207^1, 263^3, 265^2
Node 6 (Elasmotheriini): 45^1, 49^1, 59^1, 84^2, 88^1, 115^3, 130^1, 140^2, 154^1, 176^1, 194^1, 234^1, 235^1, 254^1, 256^1, 259^1, 264^3, 266^1, 275^1, 278^1
Node 7 (Elasmotheriina): 63^1, 87^1, 94^3, 95^1, 116^1, 135^2, 147^2, 149^1, 157^1, 210^1, 277^1
Node 8 (Rhinocerotinae): 46^1, 103^1, 110^3, 115^3, 125^1, 129^1, 152^2, 210^1
Node 9: 83^2, 111^3, 138^1, 160^1, 242^1
Node 10 (*Mesaceratherium*): 118^1, 226^2, 272^1
Node 11 (*Mesaceratherium gaimersheimense*, *Mesaceratherium welcommi* sp. nov.): 94^1, 102^1
Node 12: 70^1, 72^1, 84^1, 100^1, 161^1, 213^1
Node 13 (*Pleuroceros*): -36^0, 53^2, 88^1, 107^3, 112^1, 116^1, 124^1, 140^1, 148^1, 231^1, 232^1, 266^1, 282^1
Node 14: 3^1, 84^2, 105^1, -110^2, $\underline{-174^0}$, 207^1, 259^1
Node 15: $\underline{-11^0}$, 134^1, 142^1, 150^1, 151^1, **186^1**, 196^1, -212^0, 265^2
Node 16 (Aceratheriini + Rhinocerotini): $\underline{-122^0}$, 147^2, 151^2, 157^1, 224^1, 232^1
Node 17 (Aceratheriini): 22^1, 37^1, 47^1, 62^1, 80^1, -85^0, 193^1, 199^1, 223^2
Node 18 (Rhinocerotini): -3^0, 12^1, 15^1, -36^0, 67^1, 97^1, $\underline{-100^0}$, 247^1
Node 19 (Teleoceratina): 45^1, -105^0, $\underline{-146^0}$, 206^1, $\underline{-220^0}$, **229^1**, 241^1, 257^1, **262^1**, 282^1
Node 20: $\underline{-72^0}$, $\underline{-119^0}$, 144^1, 199^2, 202^1, $\underline{-226^1}$, -238^0, 252^2, 275^1, 279^1
Node 21 (Rhinocerotina): $\underline{24^1}$, $\underline{27^1}$, 83^3, 109^3, $\underline{-110^0}$, 114^2, $\underline{-115^2}$, 149^1, 154^1, 230^2, 263^2, 280^1
Node 22: 94^1, 102^1, 143^1, $\underline{-151^1}$, 157^3, $\underline{-161^0}$
Node 23: 77^1, 91^1, 101^1, $\underline{-111^2}$, 112^1, $\underline{-125^0}$, -204^0, 216^1, 256^1, 277^1
Node 24: -18^0, **31^1**, 38^1, 121^1, 187^2, $\underline{-210^0}$, 214^2, 228^2, $\underline{-232^0}$, 234^1

Superscript numbers correspond to character states. Reversions are preceded by '-'. Nonhomoplastic synapomorphies [consistency index = retention index (RI) = 1] are in bold; weakly homoplastic apomorphies (RI ≥ 0.80) and unique reversions are underlined. Other characters are strongly homoplastic.

less homoplastic are a crochet always present on P2–4, a protocone always constricted on M1–2, the presence of vertical external rugosities on d2–3, a medially stiff femoral head, an astragalus with a trochlea and a distal articulation sharing the same axis, and nearly anterior symmetric insertions on MtIII first phalanges.

The Elasmotheriina, represented by the Early Miocene *Bugtirhinus praecursor* and *Hispanotherium beonense*, are monophyletic (Fig. 13, node 7), and characterized by 11 derived homoplastic features, including a short premolar row, a lingual wall on P2, a protocone strongly constricted on upper molars, the absence of a labial cingulum on lower premolars, a scaphoid higher posteriorly than anteriorly, and a pad-shaped and continuous posteroproximal tuberosity on MtIV.

Both taxa of interest (*P. blanfordi* and *M. welcommi* sp. nov.) belong to the Rhinocerotinae (Fig. 13, node 8), with the Oligocene *Protaceratherium albigense* as the first offshoot. This Rhinocerotinae clade is defined by eight homoplastic synapomorphies: processus posttympanicus and processus paraoccipitalis distant, hypocone posterior to metacone on P3–4, antecrochet always present on upper molars, protocone always constricted on M1–2, hypocone isolated on M1 and M2, one-rooted d1, and scaphoid higher posteriorly than anteriorly (convergence with Elasmotheriina). *Protaceratherium albigense* is set well apart from the type species of the genus (*Protaceratherium minutum*; Fig. 13, node 14).

Node 9 (unnamed clade) sets *Mesaceratherium* – including its three representatives – as the sister group of other Rhinocerotinae (Fig. 13), on the basis of five dental and postcranial homoplastic synapomorphies, such as the labial cingulum usually absent on the upper premolars, the crochet always present on upper molars, the absence of a posterior groove on the ectometaloph of M3, a reduced labial cingulum on lower molars, and the absence of an anterodistal groove on the tibia.

Node 10 sets *M. paulhiacense* as the sister group of the *M. gaimersheimense* + *M. welcommi* sp. nov. clade (Fig. 13). Therefore, *Mesaceratherium* appears as a monophyletic genus, including the three species mentioned above, and diagnosed by a weak paracone fold, a posterior McIII-facet always present on McII, but no posterior MtII-facet on MtIII.

Mesaceratherium gaimersheimense and *M. welcommi* sp. nov. are sister groups (Fig. 13, node 11),

based on the presence of a lingual bridge on upper premolars, which in turn confirms that *M. gaimersheimense* Heissig, 1969 cannot be considered as a junior synonym of *M. paulhiacense* (Richard, 1937).

The clade formed by *Pleuroceros* and more derived Rhinocerotinae (Fig. 13, node 12) is defined by upper cheek teeth with joined roots, I1s oval in cross-section, a crochet usually present on P2–4, a medifossette usually absent on P3–4, a hypolophid oblique on lower molars, and a smooth anterior side on the lunate.

Pleuroceros (Fig. 13, node 13) is a clade including *P. pleuroceros* and *P. blanfordi* comb. nov. Both species share 12 homoplastic synapomorphies: a concave occipital crest in dorsal view (reversion), a nearly horizontal mandibular symphysis, a reduced lingual cingulum on upper premolars, a strong antecrochet on P4, a protocone deeply constricted and a low and reduced posterior cingulum on M1–2, a smooth and U-shaped external groove on lower cheek teeth, a continuous lingual cingulum on lower premolars, a tridactyl manus (vestigial McV), a salient insertion of the m. extensor carpalis on metacarpals, a slender tuber calcanei, and a short insertion of the m. interossei on lateral metapodials.

The following node (Fig. 13, node 14) puts *Protaceratherium minutum* as the sister group of the [*Plesiaceratherium mirallesi* [Aceratheriini, Rhinocerotini]] clade. This node is characterized by seven synapomorphies, of which only one is weakly homoplastic (presence of a protoconid fold on lower deciduous teeth; unique reversion): nasal notch above P4–M1, crochet always present on P2–4, crista usually absent on P3, antecrochet usually present on upper molars (reversion), posteroproximal lunate-facet absent on the scaphoid, and astragalus with a trochlea and a distal articulation sharing the same axis.

Plesiaceratherium mirallesi is the sister group of the [Aceratheriini, Rhinocerotini] clade. Terminals from node 15 (Fig. 13) share kidney-like condyle-facets on the atlas (consistency index = retention index = 1), a low zygomatic arch (unique reversion), a triangular M3, a rounded trigonid on lower cheek teeth, a reduced labial cingulum on lower premolars, d1/p1 usually present in adults, a distal gutter on the lateral epicondyle of the humerus, a lunate with a rounded distal border in anterior view (reversion), and a tibia-facet always present on the calcaneus.

The next node (Fig. 13, node 16) highlights the phylogenetic relationships amongst aceratheriines, teleoceratines, and rhinocerotines: the Aceratheriini appear as the sister group of the Rhinocerotini (the latter including Rhinocerotina and Teleoceratina as sister groups). Such relationships were not solved in Antoine *et al.* (2003b: fig. 4). The concerned taxa (node 16) are defined by an unique reversion (posterior part of the ectoloph straight on M1–2), and five homoplastic dental and postcranial synapomorphies: lingual cingulum usually absent on lower premolars and usually present on lower molars, d1/p1 usually absent in adults, magnum-facet straight on McII, and insertion of the m. extensor carpalis salient on metacarpals (convergence with *Pleuroceros*).

Node 17 (Fig. 13, Aceratheriini) is a polytomy with *Aceratherium incisivum*, *Alicornops simorrense*, and *Chilotherium anderssoni*. The three of them are characterized by a nearly vertical posterior margin on the pterygoid, a brutal anterior tip on the processus zygomaticus maxillary in palatine view, a small processus post-tympanicus, a foramen mandibulare open above the teeth neck line, divergent i2s, simple crochets on P2–4 (reversion), a wide and low fossa olecrani on the humerus, proximal ulna-facets usually separate on the radius, and a posterior expansion usually present on the pyramidal-facet of the unciform.

The aceratheriines as classically defined, i.e. including hornless taxa such as *Plesiaceratherium*, *Mesaceratherium*, and sometimes *Protaceratherium*, along with *Aceratherium*, *Chilotherium*, and *Alicornops*, appear as an unnatural group. We propose the restriction of the use of 'Aceratheriini' or 'Aceratheriina' in the current analysis to the clade (*Aceratherium incisivum*, *Alicornops simorrense*, *Chilotherium anderssoni*) and their close relatives (such as *Hoploaceratherium tetradactylum* and *Acerorhinus zernowi*; Antoine *et al.*, 2003b).

The Rhinocerotini (Fig. 13, node 18) include the Teleoceratina (node 19) and the Rhinocerotina (node 21) as sister groups; they share eight synapomorphies amongst which a unique reversion (medifossette always absent on P3–4), and homoplastic features, such as a nasal notch retracted above P1–P3 (reversion), the processus postorbitalis absent on the zygomatic arch, the dorsal profile of the skull concave in lateral view, the concave occipital crest (reversion), wrinkled and corrugated enamel on cheek teeth, a protocone less developed than the hypocone on P2, and a rounded posterior apophysis on the tibia.

The early Teleoceratina included in the present analysis (Fig. 13, node 19), arranged as follows: [*Diaceratherium aginense* [*Prosantorhinus douvillei*, *Brachypotherium brachypus*]], are defined by two nonhomoplastic postcranial synapomorphies (magnum-facet invisible in anterior view on McIII and calcaneus-facet 1 nearly flat on the astragalus), two unique reversions (U-shaped lingual opening of the posterior valley on lower premolars in lingual view and posterior tuberosity short on the magnum), and six homoplastic features: posterior groove present on the processus zygomaticus of the squamosal, crista always absent on P3 (reversion), anterior tubercle

present on the distal end of the ulna, proximal border of the patellar articulation straight on the femur, posterior stop absent on the cuboid-facet of the astragalus, and insertion of the m. interossei short on lateral metapodials. As usual, the Teleoceratina are essentially diagnosed by postcranial characters.

Prosantorhinus douvillei and *B. brachypus* share three unique reversions (Fig. 13, node 20; I1 almond-shaped in cross-section, metacone fold present on M1–2, and posterior McIII-facet usually absent on McII), and seven homoplastic synapomorphies: constricted metaconid on lower cheek teeth, proximal ulna-facets usually fused on the radius, gutter for the m. extensor carpi weak on the radius, fovea capitis high and narrow on the femur (reversion), transverse diameter/height ratio higher than 1.2 on the astragalus, presence of a cuboid-facet on MtIII, and shortened limbs (brachypody). Once again, seven derived features out of ten are postcranial.

The Rhinocerotina included in this phylogenetic analysis are monophyletic (Fig. 13, node 21), and split into two clades: one-horned extinct rhinocerotines *Lartetotherium sansaniense* and *Gaindatherium browni* on the one hand (Fig. 13, node 22), and Recent rhinocerotines on the other (Fig. 13, node 23). The Rhinocerotina (node 21) are notably characterized by a broad anterior tip on the nasals, the presence of a nasal horn, the antecrochet absent on upper molars and a protocone usually constricted on M1–2 (unique reversions), and the labial cingulum always absent on upper molars.

The *Lartetotherium–Gaindatherium* clade (Fig. 13, node 22) is defined by six dental features: d1/p1 usually present in adults and hypolophid transverse on lower molars (unique reversions), lingual bridge present on upper premolars, trigonid of lower cheek teeth forming an acute dihedron, and lingual cingulum always absent on lower molars.

The Recent rhinocerotines included in this analysis share ten dental and postcranial features, amongst which are two unique reversions (crochet usually present on upper molars and hypocone unconstricted on M1), a P1 usually present in adults, a collum tali low on the astragalus, a pad-shaped posteroproximal tuberosity on MtIV (convergence with Elasmotheriina), and several highly homoplastic characters.

The two-horned Recent rhinos included in the present work, *Diceros bicornis* and *Dicerorhinus sumatrensis*, form a clade essentially diagnosed by cranial and postcranial synapomorphies rather than by mandibular and dental features (Fig. 13, node 24), including the presence of a frontal horn (consistency index = retention index = 1), the scaphoid with equal anterior and posterior heights and the insertion of the m. extensor carpalis flat on the metacarpals (unique reversions), and a rounded vomer. The other ones are quite homoplastic (Appendix 1).

Mesaceratherium and *Pleuroceros* appear as monophyletic genera, quite distinct but branching at the same level in the cladogram (Fig. 13), which confirms that *M. welcommi* sp. nov. could be misidentified, as occurred throughout the last century. Both can be referred to Rhinocerotinae incertae sedis, a paraphyletic ensemble we propose to name 'aceratheres *sensu lato*'.

CONCLUSION

The revision of the hypodigm of '*Aceratherium blanfordi*, n. sp., *nobis* Lydekker, 1884' led us to split up this taxon into two co-occurring but distinct species, namely *P. blanfordi* (Lydekker, 1884) comb. nov. and *M. welcommi* Antoine & Downing sp. nov. This work highlights the identificatory/discriminatory skills of postcranial skeleton elements for rhinocerotids, especially for the ones which display globally similar – and therefore potentially homoplastic – dental patterns and features: although being associated in various localities and having comparable cheek teeth morphologies, *P. blanfordi* and *M. welcommi* can be easily distinguished thanks to their limb bones. The small, short, and robust chilothere-like postcranial bones of the tridactyl *P. blanfordi* are highly divergent from the large, long, and slender ones of the tetradactyl *M. welcommi*.

In the Bugti area, *P. blanfordi* and *M. welcommi* are found in association with a surprisingly diversified rhinocerotid fauna, especially in the locus Kumbi 4f (Level 4, earliest Miocene, MN2; Table 30), in which they co-occur with the rhinocerotine *Gaindatherium* cf. *browni*, the teleoceratines *Brachypotherium fatehjangense* (Pilgrim, 1910), *Brachypotherium gajense* (Pilgrim, 1912), and *Prosantorhinus shahbazi* (Pilgrim, 1910), the aceratheriine *Plesiaceratherium naricum* (Pilgrim, 1910), the minute *Protaceratherium* sp., and the early elasmotheriine *Bugtirhinus praecursor* (Antoine & Welcomme, 2000; Welcomme *et al.*, 2001; Métais *et al.*, 2009). To our knowledge, such a rhinocerotid specific diversity – up to nine coeval/associated species in the same locus – is unique in the world. It testifies notably to an exceptional food supply for the Dera Bugti area in the Early Miocene, in as far as these rhinocerotids were found associated with a diversified megaherbivore and macroherbivore fauna, including proboscideans, chalicotheriids, anthracotheriids, and ruminants (Antoine & Welcomme, 2000; Métais *et al.*, 2009). Given that the number of plant species included in a natural diet increases with the size of the herbivore(s) (Freeland, 1991) and that a reduction in available plant variety may cause the decline of megamammals

Table 30. Stratigraphical distribution of the rhinocerotids identified in the Early Miocene of the Bugti Hills (Balochistan. Pakistan), locality by locality

Formation	Chitarwata Formation (upper member)									Vihowa Formation (base)			
Levels	3bis	4								5		6	6sup
		Kumbi 4						Gandô		Kumbi			
Loci	DB 3bis	4a	4b	4c	4d	4e	4f	4	DB 4	5	DB 5	DB 6	DB 6sup
Bugtirhinus praecursor	◆		◆	◆			◆						
Protaceratherium sp.	◆						◆	◆					
Plesiaceratherium naricum	◆	◆				◆	◆	◆	◆	?			
Brachypotherium gajense		◆	◆	◆	◆		◆	◆	◆	◆	◆	◆	◆
Brachypotherium fatehjangense		◆	◆	◆	◆	◆	◆	◆	◆	◆	◆	◆	◆
Gaindatherium cf. *browni*			◆	◆			◆						
***Mesaceratherium welcommi* sp. nov.**		◆		◆			◆	◆	◆	◆	◆	◆	◆
Pleuroceros blanfordi		◆	◆	◆	◆		◆	◆	◆		◆	◆	
Prosantorhinus shahbazi		◆	◆			◆	◆	◆					
Rhinocerotina indet., cf. *Rhinoceros*		?								◆		◆	◆
Number of co-occurring rhinocerotid species	3	6	6	6	3	3	**9**	7	5	4	4	5	4

Modified and completed from Antoine & Welcomme (2000); Welcomme *et al.* (2001); Métais *et al.* (2009). See Material and methods for level numbers and corresponding letters (loci and levels).

(Guthrie, 1984), high plant diversity under a favourable climate may be suspected for the Early Miocene of the Sulaiman Lobe. Yet, in the absence of available climatic, palynological, and palaeobotanical data for this period and area (Collinson & Hooker, 2003; De Franceschi *et al.*, 2008; Métais *et al.*, 2009), this hypothesis cannot yet be tested.

The co-occurrence of *P. blanfordi*, *M. welcommi*, *Protaceratherium* sp., *Plesiaceratherium naricum*, and *Brachypotherium gajense* in both the Bugti and Zinda Pir areas (our unpublished data) allows the refinement of the stratigraphical correlations proposed by Lindsay *et al.* (2005) and Métais *et al.* (2009) for the upper member of the Chitarwata Formation throughout the Sulaiman Lobe. The *Pleuroceros–Mesaceratherium–Protaceratherium* assemblage defines the earliest Miocene European Land Mammal Age (Agenian ELMA; MN1+MN2) in western Europe (Bruijn *et al.*, 1992; Antoine *et al.*, 2006). Hence, their co-occurrence in the Bugti Hills and Zinda Pir – recorded for the first time outside Europe – confirms the earliest Miocene age of the upper member of the Chitarwata Fm as a whole. Compatible environmental conditions might have occurred at these times in both areas, although geographically remote. Heissig & Fejfar (2007) recently described a rhinocerotid fauna from the Early Miocene of Tuchořice (MN3) in the Czech Republic, consisting of the small teleoceratine *Prosantorhinus laubei* sp. nov., the small and slender acerathere *Protaceratherium minutum*, and the large and slender acerathere '*Aceratherium* (*Alicornops*) aff. *pauliacense*'. The latter 'can not be distinguished from the earlier type population [of *Mesaceratherium paulhiacense* (Richard, 1937)] from Paulhiac (MN1)' (Heissig & Fejfar, 2007: 19). The rhinocerotid assemblage recognized in Level 4 in the Bugti area (~MN2) includes notably *Prosantorhinus shahbazi*, *Protaceratherium* sp., and *M. welcommi* sp. nov. (Métais *et al.*, 2009; this work) Similarly, the teleoceratine *Brachypotherium fatehjangense* and the acerathere *Mesaceratherium welcommi* from the Sulaiman Range (Pakistan) have strong affinities to the earliest African rhinocerotids, *Brachypotherium heinzelini* and *Aceratherium acutirostratum*, respectively, recognized in Napak II and Songhor by Hooijer (1966, 1973) and Hooijer & Patterson (1972). Moreover, the earliest elasmotheriine *Bugtirhinus praecursor* from the earliest Miocene of the Bugti Hills (Levels 3bis and 4; Table 30; Antoine & Welcomme, 2000) has close affinities with *Ougandatherium napakense* from Napak I (Guérin & Pickford, 2003). The radiometric age of Songhor is ~19.5 Myr (Pickford, 1986; Cote *et al.*, 2007) and Napak might be slightly older (Tassy, 1986; Cote *et al.*, 2007). In the light of such coeval and comparable assemblages (Pakistan/East Africa), it might be worth revising the earliest

remains of the African 'chilothere' *Chilotheridium pattersoni* Hooijer, 1971, from the Early Miocene of Kenya and Uganda (Rusinga, Bukwa, Loperot, and Ombo; 18–16 Myr interval; Guérin & Pickford, 2003), and comparing them to both *P. blanfordi* and *M. welcommi*, with a special emphasis on referable postcranials: (1) true chilotheres have their First Appearance Datum much later, i.e. during the late Middle Miocene in Eurasia, with a late Miocene climax in Asia (Hooijer, 1966; Antoine *et al.*, 2003b); (2) as a result of convergent cheek teeth patterns, '*Aceratherium blanfordi*' as a whole had been mistakenly referred to the genus *Chilotherium* for decades; and (3) figured teeth from Rusinga (18 Myr; Hooijer, 1966: 151, pl. 6) and Ombo (16 Myr; Hooijer, 1973: pl. 1, figs 3, 9, 10) have strong similarities to *P. blanfordi* and/or *M. welcommi*.

All these homotaxic assemblages constrain the existence of broad and sustainable rhinocerotid interchanges amongst South Asia, Europe, and Africa under comparable environmental conditions throughout earliest Miocene times (*c.* 23–19 Myr interval).

ACKNOWLEDGEMENTS

We thank J.-L. Welcomme for his prominent role in the French-Baloch Palaeontological Expeditions 1995–2004 in the Bugti Hills, in which Léonard Ginsburg, Marc Delcorso, Jérôme Proriol, Mouloud Benammi, Jean-Jacques Jaeger, Yaowalak Chaimanee, and Dario De Franceschi participated and suffered. Michèle E. Morgan, John C. Barry, David Pilbeam, Everett H. Lindsay, Iqbal U. Cheema, and Susanne Cote provided valuable help and discussion. We are grateful to H. E. Iqbal Akhund and Kamal Majidullah (Karachi) for their indefectible support. Jerry J. Hooker, Andy Currant, and Peter J. Whybrow (NHM, London), Sophie Hervet (Rhinopolis), Abel Prieur (UCBL, Lyon-Villeurbanne), Christine Argot, Claire Sagne, and Pascal Tassy (MNHN, Paris), Malcolm C. McKenna (AMNH, New York), and David Pilbeam and John C. Barry (Peabody Museum, Harvard University) granted access to the collections of which they are/were in charge. Peter Hayward, Hans Larsson, and an anonymous reviewer significantly improved the original manuscript. This article is dedicated to the memory of Annie Antoine, Nawab M. A. K. Bugti, Will Downs, and Malcolm C. McKenna. This research was supported by the French ANR-PALASIAFRICA Program (ANR-08-JCJC-0011-01 – ANR-ERC). MPFB publication n°38.

REFERENCES

Antoine PO. 1997. *Aegyrcitherium beonensis* nov. gen. nov. sp., nouvel élasmothère (Mammalia, Rhinocerotidae) du gisement miocène (MN 4b) de Montréal-du-Gers (Gers, France). Position phylogénétique au sein des Elasmotheriini. *Neues Jahrbuch für Geologie und Paläontologie, Abhandlungen* **204:** 399–414.

Antoine PO. 2002. Phylogénie et évolution des Elasmotheriina (Mammalia, Rhinocerotidae). *Mémoires du Muséum National d'Histoire Naturelle* **188:** 1–359.

Antoine PO. 2003. Middle Miocene elasmotheriine Rhinocerotidae from China and Mongolia: taxonomic revision and phylogenetic relationships. *Zoologica Scripta* **32:** 95–118.

Antoine PO, Bulot C, Ginsburg L. 2000. Une faune rare de rhinocérotidés (Mammalia, Perissodactyla) dans le Miocène inférieur de Pellecahus (Gers, France). *Geobios* **33:** 249–255.

Antoine PO, Ducrocq S, Marivaux L, Chaimanee Y, Crochet JY, Jaeger JJ, Welcomme JL. 2003a. Early rhinocerotids (Mammalia, Perissodactyla) from South Asia and a review of the Holarctic Paleogene rhinocerotid record. *Canadian Journal of Earth Sciences* **40:** 365–374.

Antoine PO, Duranthon F, Hervet S, Fleury G. 2006. Vertébrés de l'Oligocène terminal (MP30) et du Miocène basal (MN1) du métro de Toulouse (SW de la France). *Comptes Rendus Palevol* **5:** 875–884.

Antoine PO, Duranthon F, Tassy P. 1997. L'apport des grands mammifères (Rhinocérotidés, Suoidés, Proboscidiens) à la connaissance des gisements du Miocène d'Aquitaine (France). In: Aguilar JP, Legendre S, Michaux J, eds. *Actes du Congrès biochrom'97*, Vol. 21. Montpellier: Mémoires et Travaux de l'Ecole Pratique des Hautes Etudes, Institut de Montpellier, 581–590.

Antoine PO, Duranthon F, Welcomme JL. 2003b. *Alicornops* (Mammalia, Rhinocerotidae) dans le Miocène supérieur des Collines Bugti (Balouchistan, Pakistan): implications phylogénétiques. *Geodiversitas* **25:** 575–603.

Antoine PO, Karadenizli L, Saraç G, Sen S. 2008. A giant rhinocerotoid (Mammalia, Perissodactyla) from the Late Oligocene of north-central Anatolia (Turkey). *Zoological Journal of the Linnean Society* **152:** 581–592.

Antoine PO, Shah SMI, Cheema IU, Crochet JY, de Franceschi D, Marivaux L, Métais G, Welcomme JL. 2004. New remains of the baluchithere *Paraceratherium bugtiense* (Pilgrim, 1910) from the Late/latest Oligocene of the Bugti Hills, Balochistan, Pakistan. *Journal of Asian Earth Sciences* **24:** 71–77.

Antoine PO, Welcomme JL. 2000. A new rhinoceros from the Bugti Hills, Baluchistan, Pakistan: the earliest elasmotheriine. *Palaeontology* **43:** 795–816.

Barbour EH. 1906. Notice of a new Miocene rhinoceros, *Diceratherium arikarense*. *Science New Series* **24:** 780–781.

Barry JC, Morgan ME, Flynn LJ, Pilbeam D, Behrensmeyer A, Raza S, Khan I, Badgley C, Hicks J, Kelley J. 2002. Faunal and environmental change in the Late Miocene Siwaliks of Northern Pakistan. *Paleobiology* **28:** Memoir 3 (Supplement to Number 2), 1–71.

Beliajeva EI. 1954. New rhinoceros remains from Kazakhstan. *Travaux de l'Institut Paléozoologique de l'Académie des Sciences de l'URSS, Moscou* **47:** 44–54 [in Russian].

de Blainville HMD. 1839–1864. *Ostéographie des mammifères récents et fossiles. Atlas – Tome troisième (Quaternatès)*, Paris: Baillière.

Blanford WT. 1876. On the geology of Sind. *Indian Geological Survey Records* **9:** 8–22.

Blanford WT. 1879. The geology of Sindh. *Memoirs of the Geological Survey of India* **18:** 1–196.

de Bonis L. 1973. *Contribution à l'étude des mammifères de l'Aquitanien de l'Agenais. Rongeurs-Carnivores-Périssodactyles*, Vol. 28. Paris: Mémoires du Muséum National d'Histoire Naturelle, 1–192.

Borissiak AA. 1944. *Aceratherium aralense* n. sp. *Doklady Akademiye Nauk SSSR* **43:** 30–32 [In Russian].

Brunet M. 1979. *Les grands mammifères chefs de file de l'immigration oligocène et le problème de la limite Eocène-Oligocène en Europe*, Paris: Fondation Singer-Polignac (ed.).

Cerdeño E. 1993. Etude sur *Diaceratherium aurelianense* et *Brachypotherium brachypus* (Rhinocerotidae, Mammalia) du Miocène moyen de France. *Bulletin du Muséum National d'Histoire Naturelle, Paris* **15:** 25–77.

Cerdeño E, Sánchez B. 2000. Intraspecific variation and evolutionary trends of *Alicornops simorrense* (Rhinocerotidae) in Spain. *Zoologica Scripta* **29:** 275–305.

Colbert EH. 1934. A new rhinoceros from the Siwalik Beds of India. *American Museum Novitates* **749:** 1–13.

Collinson M, Hooker JJ. 2003. Paleogene vegetation of Eurasia: framework for mammalian faunas. *Deinsea* **10:** 41–83.

Cote S, Werdelin L, Seiffert ER, Barry JC. 2007. Additional material of the enigmatic Early Miocene mammal Kelba and its relationship to the order Ptolemaiida. *Proceedings of the National Academy of Sciences of the United States of America* **104:** 5510–5515.

Crusafont M, Villalta JF, Truyols J. 1955. El Burdigaliense continental de la Cuenca del Vallés-Penedés. *Memorias y Comunicaciones del Instituto Geológico de Barcelona, Barcelona* **12:** 1–272.

Cuvier G. 1822. *Recherches sur les ossemens fossiles*, Vol. 5, 2nd edn. Paris: Edmond d'Ocagne.

De Bruijn H, Daams R, Daxner-Höck G, Fahlbusch V, Ginsburg L, Mein P, Morales J. 1992. Report of the RCMNS working group on fossil mammals, Reisenburg 1990. *Newsletters on Stratigraphy* **26:** 65–118.

De Franceschi D, Hoorn C, Antoine PO, Cheema IU, Flynn LJ, Lindsay EH, Marivaux L, Métais G, Rajpar AR, Welcomme JL. 2008. Floral Data from the Mid-Cenozoic of central Pakistan. *Review of Palaeobotany and Palynology* **150:** 115–129.

Downing KF. 2005. A new enigmatic large rhinocerotid from the upper unit of the Chitarwata Formation at Zinda Pir Dome, Western Pakistan. *Palaeontologia Electronica* **8** (21A)**:** 1–8.

Duvernoy GL. 1853. Nouvelles études sur les rhinocéros fossiles. *Archives du Muséum d'Histoire Naturelle, Paris* **7:** 1–144.

Duvernoy GL. 1854–1855. Nouvelles études sur les rhinocéros fossiles. *Archives du Muséum National d'Histoire Naturelle, Paris* **7:** 1–144.

Falconer H, Cautley PT. 1846–1849. Fauna antiqua sivalensis, *being the fossil zoology of the Sewalik Hills, in the north of India*. London: Falconer H.

Farris JS. 1988. *Hennig86 reference*. Version 1.5 (software). New York: Port Jefferson Station.

Fischer von Waldheim GF. 1814. *Zoögnosia tabulis synopticis illustrate, in usum Paeselectionum Academiae Imperialis Medicochirurgae*. Moscow: Nicolai Sergeidis Vsevolozsky.

Forster-Cooper C. 1915. New genera and species of mammals from the Miocene deposits of Baluchistan. Preliminary notice. *Annual Magazine of Natural History* **16:** 404–410.

Forster-Cooper C. 1924. On the skull and dentition of *Paraceratherium bugtiense*: a genus of aberrant rhinoceros from the lower Miocene deposits of Dera Bugti. *Philosophical Transactions of the Royal Society of London, Series B* **212:** 369–394.

Forster-Cooper C. 1934. XIII. The Extinct Rhinoceroses of Baluchistan. *Philosophical Transactions of the Royal Society of London, Series B* **223:** 569–616.

Freeland WJ. 1991. Plant secondary metabolites: biochemical coevolution with herbivores. In: Palo RT, Robbins CT, eds. *Plant defenses against mammalian herbivory*. Boca Raton: CRC Press, 61–81.

Gentry AW. 1987. Rhinoceroses from the Miocene of Saudi Arabia. *Bulletin of the British Museum (of Natural History)* **41:** 409–432.

Ginsburg L, Bulot C. 1984. Les Rhinocerotidae (Perissodactyla, Mammalia) du Miocène de Bézian à La Romieu (Gers). *Bulletin du Muséum National d'Histoire Naturelle, Paris* **6:** 353–377.

Gradstein FM, Ogg JG, Smith AG. 2005. *A geological time scale 2004*. Cambridge: Cambridge University Press.

Gray JE. 1821. On the natural arrangements of vertebrose animals. *London Medical Repository* **15:** 296–310.

Guthrie RD. 1984. Mosaics, allelochemics and nutrients. In: Martin PS, Klein RG, eds. *Quaternary extinctions. A prehistoric evolution*. Tucson: University of Arizona Press, 259–298.

Guérin C. 1980. *Les Rhinocéros (Mammalia, Perissodactyla) du Miocène terminal au Pléistocène supérieur en Europe occidentale. Comparaison avec les espèces actuelles*. Lyon: Documents du Laboratoire de Géologie de l'Université de Lyon, Sciences de la Terre 79, Vol. 3.

Guérin C, Pickford M. 2003. *Ougandatherium naMHNT Pak ense* nov. gen. nov. sp., le plus ancien Rhinocerotidae Iranotheriinae d'Afrique. *Annales de Paléontologie* **89:** 1–35.

Hatcher JB. 1894. On a small collection of vertebrate fossils from the Loup Fork beds of northwestern Nebraska, with note on the geology of the region. *American Naturalist* **28:** 236–248.

Heissig K. 1969. Die Rhinocerotidae (Mammalia) aus der oberoligozänen Spaltenfüllung von Gaimersheim. *Abhandlungen der Bayerischen Akademie der Wissenschaften, Mathematisch-Naturwissenschaftliche Klasse* **138:** 1–133.

Heissig K. 1972. Paläontologische und geologische Untersuchungen im Tertiär von Pakistan. 5. Rhinocerotidae

(Mamm.) aus den unteren und mittleren Siwalik-Schichten. *Abhandlungen der Bayerischen Akademie der Wissenschaften Mathematisch-Naturwissenschaftliche Klasse* **152:** 1–112.

Heissig K. 1976. Rhinocerotidae (Mammalia) aus der *Anchitherium*-Fauna Anatoliens. *Geologisches Jahrbuch B* **19:** 3–121.

Heissig K, Fejfar O. 2007. Die Säugetiere aus dem Untermiozän von Tuchořice in Nordwestböhmen. I. Die fossilen Nashörner (Mammalia, Rhinocerotidae). *Acta Musei Nationalis Pragae, Series B, Historia Naturalis, Prague* **63:** 19–64.

Hooijer DA. 1966. Miocene rhinoceroses of East Africa. *Bulletin of the British Museum (of Natural History), Fossil Mammals of Africa* **21:** 117–190.

Hooijer DA. 1971. A new rhinoceros from the late Miocene of Loperot, Turkana District, Kenya. *Bulletin of the Museum of Comparative Zoology, Cambridge (Mass.)* **142:** 339–392.

Hooijer DA. 1973. Additional Miocene to Pleistocene rhinoceroses of Africa. *Zoological Mededelingen* **46:** 149–178.

Hooijer DA, Patterson B. 1972. Rhinoceroses from the Pliocene of Northwestern Kenya. *Bulletin of the Museum of Comparative Zoology, Cambridge (Mass.)* **144:** 1–26.

Hünermann KA. 1989. Die Nashornskelette (*Aceratherium incisivum* Kaup 1832) aus dem Jungtertiär vom Höwenegg im Hegau (Südwestdeutschland). *Andrias* **6:** 5–116.

International Commission On Zoological Nomenclature. 1999. *International Code of Zoological Nomenclature, 4ème édition*. London: The International Trust for Zoological Nomenclature.

Kaup JJ. 1832. *Description d'Ossements fossiles de Mammifères inconnus jusqu'à présent, qui se trouvent au Musée grand-ducal de Darmstadt*. Darmstadt: Heyer, J.G.

Klaits BG. 1973. Upper Miocene rhinoceroses from Sansan (Gers), France: the manus. *Journal of Paleontology* **47:** 315–326.

Lartet E. 1837. Note sur les ossements fossiles des terrains tertiaires de Simorre, de Sansan, etc., dans le département du Gers, et sur la découverte récente d'une mâchoire de singe fossile. *Comptes Rendus de l'Académie des Sciences, Paris* **4:** 85–93.

Lartet E. 1851. *Notice sur la colline de Sansan*. Auch: Portes.

Laudet F, Antoine PO. 2004. Des chambres de pupation de Dermestidae (Insecta : Coleoptera) sur un os de mammifère tertiaire (phosphorites du Quercy). Implications taphonomiques et paléoenvironnementales. *Geobios* **37:** 376–381.

Leidy J 1851. Remarks on *Oreodon priscus* and Rhinoceros occidentalis. *Proceedings of the Academy of Natural Sciences of Philadelphia* **5:** 276.

Leidy J. 1871. Report on the vertebrate fossils of the Tertiary formations of the West. *Annals and Reports of the United States Geological and Geographic Survey, Hayden* **2:** 340–370.

Lihoreau F, Ducrocq S, Antoine PO, Vianey-Liaud M, Rafaÿ S, Garcia G, Valentin X. 2009. First complete skulls of *Elomeryx crispus* (Gervais, 1849) and of *Protaceratherium albigense* (Roman, 1912) from a new Oligocene locality near Moissac (SW France). *Journal of Vertebrate Paleontology* **29:** 242–253.

Lindsay EH, Flynn LJ, Cheema IU, Barry JC, Downing KF, Rajpar AR, Raza SM. 2005. Will Downs and the Zinda Pir Dome. *Palaeontologia Electronica* **8:** 1–19.

von Linnaeus C. 1758. *Systema Naturae per regna tria naturae, secundum classes, ordines, genera, species, cum characteribus, differentiis, synonymis, locis*, 10th edn, Vol. 1: *Regnum animale*. Stockholm.

Lucas FA. 1900. A new rhinoceros, *Trigonias osborni*, from the Miocene of South Dakota. *United States National Museum Proceedings* **23:** 221–224.

Lydekker R. 1881. Siwalik Rhinocerotidae. *Memoirs of the Geological Survey of India – Palaeontologica Indica* **2:** 1–62.

Lydekker R. 1884. Additional Siwalik Perissodactyla and Proboscidea. *Memoirs of the Geologcal Survey of India – Palaeontologia Indica* **3:** 1–34.

Lydekker R. 1886. *Catalogue of the fossil mammalia in the British Museum (Natural History), Part III*. London: Taylor and Francis.

Marsh OC. 1875. Notice of new Tertiary mammals. IV. *American Journal of Sciences and Arts* **109:** 239–250.

Matthew WD. 1929. Critical observations upon Siwalik mammals. *Bulletin of the American Museum of Natural History* **56:** 437–560.

Métais G, Antoine PO, Baqri SRH, Marivaux L, Welcomme JL. 2009. Lithofacies, depositional environments, regional biostratigraphy, and age of the Chitarwata Formation in the Bugti Hills, Balochistan, Pakistan. *Journal of Asian Earth Sciences* **34:** 154–167.

Mihlbachler MC. 2005. Linking sexual dimorphism and sociality in rhinoceroses: insights from *Teleoceras proterum* and *Aphelops malacorhinus* from the late Miocene of Florida. *Bulletin of the Florida Museum of Natural History* **45:** 495–520.

Osborn HF. 1900. Phylogeny of Rhinoceroses of Europe. *Memoirs of the American Museum of Natural History* **13:** 229–267.

Owen R. 1848. *The archetype and homologies of the vertebrate skeleton*. London.

Pickford M. 1986. A revision of the Miocene Suidae and Tayassuidae (Artiodactyla, Mammalia) of Africa. *Tertiary Research, Special Papers* **7:** 1–83.

Pilgrim GE. 1908. The Tertiary and post-Tertiary freshwater deposits of Baluchistan and Sind, with notices of new vertebrates. *Records of the Geological Survey of India* **37:** 139–166.

Pilgrim GE. 1910. Notice on new mammal genera and species from the Tertiaries of India. *Records of the Geological Survey of India* **15:** 63–71.

Pilgrim GE. 1912. The vertebrate fauna of the Gaj Series in the Bugti Hills and the Punjab. *Paleontologia Indica* **4:** 1–83.

Prothero DR. 1998. 42 Rhinocerotidae. In: Janis CM, Scott KM, Jacobs LL, eds. *Evolution of tertiary mammals of North America. Terrestrial carnivores, ungulates and ungulatelike mammals*, Vol. 1. New York: Cambridge University Press, 595–605.

Prothero DR. 2005. *The evolution of North American Rhinoceroses*. Cambridge; New York; Melbourne: Cambridge University Press.

Qiu Z, Xie J. 1997. A new species of *Aprotodon* (Perissodactyla, Rhinocerotidae) from Lanzhou Basin, Gansu, China. *Vertebrata PalAsiatica* **35:** 250–267 [in Chinese and English].

Répelin J. 1917. Études paléontologiques dans le sud-ouest de la France (Mammifères). Les rhinocérotidés de l'Aquitanien supérieur de l'Agenais (Laugnac). *Annales du Muséum d'Histoire naturelle de Marseille* **16:** 1–47.

Richard M. 1937. Une nouvelle espèce de Rhinocérotidé aquitanien: *Diaceratherium pauliacensis*. *Bulletin de la Société d'Histoire Naturelle de Toulouse* **71:** 165–170.

Ringström TJ. 1924. Nashörner der *Hipparion*-Fauna Nord-Chinas. *Geological Survey of China* **11:** 1–156.

Roger O. 1898. Wirbeltierreste aus dem Dinotheriensande der bayerisch-schwäbischen Hochebene. *Bericht des Naturwissenschaftlichen Vereins für Schwaben, Neuburg* **33:** 1–46, 383–396.

Roman F. 1912. Les rhinocérotidés de l'Oligocène d'Europe. *Archives du Musée des Sciences Naturelles de Lyon* **11:** 1–92.

Roman F. 1924. Contribution à l'étude de la faune de mammifères des Littorinenkalk (Oligocène supérieur) du Bassin de Mayence. *Travaux du Laboratoire de Géologie de la Faculté de Sciences de Lyon* **VII:** 55.

Roman F, Viret J. 1930. Le Miocène continental de l'Armagnac et le gisement burdigalien de La Romieu (Gers). *Livre Jubilaire de la Société Géologique de France, Paris* **2:** 576–604.

Roman F, Viret J. 1934. *La faune de Mammifères du Burdigalien de La Romieu (Gers)*, Vol. 21. Paris: Mémoires de la Société Géologique de France.

Scott WB. 1941. Perissodactyla. The mammalian fauna of the White River Oligocene. *Transactions of the American Philosophical Society* **28:** 747–980.

Steininger FF. 1999. Chronostratigraphy, geochronology and biochronology of the Miocene 'European Land Mammal Mega-Zones' (ELMMZ) and the Miocene 'Mammal-Zones' (MN). In: Rössner GE, Heissig K, eds. *The Miocene land mammals of Europe*. Munich: Pfeil, 9–24.

Swofford DL. 1998. *PAUP, Phylogenetic analysis using parsimony*, version 4.0 (software). Sunderland: Smithsonian Institution, Sinauer Associates.

Tanner LG. 1969. A new rhinoceros from the Nebraska Miocene. *Bulletin of the University of Nebraska State Museum* **8:** 395–412.

Tassy P. 1986. *Nouveaux Elephantoidea (Mammalia) dans le Miocène du kenya*. Paris: Cahiers de Paléontologie, Editions du Centre National de la Recherche Scientifique.

Uhlig U. 1999. Die Rhinocerotidae (Mammalia) aus der unteroligozänen Spaltenfüllung Möhren 13 bei Treuchtlingen in Bayern. *Verlag der Bayerischen Akademie der Wissenschaften Abhandlungen*. Neue Folge **170**.

Welcomme JL, Antoine PO, Duranthon F, Mein P, Ginsburg L. 1997. Nouvelles découvertes de Vertébrés miocènes dans le synclinal de Dera Bugti (Balouchistan, Pakistan). *Comptes Rendus de l'Académie des Sciences, Sciences de la terre et des planètes* **325:** 531–536.

Welcomme JL, Benammi M, Crochet JY, Marivaux L, Métais G, Antoine PO, Baloch I. 2001. Himalayan Forelands: palaeontological evidence for Oligocene detritic deposits in the Bugti Hills (Baluchistan, Pakistan). *Geological Magazine* **138:** 397–405.

Welcomme JL, Ginsburg L. 1997. Mise en évidence de l'Oligocène sur le territoire des Bugti (Balouchistan, Pakistan). *Comptes Rendus de l'Académie des Sciences, Sciences de la Terre et des Planètes* **325:** 999–1004.

Welcomme JL, Marivaux L, Antoine PO, Benammi M. 1999. Mammifères fossiles des Collines Bugti (Balouchistan, Pakistan). Nouvelles données. *Bulletin de la Société d'Histoire Naturelle de Toulouse* **135:** 135–139.

Wermelinger M. 1998. Prosantorhinus *cf.* douvillei *(Mammalia, Rhinocerotidae), petit rhinocéros du gisement miocène (MN 4b) de Montréal-du-Gers (Gers, France). Etude ostéologique du membre thoracique*. Unpublished PhD, University Toulouse III, France.

Wiens JJ. 2001. Character analysis in morphological phylogenetics: problems and solutions. *Systematic Biology* **50:** 689–699.

Wood HE II. 1927. Some early Tertiary rhinoceroses and hyracodonts. *Bulletin of the American Paleontologists* **13:** 5–105.

Yan D, Heissig K. 1986. Revision and autopodial morphology of the Chinese-European rhinocerotid genus *Plesiaceratherium* Young 1937. *Zitteliana Abhandlungen der Bayerische Staatssammlung für Paläontologie und historisches Geologie, München* **14:** 81–110.

Young C-C. 1937. On a Miocene mammalian fauna from Shantung. *Bulletin of the Geological Society of China* **17:** 209–245.

APPENDIX 1

CHARACTER LISTING

This list coincides with the character list proposed by Antoine (2003) and Antoine *et al.* (2003b).

Cranium

(1) Nasal: lateral apophysis = 0, absent; 1, present
(2) Maxillary: foramen infraorbitalis = 0 above premolars; 1, above molars
(3) Nasal notch = 0, above P1–3; 1, above P4–M1
(4) Nasal septum = 0, never ossified; 1, ossified (even sometimes)
(5) Nasal septum: ossified = 0, partially; 1, totally
(6) Nasal/lacrymal: contact = 0, long; 1, punctual or absent
(7) Orbit: anterior border = 0, above P4–M2; 1, above M3; 2, behind M3
(8) Lacrymal: processus lacrymalis = 0, present; 1, absent

(9) Frontal: processus postorbitalis = 0, present; 1, absent
(10) Maxillary: anterior base of the processus zygomaticus maxillari = 0, high; 1, low
(11) Zygomatic arch = 0, low; 1, high; 2, very high
(12) Zygomatic arch: processus postorbitalis = 0, present; 1, absent
(13) Zygomatic arch: processus postorbitalis = 0, on jugal; 1, on squamosal
(14) Jugal/squamosal: suture = 0, smooth; 1, rough
(15) Skull: dorsal profile = 0, flat; 1, concave; 2, very concave
(16) Sphenoid: foramen sphenorbitale and f. rotundum = 0, distinct; 1, fused
(17) Squamosal: area between temporal and nuchal crests = 0, flat; 1, depression
(18) External auditory pseudomeatus = 0, open; 1, partially closed; 2, closed
(19) Occipital side = 0, inclined forward; 1, vertical; 2, inclined backward
(20) Occipital: nuchal tubercle = 0, little developed; 1, developed; 2, very developed
(21) Skull: back of teeth row = 0, in the posterior half; 1, restricted to the anterior half
(22) Pterygoid: posterior margin = 0 nearly horizontal; 1, nearly vertical
(23) Skull = 0, dolichocephalic; 1, brachycephalic
(24) Nasal bones: rostral end = 0, narrow; 1, broad; 2, very broad
(25) Nasal bones = 0, totally separated; 1, anteriorly separated; 2, fused
(26) Nasal bones = 0, long; 1, short; 2, very long
(27) Median nasal horn = 0, absent; 1, present
(28) Median nasal horn = 0, small; 1, developed
(29) Paired nasal horns = 0, absent; 1, present
(30) Paired nasal horns = 0, terminal bumps; 1, lateral crests
(31) Frontal horn = 0, absent; 1, present
(32)*Frontal horn = 0, small; 1, huge [*Elasmotherium*]
(33) Orbit: lateral projection = 0, absent; 1, present
(34) Zygomatic width/frontal width = 0, less than 1.5; 1, more than 1.5
(35) Frontal-parietal = 0, sagittal crest; 1, close frontoparietal crests; 2, distant crests
(36) Occipital crest = 0, concave; 1, straight; 2, forked
(37) Maxillary: processus zygomaticus maxillari, anterior tip = 0, progressive; 1, brutal
(38) Vomer = 0, acute; 1, rounded
(39) Squamosal: articular tubercle = 0, smooth; 1 high
(40) Squamosal: transversal profile of articular tubercle = 0, straight; 1, concave
(41) Squamosal: foramen postglenoideum = 0, distant from the processus postglenoidalis; 1, close to it
(42) Squamosal: processus postglenoidalis = 0, flat; 1, convex; 2, dihedron
(43) Basioccipital: foramen nervi hypoglossi = 0, in the middle of the fossa; 1 shift anteroexternally
(44) Basioccipital: sagittal crest on the basilar process = 0, absent; 1, present
(45) Squamosal: posterior groove on the processus zygomaticus = 0, absent; 1, present
(46) Squamosal-occipital: processus post-tympanicus and processus paraoccipitalis = 0, fused; 1, distant
(47) Squamosal: processus post-tympanicus = 0, well developed; 1, little developed; 2, huge
(48) Occipital: processus paraoccipitalis = 0, well developed; 1, little developed
(49) Occipital: foramen magnum = 0, circular; 1, subtriangular
(50) Basioccipital: median ridge on the condyle = 0, absent; 1, present
(51) Basioccipital: medial truncation on the condyle = 0, absent; 1, present
(52) Basioccipital: medial truncation on the condyle = 0, present at juvenile stage; 1, still present at adult stage

Mandible

(53) Symphysis = 0, very upraised; 1, upraised; 2, nearly horizontal
(54) Symphysis = 0, spindly; 1, massive; 2, very massive
(55) Symphysis: posterior margin = 0, in front of p2; 1, level of p2–4
(56) Foramen mentale = 0, in front of p2; 1, level of p2–4
(57) Corpus mandibulae: lingual groove = 0, present; 1, absent
(58) Corpus mandibulae: lingual groove = 0, still present at adult stage; 1, present at juvenile stage only
(59) Corpus mandibulae: base = 0, straight; 1, convex; 2, very convex
(60) Ramus = 0, vertical; 1, inclined forward; 2, inclined backward
(61) Ramus: processus coronoideus = 0, well developed; 1, little developed
(62) Foramen mandibulare = 0, below the teeth neck; 1, above the teeth neck

Teeth

(63) Compared length of the premolars/molars rows = 0 $(100 \times L_{P3–4}/L_{M1–3}) > 50$; 1, $42 < (100 \times L_{P3–4}/L_{M1–3}) < 50$; 2 $(100 \times L_{P3–4}/L_{M1–3}) < 42$
(64) Cheek teeth: enamel foldings = 0, absent; 1, weak; 2, developed; 3, intense
(65) Cheek teeth: cement = 0, absent; 1, present
(66) Cheek teeth: cement = 0, weak or variable; 1, abundant

(67) Cheek teeth: shape of enamel = 0, wrinkled; 1, wrinkled and corrugated; 2, corrugated and arborescent
(68) Cheek teeth: crown = 0, low; 1, high
(69) Cheek teeth: crown = 0, high; 1, partial hypsodonty; 2, subhypsodonty; 3, hypsodonty
(70) Cheek teeth: roots = 0, distinct; 1, joined; 2, fused
(71) I1 = 0, present; 1, absent
(72) I1: shape of the crown (cross-section) = 0, almond; 1, oval; 2, halfmoon (NA)
(73) I2 = 0, present; 1, absent
(74) I3 = 0, present; 1, absent
(75) C1 = 0, present; 1, absent
(76) i1 = 0, present; 1, absent
(77) i1: crown = 0, developed, with a pronounced neck; 1, reduced
(78) i2 = 0, present; 1, absent
(79) i2: shape = 0, incisor-like; 1, tusk-like
(80) i2: orientation = 0, parallel; 1, divergent
(81) i3 = 0, present; 1, absent
(82) c1 = 0, present; 1, absent
(83) Upper premolars: labial cingulum = 0, always present; 1, usually present; 2, usually absent; 3, always absent
(84) P2–4: crochet = 0, always absent; 1, usually present; 2, always present
(85) P2–4: crochet = 0, always simple; 1, usually simple; 2, usually multiple
(86) P2–4: metaloph constriction = 0, absent; 1, present
(87) P2–4: lingual cingulum = 0, always present; 1, usually present; 2, usually absent; 3, always absent
(88) P2–4: lingual cingulum = 0, continuous; 1, reduced
(89) P2–4: postfossette = 0, narrow; 1, wide; 2, posterior wall
(90) P2–3: antecrochet = 0, always absent; 1, usually absent; 2, usually present; 3, always present
(91) P1 (in adults) = 0, always present; 1, usually present; 2, always absent
(92) P1: anterolingual cingulum = 0, present; 1, absent [*Rhinoceros sondaicus*]
(93) P2 = 0, present; 1, absent
(94) P2: protocone and hypocone = 0, fused; 1, lingual bridge; 2, separated; 3, lingual wall (NA)
(95) P2: metaloph = 0, hypocone posterior to metacone; 1, transverse; hypocone anterior to metacone
(96) P2: lingual groove = 0, present; 1, absent
(97) P2: protocone = 0, equal or stronger than the hypocone; 1, less strong than the hypocone
(98) P2: protoloph = 0, present; 1, absent
(99) P2: protoloph = 0, joined to the ectoloph; 1, interrupted
(100) P3–4: medifossette = 0, always absent; 1, usually absent; 2, usually present; 3, always present
(101) P3–4: constriction of the protocone = 0, always absent; 1, usually absent; 2, usually present; 3, always present
(102) P3–4: protocone and hypocone = 0, fused; 1, lingual bridge; 2, separated; 3, lingual wall (NA)
(103) P3–4: metaloph = 0, transverse; 1, hypocone posterior to metacone; 2, hypocone anterior to metacone
(104) P3: protoloph = 0, joined to the ectoloph; 1, interrupted
(105) P3: crista = 0, always absent; 1, usually absent; 2, usually present; 3, always present
(106) P3: pseudometaloph = 0, always absent; 1, sometimes present
(107) P4: antecrochet = 0, always absent; 1, usually absent; 2, usually present; 3, always present
(108) P4: hypocone and metacone = 0, joined; 1, separated
(109) Upper molars: labial cingulum = 0, always present; 1, usually present; 2, usually absent; 3, always absent
(110) Upper molars: antecrochet = 0, always absent; 1, usually absent; 2, usually present; 3, always present
(111) Upper molars: crochet = 0, always absent; 1, usually absent; 2, usually present; 3, always present
(112) Upper molars: crista = 0, always absent; 1, usually absent; 2, usually present; 3, always present
(113)* Upper molars: medifossette = 0, always absent; 1, usually absent [*Diceros bicornis*]; 2, usually present [*Ceratotherium simum*; *Coelodonta antiquitatis*; *Rhinoceros unicornis*]
(114) Upper molars: lingual cingulum = 0, always present; 1, usually present; 2, usually absent; 3, always absent
(115) M1–2: constriction of the protocone = 0, always absent; 1, usually absent; 2, usually present; 3, always present
(116) M1–2: constriction of the protocone = 0, weak; 1, strong
(117) M1–2: paracone fold = 0, present; 1, absent
(118) M1–2: paracone fold = 0, strong; 1, weak
(119) M1–2: metacone fold = 0, present; 1, absent
(120) M1–2: metastyle = 0, short; 1, long
(121) M1–2: metaloph = 0, long; 1, short
(122) M1–2: posterior part of the ectoloph = 0, straight; 1, concave

(123) M1–2: cristella = 0, always absent; 1, usually present; 2, always present
(124) M1–2: posterior cingulum = 0, continuous; 1, low and reduced
(125) M1: metaloph = 0, continuous; 1, hypocone isolated
(126) M1: antecrochet-hypocone = 0, always separated; 1, sometimes joined; 2, always joined
(127) M1: postfossette = 0, present; 1, usually absent
(128) M2: protocone, lingual groove = 0, always absent; 1, usually absent; 2, always present
(129) M2: metaloph = 0, continuous; 1, hypocone isolated
(130) M2: mesostyle = 0, absent; 1, present
(131) M2: mesostyle = 0, weak; 1, strong
(132) M2: antecrochet and hypocone = 0, separated; 1, joined
(133) M3: ectoloph and metaloph = 0, distinct; 1, fused (ectometaloph)
(134) M3: shape = 0, quadrangular; 1, triangular
(135) M3: constriction of the protocone = 0, always absent; 1, usually absent; 2, always present
(136) M3: protocone = 0, trefoil-shape; 1, indented
(137) M3: protoloph = 0, transverse; 1, lingually elongated
(138) M3: posterior groove on the ectometaloph = 0, present; 1, absent
(139)*p2–3: vertical external roughnesses = 0, absent; 1, present
(140) Lower cheek teeth: external groove = 0, developed; 1, smooth, U-shaped; 2, angular, V-shaped (NA)
(141) Lower cheek teeth: external groove = 0, vanishing before the neck; 1, developed until the neck
(142) Lower cheek teeth: trigonid = 0, angular; 1, rounded
(143) Lower cheek teeth: trigonid = 0, obtuse or right dihedron; 1, acute dihedron
(144) Lower cheek teeth: metaconid = 0, joined to the metalophid; 1, constricted
(145) Lower cheek teeth: entoconid = 0, joined to the hypolophid; 1, constricted
(146) Lower premolars: lingual opening of the posterior valley = 0, U-shape; 1, narrow, V-shape
(147) Lower premolars: lingual cingulum = 0, always present; 1, usually present; 2, usually absent; 3, always absent
(148) Lower premolars: lingual cingulum = 0, reduced; 1, continuous
(149) Lower premolars: labial cingulum = 0, present; 1, absent
(150) Lower premolars: labial cingulum = 0, continuous; 1, reduced
(151) d1/p1 (in adults) = 0, always present; 1, usually present; 2, usually absent; 3, always absent
(152) d1: 0, always two-rooted; 1, usually two-rooted; 2, always one-rooted
(153) p2 = 0, always present; 1, usually present; 2, always absent
(154) p2: paralophid = 0, isolated, spur-like; 1, curved, without constriction
(155) p2: paraconid = 0, developed; 1, reduced
(156) p2: posterior valley = 0, lingually open; 1, usually closed; 2, always closed
(157) Lower molars: lingual cingulum = 0, always present; 1, usually present; 2, usually absent; 3, always absent
(158) Lower molars: lingual cingulum = 0, reduced; 1, continuous
(159) Lower molars: labial cingulum = 0, always present; 1, usually present; 2, usually absent; 3, always absent
(160) Lower molars: labial cingulum = 0, continuous; 1, reduced
(161) Lower molars: hypolophid = 0, transverse; 1, oblique; 2, almost sagittal
(162) m2–3: lingual groove of the entoconid = 0, absent; 1, present
(163)*dI1 = 0, present; 1, absent [*Ceratotherium simum*; *Coelodonta antiquitatis*]
(164)*dI2 = 0, present; 1, absent
(165) D2: mesostyle = 0, present; 1, absent
(166) D3–4: mesostyle = 0, absent; 1, present
(167) D2: lingual wall = 0, absent; 1, present
(168) D2: secondary folds = 0, absent; 1, present
(169) D2: mesoloph = 0, absent; 1, present
(170) di1 = 0, present; 1, absent
(171) di2 = 0, present; 1, absent
(172) Lower milk teeth: constriction of the metaconid = 0, present; 1, absent
(173) Lower milk teeth: constriction of the entoconid = 0, absent; 1, present
(174) Lower milk teeth: protoconid fold = 0, present; 1, absent
(175) d1 (in juveniles) = 0, present; 1, absent
(176) d2–3: vertical external roughnesses = 0, absent; 1, present
(177) d2–3: ectolophid fold = 0, present; 1, absent
(178) d2: anterior groove on the ectolophid = 0, absent; 1, present
(179) d2: paralophid = 0, simple; 1, double
(180) d2: posterior valley = 0, always open; 1, usually open; 2, usually closed; 3, always closed
(181) d3: paralophid = 0, double; 1, simple
(182) d3: lingual groove on the entoconid = 0, always absent; 1, usually absent; 2, always present

Postcranial skeleton

(183) Atlas: outline of the rachidian canal = 0, bulb; 1, mushroom

(184) Atlas: alar notch = 0, absent; 1, present
(185) Atlas: foramen vertebrale lateralis = 0, absent; 1, present
(186) Atlas: condyle-facets = 0, comma-like; 1, kidney-like
(187) Atlas: axis-facets = 0, straight; 1, sigmoid; 2, transversally concave (NA)
(188) Atlas: foramen transversarium = 0, present; 1, absent
(189) Atlas: foramen transversarium = beside the axis-facet; 1, hidden by the axis-facet
(190) Scapula = 0, elongated ($1.5 < H/APD \leq 2$); 1, very elongated ($H/APD > 2$); 2, spatula-shaped ($H/APD \leq 1.5$)
(191) Scapula: glenoid fossa = 0, oval; 1, medial border straight
(192) Humerus: greater trochiter = 0, high; 1, low
(193) Humerus: fossa olecrani = 0, high; 1, low
(194) Humerus: distal articulation = 0, egg cup (shallow median constriction); 1, diabolo (deep median constriction)
(195) Humerus: scar on the trochlea = 0, absent; 1, present
(196) Humerus: distal gutter on the epicondyle = 0, absent; 1, present
(197) Radius: anterior border of the proximal articulation = 0, straight; 1, M-shaped
(198) Radius: medial border of the diaphysis = 0, straight; 1, concave
(199) Radius: proximal ulna-facets = 0, always separated; 1, usually separated; 2, usually fused; 3, always fused
(200) Radius: insertion of the m. biceps brachii = 0, shallow; 1, deep
(201) Radius/ulna = 0, independent; 1, in contact or fused
(202) Radius: gutter for the m. extensor carpi = 0, deep and wide; 1, weak
(203) Radius/ulna: second distal articulation = 0, absent; 1, present
(204) Radius: posterior expansion of the scaphoid-facet = 0, low; 1, high
(205) Ulna: angle between diaphysis and olecranon = 0, open; 1, closed
(206) Ulna: anterior tubercle on the distal end = 0, absent; 1, present
(207) Scaphoid: posteroproximal facet with semilunate = 0, present; 1, absent or contact
(208) Scaphoid: trapezium-facet = 0, large; 1, small
(209) Scaphoid: magnum-facet in lateral view = 0, concave; 1, straight
(210) Scaphoid: comparison between anterior and posterior heights = 0, equal; 1, H ant < H post
(211) Semilunate: ulna-facet = 0, absent; 1, present
(212) Semilunate: distal border of anterior side = 0, acute; 1, rounded
(213) Semilunate: anterior side = 0, keeled; 1, smooth
(214) Pyramidal: distal facet for semilunate = 0, symmetric; 1, asymmetric; 2, L-shaped
(215) Pyramidal: distal side = 0, triangular; 1, elliptic
(216) Trapezoid: proximal border in anterior view = 0, symmetric; 1, asymmetric
(217) Magnum: proximal border of the anterior side = 0, nearly straight; 1, concave
(218) Magnum: indentation on the medial side = 0, absent; 1, present
(219) Magnum: indentation on the medial side = 0, always shallow; 1, usually shallow; 2, always deep
(220) Magnum: posterior tuberosity = 0, short; 1, long
(221) Magnum: posterior tuberosity = 0, curved; 1, straight
(222) Unciform: pyramidal-facet and McV-facet = 0, always separate; 1, usually separate; 2, always in contact
(223) Unciform: posterior expansion of the pyramidal-facet = 0, always absent; 1, usually absent; 2, usually present; 3, always present
(224) McII: magnum-facet = 0, curved; 1, straight
(225) McII: anterior McIII-facet = 0, present; 1, sometimes absent
(226) McII: posterior McIII-facet = 0, always absent; 1, usually absent; 2, always present
(227) McII: anterior and posterior McIII-facets = 0, separated; 1, fused
(228) McII: trapezium-facet = 0, always present; 1, usually present; 2, always absent
(229) McIII: magnum-facet in anterior view = 0, visible; 1, invisible
(230) McIV: proximal facet, outline = 0, trapezoid; 1, pentagonal; 2, triangular
(231) McV: 0, functional; 1, vestigial
(232) Metacarpals: insertion of the m. extensor carpalis = 0, flat; 1, salient
(233) Coxal: acetabulum = 0, oval or circular; 1, subtriangular
(234) Femur: trochanter major = 0, high; 1, low
(235) Femur: head = 0, hemispheric; 1, medially stiff
(236) Femur: surface of epiphysis of the head = 0, flat; 1, crescent-shaped
(237) Femur: fovea capitis = 0, present; 1, absent
(238) Femur: fovea capitis = 0, high and narrow; 1, low and wide
(239) Femur: third trochanter = 0, developed; 1, very developed
(240) Femur: relations between the medial lip of the trochlea and the diaphysis = 0, broken angle; 1, ramp
(241) Femur: proximal border of the patellar trochlea = 0, curved; 1, straight

(242) Tibia: anterodistal groove = 0, present; 1, absent
(243) Tibia: mediodistal gutter (tendon m. tibialis posterior) = 0, always present; 1, usually present; 2, always absent
(244) Tibia: mediodistal gutter = 0, shallow; 1, deep
(245) Tibia–fibula = 0, independent; 1, in contact or fused
(246) Tibia: posterior apophysis = 0, high; 1, low
(247) Tibia: posterior apophysis = 0, acute; 1, rounded
(248) Fibula: proximal articulation = 0, low; 1, high
(249) Fibula: distal end = 0, slender; 1, robust
(250) Fibula: laterodistal gutter (tendon peronaeus muscles) = 0, shallow; 1, deep
(251) Fibula: position of the laterodistal gutter = 0, posterior; 1, median
(252) Astragalus: (transverse diameter/height) ratio = 0, TD/H < 1; 1, 1 ≤ TD/H < 1.2; 2, 1.2 ≤ TD/H
(253) Astragalus: (anteroposterior diameter/height) ratio = 0, APD/H < 0.65; 1, 0.65 ≤ APD/H
(254) Astragalus: orientation of the fibula-facet = 0, subvertical; 1, oblique
(255) Astragalus: fibula-facet = 0, flat; 1, concave
(256) Astragalus: collum tali = 0, high; 1, low
(257) Astragalus: posterior stop on the cuboid-facet = 0, present; 1, absent
(258) Astragalus: caudal border of the trochlea, in proximal view = 0, sinuous; 1, nearly straight
(259) Astragalus: orientation of trochlea/distal articulation = 0, very oblique; 1, same axis
(260) Astragalus: expansion of the calcaneus-facet 1 = 0, always present; 1, usually present
(261) Astragalus: expansion of the calcaneus-facet 1 = 0, always wide and low; 1, usually wide and low; 2, always high and narrow
(262) Astragalus: calcaneus-facet 1 = 0, very concave; 1, nearly flat
(263) Astragalus: calcaneus-facets 2 and 3 = 0, always independent; 1, usually independent; 2, usually fused; 3, always fused
(264) Calcaneus: fibula-facet = 0, always absent; 1, usually absent; 2, usually present; 3, always present
(265) Calcaneus: tibia-facet = 0, always absent; 1, usually absent; 2, always present
(266) Calcaneus: tuber calcanei = 0, massive; 1, slender
(267) Calcaneus: insertion of the m. fibularis longus = 0, salient; 1, invisible
(268) Navicular: cross-section = 0, lozenge; 1, rectangle
(269) Cuboid: proximal side = 0, oval; 1, triangular
(270) Ectocuneiform: posterolateral process = 0, weak; 1, developed
(271) MtIII: proximal border of the anterior side = 0, straight; 1, concave; 2, sigmoid
(272) MtIII: posterior MtII-facet = 0, present; 1, absent
(273)* MtIII: MtIV-facets = 0, distinct; 1, sometimes joined [*Coelodonta antiquitatis*]
(274) MtIII: distal widening of the diaphysis (in adults) = 0, absent; 1, present
(275) MtIII: cuboid-facet = 0, absent; 1, present
(276) MtIII: cuboid-facet = 0, small; 1, large
(277) MtIV: posteroproximal tuberosity = 0, isolated; 1, pad-shaped and continuous
(278) Phalanx I for MtIII: symmetric insertions = 0, lateral; 1, nearly anterior
(279) Limbs = 0, slender; 1, robust (brachypod)
(280) Metapodials: intermediate relief = 0, high and acute; 1, low and smooth
(281) Central metapodials: posterodistal tubercle on the diaphysis = 0, absent; 1, present
(282) Lateral metapodials: insertion of the m. interossei = 0, long; 1, short (does not reach distal half of the shaft)

APPENDIX 2

Data matrix including 282 cranial, dental, and postcranial characters controlled on 28 terminal taxa (tapirid, rhinocerotoids, and rhinocerotids). The four outgroups are *Tapirus terrestris, Hyrachyus eximius, Trigonias osborni*, and *Ronzotherium filholi*. The characters 72, 94, 102, 140 and 187 are non-additive. Missing observations and nonapplicable characters appear as '?' and '–', respectively.

	Characters
	0000000000000000000000000000000000000000000000000000000000000000000000000000000000000000000000000000000000000000000000
	0000000001111111111222222222233333333334444444445555555556666666666777777777788888888899999999999
	0123456789012345678901234567890123456789012345678901234567890123456789012345678901234567890123456789012345678901234567890123456789
Taxa	
Tapirus terrestris (outgroup)	00010-10000000000000100100010-0-0-0100000100000000000-0010000000000--0-000000000000000-0000000020-100
Hyrachyus eximius (outgroup)	00000-00?01100000001020000000-0-0-00000?000000000000-0001000100100-00-000000000000010-000000000---1-
Trigonias osborni (outgroup)	01000-1000010000?01020010000-0-0-00000?000001001010-20110000?100-00-?0100000101100-0000000020-001
Ronzotherium filholi (outgroup)	00100-?000001-01100000010000-0-0-00111100010100000000-0000010010000-00-0000110?0101100-0001000010-001
Aceratherium incisivum	00000-0000010000?10110?00000-100-01010??0??????00?????21?1??000?100-?0-?00011000101100-1001000021-000
Alicornops simorrense	00000-?000110101110220000000100-0-00101?0?0101100010111000011 0?1101011020211101010112210111000031001-
Brachypotherium brachypus	00000-1001101-12100121012101 10-10102101100101010100-00111-2201001021011-1111-1--113210000010020-101
Bugthirhinus praecursor	00001000000001-1111001000110110-10002001110100010011 0?11101-0010001010-10111101010113211110 01?020-101
Chilotherium anderssoni	00001000000000?211201011110110-0-0120001101010100110-211101011000101101011110101111321 03-0010020-101
Diaceratherium aginense	00010-?0?000100 11?1??0?10000-0-0-0020000?0201?1111 0?22111-0001000-10-100??100010111210000000020-001
Diceratherium armatum	00000-?0101100 01?12020100000-110-0000011001010???00?0?2010000000001010-10101100010113 0-0000000010-001
Dicerorhinus sumatrensis	00000-?000110001100120 1?0000-100-00?001010201110110?0?10111-1000001010-2021101-010113220010000010-001
Diceros bicornis	00?10-?0??00??00?1100???0000-0-0-0?010?10120010000 1101111000???000-00-001??100010112210000100010-001
Gaindatherium browni	00010-?0??01???0??0100?10000-0-0-0???0?0????????0?0????010??100?000-10-101??101010113220000000020-001
Hispanotherium beonense	00000-?000010100?01210010010-0-0-00020?00?1?0011010?0????1000???000-00-000111??01??100-0000000020-000
Lartetotherium sansaniense	00000-?00001??00?00100110000-0-0-0?000?00?1000010?1??11000000?00??00-001000000101110-10010000310000
Menoceras arikarense	0??001000-?01000000 1?1120-0001000011-000
Mesaceratherium gaimersheimense	01000-?000001-?1?12020?10100-0-0-01000???????11011?? 01110??000?000-10-?011110001011211000000021-100
Mesaceratherium paulhiacense	00000-?000001-?2?01010?1210110-0-00200??0??0111000??? 211100000?000-10-?011110001011?210210000010-000
***Mesaceratherium welcommi* sp. nov.**	00000-?000101-?1?0210001110110-0-0111001????00????? ??2111??0???001010-?01011??0111132003-0000010-100
Plesiaceratherium mirallesi	00010-0000010100?11110110110-0-0-00211?????0100100? ??2211??000?000-010?1-1111-011110200000300010-000
Pleuroceros blanfordi	00000-?0001000?0000110110010-0-0-0?001?10?2010110110?1111??000100??00-?011110101111210100001 0020-000
Pleuroceros pleuroceros	0?000-?????????0????????00?0-0-0-??0?1????????????? ???22?0000???100-?0-??????1-011113220010000010-001
Prosantorhinus douvillei	0??? ??0110??0???000-00-000011000101120-000000?011-001
Protaceratherium albigense	0??? ??11?????????00???0-?0????0001????0-?00??00021?000
Protaceratherium minutum	0??? ??11111?0000101000-0???????0101030-000000?010-100
Rhinoceros unicornis	00000-?0000100?1?01110?00??0-110-00?01???????11000??? 2111??00??1?????0?0?1110?0?011??????????????????
Subhyracodon occidentalis	0?00????????1??0?????1?????????????????0??1??2??1???0 10?21111-0???10110101?????0?0101121200100 0?011-100

	Characters
	1111111111111111111111111111111111111111111111111111111111111111111111111111111111111111111111111111
	0000000000111111111122222222223333333333444444444455555555556666666666777777777788888888889999999999
	0123456789012345678901234567890123456789012345678901234567890123456789012345678901234567890123456789
Taxa	
Tapirus terrestris (outgroup)	0020000000000000-000000000-0000-0000-0-0--1100000013-0100000100001000000000000000001000101000000000000
Hyrachyus eximius (outgroup)	0000100012000000-000010000-0000-0000-0-000001003-000001002-0000??00000?????????????000001-0000001003
Trigonias osborni (outgroup)	0020000010100000-0100000000000-0000-0000000100201-0000002-2-00??00000000100?0??00110?0000?0?000000
Ronzotherium filholi (outgroup)	0030020101222000-0011000000000-0000-0000000000010000000000000000??000000?0000?001000010001-?100100003
Aceratherium incisivum	1221010112231113001110100100010-01120010101000120011200001021 10??000??????????????????????0?01001001
Alicornops simorrense	1021010202331023000110000100000-0112001000010012000220000 3-1110??1001000000000011000?????0??001001001
Brachypotherium brachypus	0021000101230002001010000100010-0110-01010101003-012000102-0010??000101000?00101100????????100001002
Bugthirhinus praecursor	0131000000330013101??1100???0110010200?02001001201-3?0???101110??00000??????????????????????????????
Chilotherium anderssoni	2321020301330003101110000000001001021000001010100 1-320000103-1011110000000000001010???????0???????0?
Diaceratherium aginense	0021000002330003000110000100000-010200?00000000??01320000??011???????????????00?1????????????0?00001000
Diceratherium armatum	0011000000310002001000100000010-0100-01000010000100 3?000001001 0??000?0??1000000120001 0?01-??00000003
Dicerorhinus sumatrensis	1121010003021023000111000 0-000100110-0100010001 3-1-2100002-2-10????0??????????????????010121-0100001000
Diceros bicornis	2121010003121101001111000000000-0110-0100010001 3-1-2001002-2-1001100000 0???0010?0??001121-1001100100
Gaindatherium browni	0011000003030022000110000100000-0112001000110013-1-1201003-3-00???0??????????????????????????????????
Hispanotherium beonense	0331100001330023100011101100211001020000200110 13-1-3001002-2-10??000000000001111000010000010111101 13
Lartetotherium sansaniense	0011010003030022000110000100000-0112001000111013-1-1201003-2100??00000?????????????????????????0100010
Menoceras arikarense	2321030000332003000011101000001001 00-000200100101003?0100002-10??100010010001001000110021-1000101000
Mesaceratherium gaimersheimense	0011000000310003001110100100010-0101-01?201000110010200001021 00??????????001??????????????????????????
Mesaceratherium paulhiacense	0021000003330003001110100100?110010??0????????????0????0??
***Mesaceratherium welcommi* sp. nov.**	0311000000330003101110100100010-0102001120100113-1-120???20210-??
Plesiaceratherium mirallesi	2021010102230013000011100000000-0110-011001000100011100000000100??0001000000001000000001?1????100001000
Pleuroceros blanfordi	12110003023310131010101011000110010200111000101010002000000 0110??????????00?00110000???????????01100??
Pleuroceros pleuroceros	???11000?010100??0???00011???????????????????????????????????????
Prosantorhinus douvillei	0021000303230023000010100000000100110-0100010100001-22000200011 1??00010??000000000030211?1101210100100 2
Protaceratherium albigense	0011010000300003 0-0100100100011001020000000000101000200000000000???1????00?1000000??????????0?0000000
Protaceratherium minutum	1021020202230003000011100000010-0100-0102000101000002000000 1110??00000??0000000??000100000?00?000?0?
Rhinoceros unicornis	0221020003022232001110000 0-0000-0110-01000101013-1-2001002-2-11????010?????0????????111101-1101001003
Subhyracodon occidentalis	0030000010110000-0001110000000??0100-0?000010010100320001010010000000000???0000100??11?2??0?00001?03

Taxa	Characters
	22222222222222222222222222222222222222222222222222**2**22222222222222222222222222222222
	0000000000111111111122222222223333333333444444444**5**55555555566666666667777777777888
	0123456789012345678901234567890123456789012345678**9**0123456789012345678901234567890**1**2
Tapirus terrestris (outgroup)	**0**000000001001000000-0000000-0000000000000010100000**1**0001000000000000000000020000-000000
Hyrachyus eximius (outgroup)	**0**1000001000111000010000000-00000000?0100000000000**0**0000000000003000000021-010000000
Trigonias osborni (outgroup)	**0**000?00010000010001010010000-00?00000???00101-000?0**0**0110000000000??1?00?0000????0001
Ronzotherium filholi (outgroup)	**0**00000000000000000-1???000-202?0000?0000000000000**0**01?00001002010101001?000000-0?0000
Aceratherium incisivum	**0**10011110010010010101022102120101?00?0100000110000**0**11110001001010000010000000-000000
Alicornops simorrense	**1**000?001?000011000??0023102100?01?10???00??1?0???1**?**?11000011000032000001000100?0000
Brachypotherium brachypus	**0**01101100110001000100011100-011110000001011 2-00101**0**1211001010011220000?100011001001
Bugthirhinus praecursor	??001?010010????????1000??????21??????????????????0**1**11101??10003??1?1?02001101100?0
Chilotherium anderssoni	**0**???????????0???10???????????????1??????????????????**?**?2?100???10?0????????????10??10??
Diaceratherium aginense	**0**1001011101011000000-0100102101001?00?010011??00111**?**?101001?110103?0?00020000-000001
Diceratherium armatum	**0**100000100001010001010000000-00210?000010000000011 0**0**0100001000003120010020010-000001
Dicerorhinus sumatrensis	**0**1100100000100201010000000202021001 0?0100101-00001**1**11100101100023200010100010100000
Diceros bicornis	**1**1000100000111211010100010212001001101-110101011 10**1**1111010110002020100010000-100100
Gaindatherium browni	**?**???**?**?????????????????????????????????
Hispanotherium beonense	**1**100010111110010101211120010002101111000101011111 0**1**12111101102033211101200110110100
Lartetotherium sansaniense	**0**1001??0001101100012112?002000211?????????000101??**?**?110000?01003??0010?100?0-0?0100
Menoceras arikarense	**0**10000011000101000101003002000210111001000001001 10**0**01110100101033210110100110010000
Mesaceratherium gaimersheimense	**?**???**?**?????????????????????????????????
Mesaceratherium paulhiacense	**?**??????000101?10101011 0?1021001 0??????????????????**?**?110000?002000?0?00021-00-??00?0
***Mesaceratherium welcommi* sp. nov.**	**?**0000?00001000?0?010??0000200??00?????????101100??**?**?110000100203300000?1101????00?0
Plesiaceratherium mirallesi	**0**10000010010000000101000011000100000000000010000001**1**11100100101031200000 11-00-000010
Pleuroceros blanfordi	**0**0001??0101011??0010??01000-?0?11?????????101001?1**1**0110000100200001000010010-0?0001
Pleuroceros pleuroceros	**?**??????0101???100010??0?002000?11??????????????????**?**?110000?00?003?1?000000?0-??0001
Prosantorhinus douvillei	**0**110111000100100000-00001011110110100000011100000 1**0**121000101121032000001 1-010001001
Protaceratherium albigense	**0**1000??00010??10?01010??000-00101?????????001100??**?**?010000102-00????1??1?0?0-??0000
Protaceratherium minutum	**0**?????011010111000 11??0?000-?00?0?1????0?00??000??**?**?110010010001100000002??10-?10000
Rhinoceros unicornis	**0**1000100001000001 00-10201020002110 00?0110010001101**1**1110010110002320000001 0010-100100
Subhyracodon occidentalis	**0**10??1001??0100??0?????????????0?10000???000???0??10**?**?1?0000?00000001 00??2??00-??0???